The University of Osaka
Institutional Knowledge Archive

Title	Theoretical and Experimental Studies on Gold and Gold-Based Bimetallic Nanocluster Catalysts
Author(s)	Karanjit, Sangita
Citation	大阪大学, 2015, 博士論文
Version Type	VoR
URL	https://doi.org/10.18910/54004
rights	
Note	

The University of Osaka Institutional Knowledge Archive : OUKA

https://ir.library.osaka-u.ac.jp/

The University of Osaka

Doctoral Dissertation

Theoretical and Experimental Studies on Gold and Gold-Based Bimetallic Nanocluster Catalysts

金および含金ナノクラスター触媒の理論的および実験的研究

SANGITA KARANJIT

July 2015

Graduate School of Engineering
Division of Applied Chemistry
Osaka University

CONTENTS

Chapter 4. Theoreoretical and Experimental Studies on Gold-based Bimetallic Nanocluster Catalysts 58

Conclusion

Ackwledgement

Chapter 1

General Introduction

1.1 Gold nanoclusters

Since the ancient times, gold has been given a great value for its beauty as well as its unique physical and chemical properties. However, for catalytic purposes, bulk gold is always being regarded as inactive[1] and its use is limited to decorating materials or ornaments because of its high ionization potential, and accordingly gold has a poor affinity towards molecules. Through a number of theoretical and experimental investigations, it was demonstrated that no dissociative adsorption of small gas molecules like H_2 and O_2 occurs at low temperature,[2,3] therefore, Au should not be catalytically active for hydrogenation and oxidation reactions.[4,5] Since it was realized that the bulk properties of materials change drastically as their sizes decrease from the bulk material to small clusters[6] and proper control of these properties can lead to a new science (Figure 1),[7] nanometer sized gold clusters have attracted attention of researchers[8-11] and opened up a wide research area in chemistry. Since then, gold nanoclusters (Au NCs) have been extensively used as active catalysts in several oxidation, hydrogenation and addition reactions.[12-21] Besides the size, stability of Au NCs also largely determines the catalytic activity. Because, naked colloidal nanoparticles are thermodynamically unstable and show poor long-term stability due to agglomeration, the stabilization of such particles is essential which can be achieved by coordination of Au NCs to ligands/anionic species, polymers or by supporting them on a solid surface. For these purposes, several types of Au NCs stabilized on polymers, metal oxides and carbon materials has been developed and used until recent years.[22-27] Metal NCs suspended in solution are often used as effective heterogeneous catalysts due to the advantages of simplified isolation of product, their facile recovery and excellent recyclability which renders metal nanocatalysts environmentally friendly.

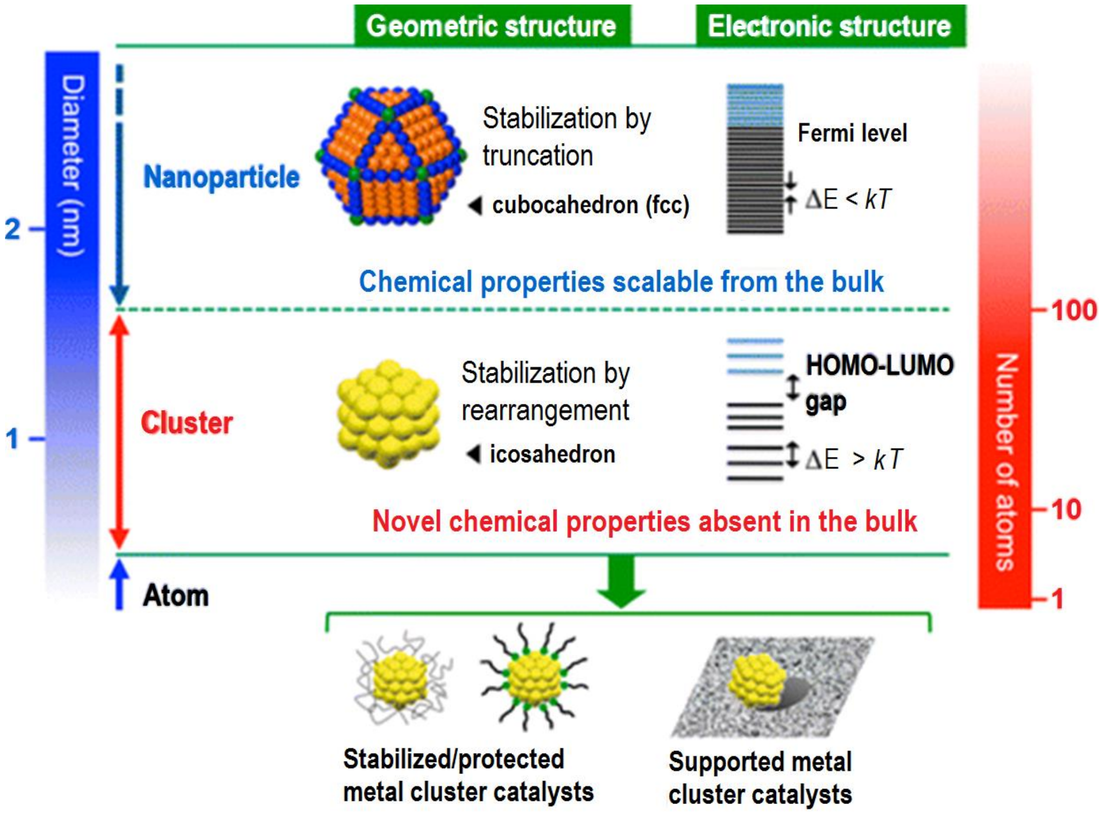

Figure 1: Development of novel catalysts based on metal clusters (reprinted from reference 7b).

Although there still has much controversy concerning the nature of the active sites of gold NCs catalysts, it has been accepted that the size, dispersion level of the nanoclusters and the interaction between Au clusters and the support are key parameters determining the performance of the supported Au NCs. Significant efforts have been invested in preparing well defined NCs, but, an in-depth understanding of the origin of the size dependence of nanogold catalysts is still lacking and identification of active species is difficult due to the wide size distribution of conventional nanoclusters.

1.2 Activity of gold nanocusters in catalysis

It has been reported that the high activity of nanocatalysts is attributed to several important factors, including the high surface-to-volume ratio, surface geometric effect (e.g., surface atom arrangement and low-coordinated atoms), the electronic effect, as well as the quantum size effect and interaction with the supporting material.[28] The properties of Au NCs differ significantly from their behavior in bulk condition because on reducing a matter to the nanoscale, its relative surface area increases and the size-dependent properties begin to dominate. It is known that the size of the Au NCs is one of the key factors for the catalytic activity and selectivity in the aerobic oxidation reactions[22] and that the best performance is exhibited by the small gold clusters (2-10 nm). In this context, the efficient catalytic activity of gold nanoparticles supported on inorganic oxides has attracted increased interest since the pioneering work of Haruta and co-workers.[10] A series of publications relating CO oxidation by gold[29–45,12] had opened up the opportunity to other reactions of practical interest such as selective alcohol and olefin oxidations,[46–53,13] C–C coupling reactions,[54-57] water gas shift,[58] direct synthesis of hydrogen peroxide from H_2 and O_2,[59] and selective hydrogenations of olefins[60–63] and aldehydes.[64–68]

It has been suggested that the increasing activity of gold catalysts with decreasing gold particle size is related to the higher concentration of low coordinated gold atoms in the smallest particles. For example, the activity for hydrogenation of gold catalysts is directly related to the number of low coordinated gold atoms[69,70] where H_2, as well as other reactants like O_2, CO or NO, are more strongly adsorbed and activated. Especially, there are several reports concerning the higher catalytic activity of gold nanoparticles supported on reducible oxides such as TiO_2, Fe_2O_3 or CeO_2.[10,29–33,36,37,71] Supported gold catalysts are exceptionally active for several reactions, however, to understand the mechanism of even relatively simple reaction such as oxidation reaction of CO is very difficult due to complex interaction of NCs with support and whether the role of the support is limited to the stabilization of small particles, to involve in the formation of cationic gold surface sites or to participate in the activation of reactants is still under debate.[72–75] Since, the nature of the active sites remains obscure (Figure 2), detailed mechanistic studies have yet to be investigated.

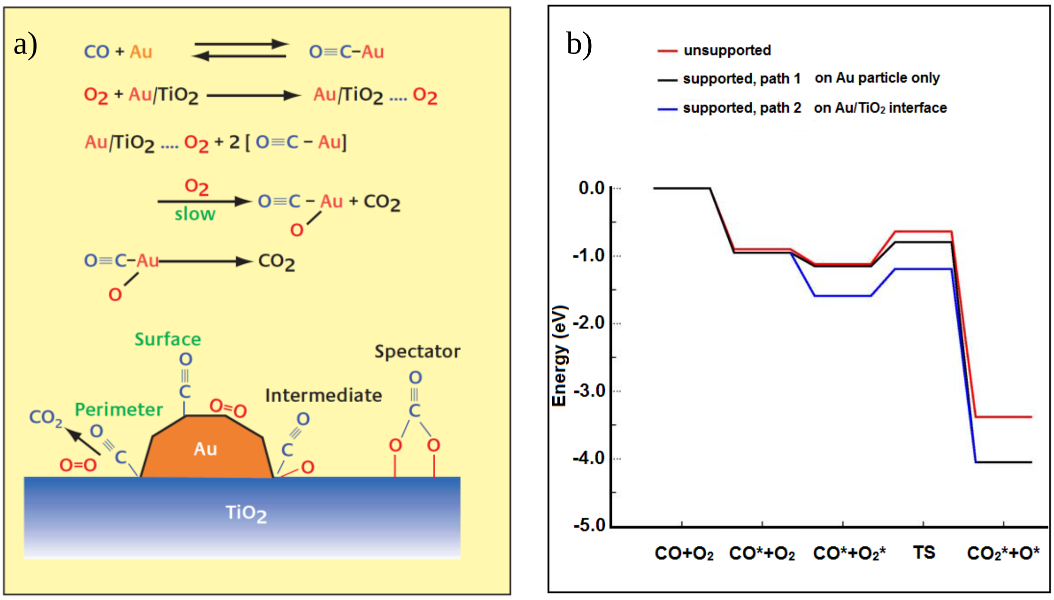

Figure 2: a) Schematic representation for CO oxidation pathways over Au/TiO_2 and possible existence of active sites b) energy profiles for the CO oxidation on a Au_{10} cluster (reprinted from reference 49).

In general, the activity of Au NCs are dependent on electronic interaction between clusters and solid support or stabilizing polymer/ligand as discussed earlier, which can be inhanced by modification of solid support or stabilizers (Figure 3). An alternative method to enhance the activity of Au NCs is impurity doping of another metal which modifies the electronic properties of Au NCs surface enhancing its activity towards several reactions. Activation of Au NCs surface directly relates to mode of adsorption and activation of molecules like O_2 or CO, which can directly participate in reaction as well as generation of more active Au sites as a result of adsorbed species. The catalysis by Au is unique, however, several concerns about nature of catalytically active site is still an unresolved problem.

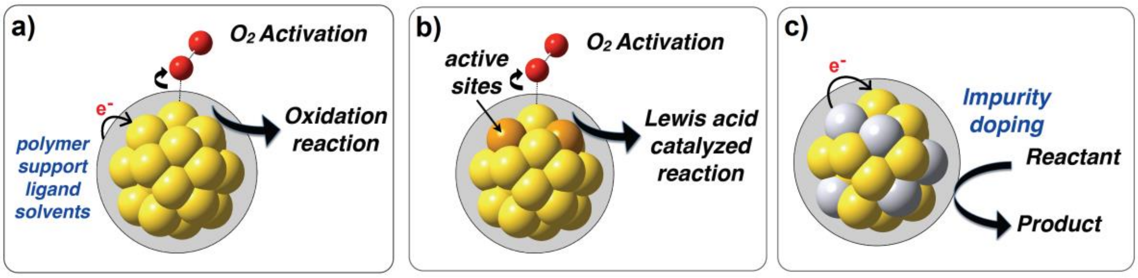

Figure 3: Schematic representation of possible routes to activate Au NCs

Selective oxidation reaction is an area in which gold can play a significant role in the development of new “green” technologies using molecular oxygen.[2,46] When dealing with oxidation reactions, one of the most important issues to be considered is O_2 activation and/or dissociation. Many experimental and theoretical studies have been carried out showing the key role played by the metal oxide or hydroxide support[76] and by special Au sites at the metal–support interface[77] to activate molecular O_2. However, there is also evidence that Au NCs supported on inert materials are able to catalyze a number of oxidation reactions, and in this case, particle size determines catalyst activity. For example, Au NCs smaller than 2 nm stabilized by poly(*N*-vinyl-2-pyrrolidone)[22] show good catalytic performance in the aerobic oxidation of alcohols.

Mechanism of O_2 activation by Au NCs is the most important but the least understood phenomenon yet, so, it must be studied in detail. Several theoretical calculations regarding activation of O_2 has been carried out specially on the model cluster representing cationic Au NCs supported on oxide such as CeO_2. The dissociative adsorption of O_2 has been considered (Figure 4) and in such mode of O_2 activation, gold support interface and particle morphology rather than particle size plays a dominating role in the catalytic properties of gold. However, it cannot be considered for all the cases because only the presence of low-coordinate Au atoms, strong adsorption of molecular oxygen on Au NCs is a necessary but not sufficient condition for O_2

dissociation, there is a critical size for Au NCs to dissociate O_2.[28b]

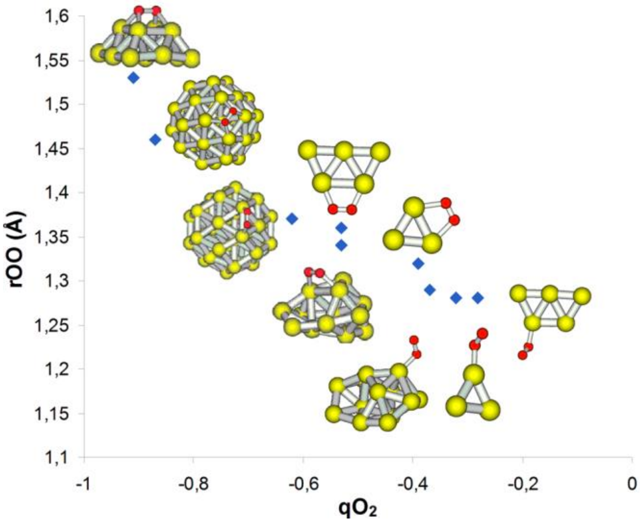

Figure 4: Optimized structures of O_2 interacting with Au_{38}, Au_{13}, Au_5, and Au_3 clusters, and correlation between optimized O–O bond length and charge transferred to O_2 (reprinted from reference 28).

On the other hand, activation of molecular O_2 by PVP stabilized small anionic gold cluster in the form of superoxide has been reported, too (Figure 5).[22,78,79] Such activated oxygen takes part directly in several oxidation reaction or helps in activation of Au NCs surface for other types of lewis acid catalyzed reactions such as oxidative homocoupling[78] and intramolecular addition of alcohol/amine to alkene.[22c,79] It is widely accepted that the activation of molecular oxygen (O_2) is a crucial step for the aerobic oxidation reaction over gold catalysts, as shown in theoretical studies.[80,81] In small Au clusters and rough surfaces, the highest occupied molecular orbital of gold is localized and its charge density sticks out in the vacuum, facilitating electron density transfer into the π*-orbital of O_2 and inducing the binding of O_2 to gold. The electronic charge transfer from gold cluster to the adsorbed O_2 in the form of peroxo- and superoxo-like species are capable of selective oxidation of many chemical substances.

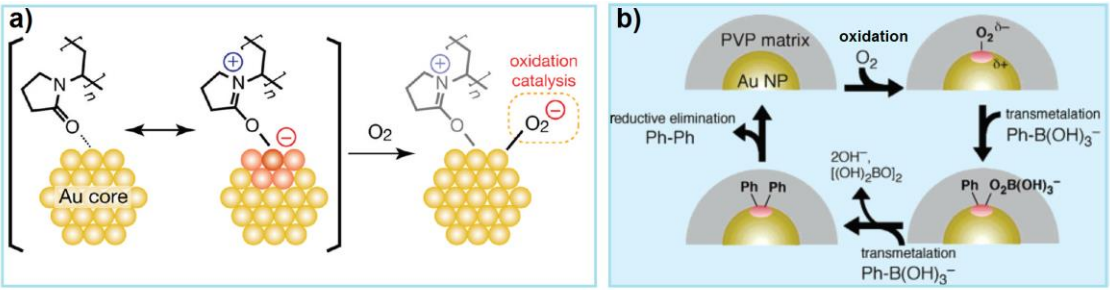

Figure 5: Mechanism for the activation of molecular oxygen by Au cluster in Au:PVP (reprinted from reference 22d and reference 78).

Therefore, it is the most important to attain atomically precise Au NCs and use such NCs as well defined catalysts. By solving the atomic structure of the NCs, precise correlation between catalytic properties and the exact atomic structure of the NCs can be made and detail information about the factors that controls the surface activation, nature of surface active sites, their structure and catalytic mechanism can be achieved. For that purpose, colloidal Au NCs stabilized by weakly coordinating polymers such as PVP has been developed as a model catalyst. The Au:PVP clusters not only work as practical *quasi*-homogenous catalysts for aerobic oxidations but also provide an ideal opportunity to address several fundamental questions regarding the nature of catalytically active sites including the reaction mechanism without considering the direct effect of stabilizer. Moreover, the convinient wet chemical method of preparing small sized (1.3-10 nm) monodispersed Au:PVP clusters enabled the study of size-dependent catalytic activity and the nature of the active sites.

Theoretical methods are capable of analyzing the possible contributions to the enhanced activity of Au NCs. Especially, density functional theory (DFT) calculations can provide a clearer insight into the activity of Au NCs. The model that represent colloidal nanogold stabilized by weakly coordinating polymer could be a simple model for obtaining the contributions from the finite size and shape effects of the gold particle without including the complicated effects from the support in a subsequent reaction steps. This will allow the easy identification of the different aspects involved in the catalysis by gold and provide the detail information about the contributions of the different factors such as structure and composition of the system.

1.3 Colloidal gold nanocusters in catalysis

Metal NCs can be stabilized by polymers through the steric bulk of their framework. Polymers play the role of ligand by weakly coordinating to the cluster surface through heteroatoms.[82] In the core/shell metal NCs, a polymer layer may be physically[83] or chemically[84] bound to metal core. Polymer-stabilized metal NCs are homogenously dispersed in reaction medium with reactant and products, hence known as *quasi*-homogenous catalyst. Au NCs which are *quasi*-homogenously dispersed in medium has attracted tremendous interest of researchers due to their high catalytic activities and selectivities towards the desired product. The coordinatively unsaturated metal atoms in the cluster are exposed for catalysis, hence, strongly bound protective agents hinder the reaction site.[85]

In order to understand the origin of catalysis and the reaction mechanism, Au clusters stabilized by weakly interacting polymers such as PVP were developed. This model catalyst is free of any noticeable influence from the stabilizer on the intrinsic properties of the clusters. Through a series of publications it has been demonstrated that the Au NCs stabilized by a hydrophilic polymer PVP (Au:PVP) clusters dispersed in water act as real-world catalysts under mild conditions for aerobic oxidations, homocoupling of arylboronic acids, H_2O_2 formation from ammonium formate[22,78,86] and so on (Figure 6). The protective agent such as PVP not only has a major role to stabilize the gold cluster protecting from agglomeration but also has an additional role to donate electron for Au clusters. After careful characterization of Au:PVP, it was revealed that Au clusters are negatively charged by electron donation from PVP, due to which it act as ideal catalyst for aerobic oxidation reactions. It has been proposed that a superoxo-like species generated by adsorption of molecular oxygen on the cluster surface plays a key role in these oxidation reactions. The hetero-junction effect between PVP and gold clusters has been theoretically studied by Okumura *et al.*[87,88] as an electron donor to the gold clusters, whose catalytic activity is affected by the adsorbed PVPs.

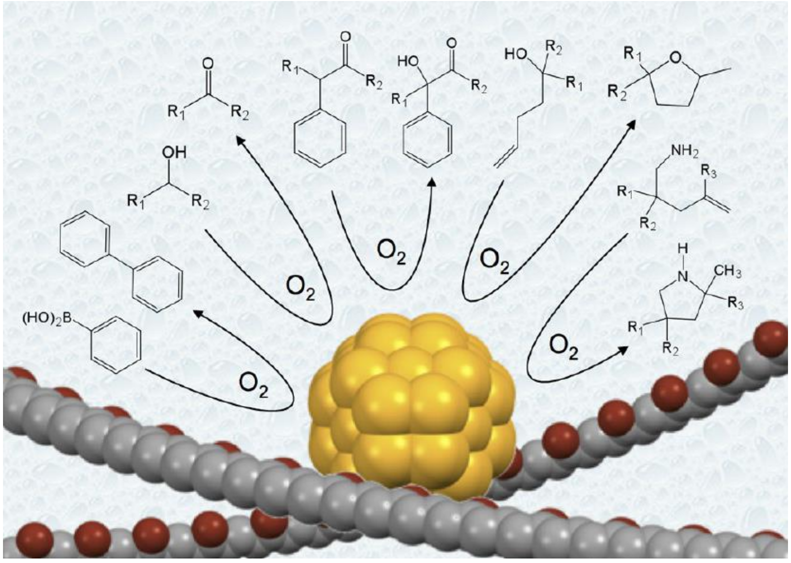

Figure 6: Oxidation reactions catalyzed by Au:PVP (reprinted from reference 7b).

1.4 Bimetallic nanoclusters

Bimetallic NCs, composed of two distinct metal elements, are emerging as a new class of materials.[89] They usually show a combination of the properties associated with two different metals.[90] Bimetallic NCs are of wide interest since they lead to many interesting size-dependent electrical, chemical, and optical properties and are particularly important in the field of catalysis because, going from monometallic to bimetallic nanoparticles there is a great enhancement in specific physical and chemical properties of bimetallic NCs due to synergistic effects.[91] Gold is very useful as an alloying metal and has been used in conjunction with various metals such as palladium and platinum due to their similar lattice constants. The structure of bimetallic combination (Figure 7) depends mainly on the preparation conditions and the miscibility of the two components.

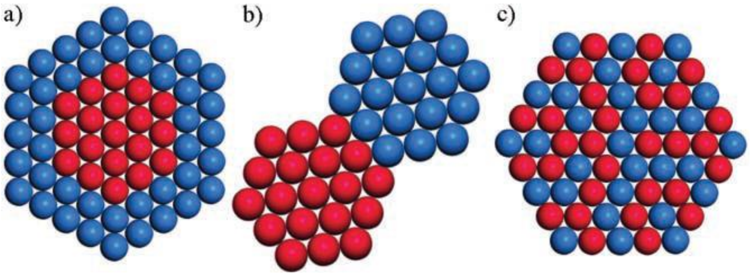

Figure 7: Bimetallic NCs with different structures: a) core/shell, b) heterostructure; c) intermetallic or alloyed structures. (reprinted from reference 92).

Alloys are an important class of catalysts as they exhibit enhanced catalytic activities and selectivities as compared with their single-metal constituents (Figure 7).[93] Among alloy catalysts, Pd–Au has received a great deal of attention because of its superior activity in a number of reactions.[94-97] Alloying induces multiple changes in the physical and chemical properties of the metallic components that are directly concerned with the catalytic properties. Two alloy effects are significant: (1) ensemble effects, i.e., a finite number of atoms in a particular geometric orientation that are required for facilitating a particular catalytic process; and (2) ligand effects, i.e., electronic modifications resulting from hetero-nuclear metal–metal bond formation. Furthermore, bimetallization can result in stabilization of nanoclusters when one metal acts as stabilizer for the another, preventing aggregation (Figure 8).[96f] Such stabilization effect is scarcely understood experimentally and theoretically.

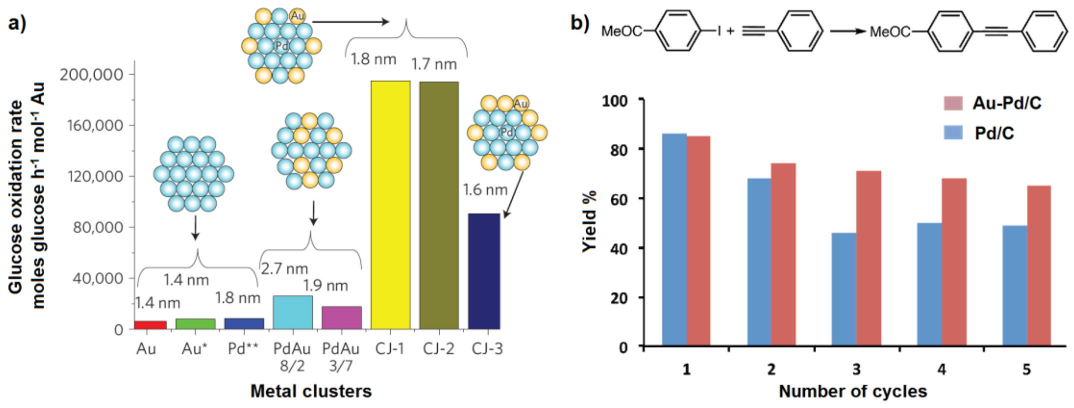

Figure 8: a) Comparison of the catalytic activity of Au/Pd, Au, Pd and Pd/Au alloy NCs for aerobic glucose oxidation (reprinted from reference 95a), b) recycling study for sonogashira cross coupling reaction.

1.5 Objectives

Theoretical modeling is a powerful tool to get information about fundamental aspects of catalysis, such as identification of active sites in catalysts and determination of reaction mechanisms. A detailed knowledge of the mode of adsorption and activation of reactants and reaction intermediates, of the energy barriers that have to be overcome, and the nature of the active sites involved in each elementary step of the overall process, including the desired reaction and the competing routes leading to byproducts, is necessary to design highly selective catalysts. So, the objective of this thesis is to analyze the origin of high catalytic activity and to investigate nature of the active sites generated on small unsupported Au NCs due to adsorption of molecular oxygen, and to establish their role in reactions of fundamental and industrial interest such as alcohol oxidation and homocoupling of phenylboronic acid from a theoretical point of view. The common feature of these apparently different reactions is that they are catalyzed by Au NCs smaller than 2 nm in the presence of molecular O_2, suggesting that similar active species might be involved. In addition, a comprehensive study to illustrate the origin of several bimetallic effects and its mechanism that cause difference in catalytic activity of bimetallic NCs compared to monometallic ones is another goal of this thesis. A detailed mechanistic study that addresses the influence of the gold cluster size and morphology in the nature of active site is helpful to design a new generation of more active gold catalysts.

1.6 References

[1] a) B. Armer, H. Schmidbaur, *Organogoldchemie. Angew. Chem.* **1970**, *82*, 120. b) G. C. Bond, *Gold Bull.* **1972**, *5*, 11. c) B. Hammer, J. K. Nørskov, *Nature* **1995**, 376, 238

[2] a) J. J. Pireaux, M. Chtaïb, J. P. Delrue, P. A. Thiry, M. Liehr, R. Caudano, *Surf. Sci.* **1984**, *141*, 211. b) N. Saliba, D. H. Parker, B. E. Koel, *Surf. Sci.* **1998**, *410*, 270. c) J. Wang, B. E. Koel, *J. Phys. Chem. A* **1998**, *102*, 8573.

[3] L. McEwana , M. Juliusa, S. Robertsa, J. C. Q. Fletcher, *Gold Bull.*, **2010**, *43*, 298.

[4] A. G. Sault, R. J. Madix, C. T. Campbell, *Surf. Sci.* **1986**, *169*, 347.

[5] B. Hammers, J. K. Nørskov, *Nature* **1995**, *376*, 238.

[6] R. F. Service, *Science* **2004**, *304*, 1732.

[7] a) C. N. R. Rao, A. K. Cheetham, *J. Mater. Chem.* **2001**, 11, 2887. b) S. Yamazoe, K. Koyasu, T. Tsukuda, *Acc. Chem. Res.* **2014**, *47*, 816.

[8] G. C. Bond, P. A. Sermon, G. Webb, D. A. Buchanan and P. B. Wells, *J. Chem. Soc., Chem. Commun.* **1973**, 444.

[9] G. J. Hutchings, *J. Catal.* **1985**, *96*, 292.

[10] M. Haruta, T. Kobayashi, H. Sano, N. Yamada, *Chem. Lett.* **1987**, *16*, 405.

[11] L. Prati and M. Rossi, *J. Catal.* **1998**, *176*, 552.

[12] a) S. E. Davis, M. S. Ide, R. J. Davis, *Green Chem.* **2013**, *15*, 17. b) M. Haruta, *Nature* **2005**, *437*, 1098. c) A. Corma, P. Serna, *Science* **2006**, *313*, 332. d) A. S. K.

Hashmi, G. J. Hutchings, *Angew. Chem.* **2006**, *118*, 8064. e) A. S. K. Hashmi, G. J. Hutchings, *Angew. Chem. Int. Ed.* **2006**, *45*, 7896.

[13] A. Abad, C. Almela, A. Corma, H. García, *Chem. Commun.* **2006**, 3178.

[14] C. D. Pina, E. Falletta, M. Rossi, *Chem. Soc. Rev.* **2012**, *41*, 350.

[15] A. Corma, P. Serna, *Science* **2006**, *313,* 332.

[16] M. Pan, H. C. Ham, W. Y. Yu, G. S. Hwang, C. B. Mullins, *J. Am. Chem. Soc.* **2013**, *135,* 436.

[17] M, Pan, Z. D. Pozun, A. J. Brush, G. Henkelman, C. B. Mullins, *ChemCatChem* **2012**, *4*, 1241.

[18] M. Pan, A. J. Brush, Z. D. Pozun, H. C. Ham, W. Y. Yu, G. Henkelman, G. S. Hwang, C. B. Mullins, *Chem. Soc. Rev.* **2013**, *42*, 5002.

[19] Y. Maeda, Y. Iizuka, M. Kohyama, *J. Am. Chem. Soc.* **2013**, *135*, 906.

[20] Z. Wu, S. Zhou, H. Zhu, S. Dai, S. H. Overbury, *J. Phys. Chem. C* **2009**, *113*, 3726.

[21] M. Bandini, *Chem. Soc. Rev.* **2011**, *40*, 1358.

[22] a) T. Tsukuda, H. Tsunoyama, H. Sakurai, *Chem. Asian J.* **2011**, *6*, 736. b) H. Tsunoyama, H. Sakurai, Y. Negishi, T. Tsukuda, *J. Am. Chem. Soc.* **2005**, *127*, 9374. c) I. Kamiya, H. Tsunoyama, T. Tsukuda, H. Sakurai, *Chem. Lett.* **2007**, *36*, 646. d) H. Tsunoyama, N. Ichikuni, H. Sakurai, T. Tsukuda, *J. Am. Chem. Soc.* **2009**, *131*, 7086.

[23] F. Shi, Q. Zhang, Y. Ma, Y. He, Y. Deng, *J. Am. Chem. Soc.* **2005**, *127*, 4182.

[24] C. Y. Ma, Z. Mu, J. J. Li, Y. G. Jin, J. Cheng, G. Q. Lu, Z. P. Hao and S. Z. Qiao, *J. Am. Chem. Soc.* **2010**, *132*, 2608.

[25] Y. Guan and E. J. M. Hensen, *Appl. Catal. A* **2009**, *361*, 49.

[26] Z. Wang, J. Zhang, Z. Yin, S. Wu, D. Mandler, H. Zhang, *Nanoscale* **2012**, *4*, 2728.

[27] Z. Zanolli, R. Leghrib, A. J. Felten, Pireaux, E. Llobet and J. C. Charlier, *ACS*

Nano **2011**, *5*, 4592.

[28] a) M. Boronat, A. Leyva-Pérez, A. Corma, *Acc. Chem. Res.* **2014**, *47*, 834. b) A. Roldan, S. Gonzalez, J. M. Ricart, F. Illas, *ChemPhysChem* **2009**, *10*, 348.

[29] M. Haruta, *Catal. Today* **1997**, *36*, 153.

[30] M. Valden, X. Lai, D. W. Goodman, *Science* **1998**, *281*, 1647.

[31] M. S. Chen, D. W. Goodman, *Science* **2004**, *306*, 252.

[32] G. C. Bond, D. T. Thomson, *Catal. Rev. Sci. Eng.* **1999**, *41*, 319.

[33] G. C. Bond, D. T. Thomson, *Gold Bull.* **2000**, *33*, 41.

[34] G. J. Hutchings, *Gold Bull.* **2004**, *37*, 3.

[35] G. J. Hutchings, *Catal. Today* **2005**, *100*, 55.

[36] S. Carretin, P. Concepci´on, A. Corma, J. M. L´opez-Nieto and V. F. Puntes, *Angew. Chem. Int. Ed.* **2004**, *43*, 2538.

[37] J. Guzman, S. Carrettin, A. Corma, *J. Am. Chem. Soc.* **2005**, *127*, 3286.

[38] B. Schumacher, Y. Denkwitz, V. Plzak, M. Kinne, R. J. Behm, *J. Catal.* **2004**, *224*, 449.

[39] N. Weiher, A. M. Beesley, N. Tsapatsaris, L. Delannoy, C. Louis, J. A. van Bokhoven, S. L. M. Schroeder, *J. Am. Chem. Soc.* **2007**, *129*, 2240.

[40] H. Hakkinen, S. Abbet, A. Sanchez, U. Heiz, U. Landman, *Angew. Chem. Int. Ed.* **2003**, *42*, 1297.

[41] G. J. Wang and B. Hammer, *Phys. Rev. Lett.* **2006**, *97*, 136107.

[42] N. L´opez, T. V. J. Janssens, B. S. Clausen, Y. Xu, M. Mavrikakis, T. Bligaard, J. K. Nørskov, *J. Catal.* **2004**, *223*, 232.

[43] I. N. Remediakis, N. Lopez, J. K. Nørskov, *Angew. Chem. Int. Ed.* **2005**, *44*, 1824.

[44] N. C. Hern´andez, J. F. Sanz, J. A. Rodriguez, *J. Am. Chem. Soc.* **2006**, *128*, 15600.

[45] T. V. W. Janssens, B. S. Clausen, B. Hvolbaek, H. Falsig, C. H. Christensen, T.

Bligaard, J. K. Nørskov, *Top. Catal.* **2007**, *44*, 15.

[46] M. Comotti, C. Della Pina, R.Matarrese, M. Rossi, *Angew. Chem. Int. Ed.* **2004**, *43,* 5812.

[47] D. I. Enache, J. K. Edwards, P. Landon, B. Solsona-Espriu, A. F. Carley, A. A. Herzing, M. Watanabe, C. J. Kiely, D. W. Knight, G. J. Hutching, *Science* **2006**, *311*, 362.

[48] A. Abad, C. Almela, A. Corma, H. Garc´ıa, *Chem. Commun.* **2006**, 3178.

[49] a) M. Haruta, *J. New. Mat. Electrochem. Systems* **2004**, *7*, 163. b) I. N. Remediakis, N. Lopez, J. K. Nørskov, *Applied Catalysis A: General* **2005**, *291*, 13.

[50] M. D. Hughes, Y. J. Xu, P. Jenkins, P. McMorn, P. Landon, D. I. Enache, A. F. Carley, G. A. Attard, G. J. Hutchings, F. King, E. H. Stitt, P. Johnston, K. Griffin, C. J. Kiely, *Nature* **2005**, *437*, 1132.

[51] T. A. Nijhuis, T. Visser, B. M.Weckhuysen, *Angew. Chem. Int. Ed.* **2005**, *44*, 1115.

[52] A. M. Joshi, W. N. Delgass, K. T. Thomson, *J. Phys. Chem. C* **2007**, *111*, 7841.

[53] J. J. Bravo-Ju´arez, K. K. Bando, J. Lu, M. Haruta, T. Fujitani, T. Oyama, *J. Phys. Chem. C* **2008**, *112*, 1115.

[54] A. S. K. Hashmi, J. P. Weyrauch, M. Rudolph and E. Kurpejovic, *Angew. Chem., Int. Ed.* **2004**, *43*, 6545.

[55] S. Carrettin, J. Guzman, A. Corma, *Angew. Chem. Int. Ed.* **2005**, *44*, 2242.

[56] C. Gonz´alez-Arellano, A. Corma, M. Iglesias, F. S´anchez, *Chem. Commun.* **2005**, 3451.

[57] C. Gonz´alez-Arellano, A. Abad, A. Corma, H. Garc´ıa,M. Iglesias, F. S´anchez, *Angew. Chem. Int. Ed.* **2007**, *46*, 1536.

[58] Q. Fu, H. Saltsburg, M. Flytzani-Stephanopoulos, *Science* **2003**, *301*, 935.

[59] J. K. Edwards, B. Solsona, N. N. Edwin, A. F. Carley, A. A. Herzing, C. J. Kiely, G.

J. Hutchings, *Science* **2009**, *323*, 1037.

[60] J. Jia, K. Haraki, J. N. Kondo, K. Domen, K. Tamaru, *J. Phys. Chem. B* **2000**, *104*, 11153.

[61] T. V. Choudhary, C. Sivadinarayana, A. K. Dayte, D.Kumar, D. W. Goodman, *Catal. Lett.* **2003**, *86*, 1.

[62] M. Neurock, D. H. Mei, *Top. Catal.* **2002**, *20*, 5.

[63] D. H. Mei, E. W. Hansen, M. Neurock, *J. Phys. Chem. B* **2003**, *107*, 798.

[64] S. Schimpf, M. Lucas, C. Mohr, U. Rodemerck, A. Bruckner, J. Radnik, H. Hofmeister, P. Claus, *Catal. Today* **2002**, *72*, 63.

[65] C. Mohr, H. Hofmeister, J. Radnik, P. Claus, *J. Am. Chem. Soc.* **2003**, *125*, 1905.

[66] J. E. Bailie, G. J. Hutchings, *Chem. Commun.* **1999**, 2151.

[67] C. Milone, M. L. Tropeano, G. Guline, G. Neri, R. Ingoglia, S. Galvagno, *Chem. Commun.* **2002**, 868.

[68] R. Zanella, C. Louis, S. Giorgio, R. Touroude, *J. Catal.* **2004**, *223*, 328.

[69] I. N. Remediakis, N. Lopez, J. K. Norskov, *Angew. Chem.* **2005**, *44*, 1824.

[70] S. N. Rashkeev, A. R. Lupini, S. H. Overbury, S. J. Pennycook, S. T. Pantelides, *Phys. Rev.* **2007**, *76*, 035438.

[71] T. Risse, S. K. Shaikhutdinov, N. Nilius, M. Sterrer, H. J. Freund, *Acc. Chem. Res.* **2008**, *41*, 949.

[72] M. M. Schubert, S. Hackenbertg, A. C. van Veen, M. Muhler, V. Plzak, J. Behm, *J. Catal.* **2001**, *197*, 113.

[73] Z. P. Liu, P. Hu, A. Alavi, *J. Am. Chem. Soc.* **2002**, *124*, 14470.

[74] G. J. Wang, B. Hammer, *Top. Catal.* **2007**, *44*, 49.

[75] S. Laursen, S. Linic, *J. Phys. Chem. C* **2009**, *113*, 6689.

[76] T. Takei, I. Okuda, K. K. Bando, T. Akita, M. Haruta, *Chem. Phys. Lett.* 2010, *493*,

207.

[77] a) A. A. Herzing, C. J. Kiely, A. F. Carley, P. Landon, G. J. Hutchings, *Science* 2008, *321*, 1331. b) D. Widmann, R. J. Behm, *Angew. Chem. Int. Ed.* doi:10.1002/ anie.201102062. c) M. Haruta, *Chem. Rec.* **2003**, 3, 75. d) J. A. Rodriguez, L. Feria, T. Jirsak, Y. Takahashi, K. Nakamura, F. Illas, *J. Am. Chem. Soc.* **2010**, 132, 3177.

[78] a) H. Tsunoyama, H. Sakurai, N. Ichikuni, Y. Negishi, T. Tsukuda, *Langmuir* **2004**, *20*, 11293. b) H. Sakurai, H. Tsunoyama, T. Tsukuda, *J. Organomet. Chem*. **2007**, *692*, 368. c) R. N. Dhital, A, Murugadoss, H. Sakurai, *Chem. Asian J.* **2012,** *7,* 55-59.

[79] H. Kitahara, H. Sakurai, *Chem. Lett.* **2010**, *39*, 46.

[80] R. Coquet, K. L. Howard, D. J. Willock, *Chem. Soc. Rev.* **2008**, *37*, 2046.

[81] L. M. Molina, B. Hammer, *Appl. Catal. A: General* **2005**, *291*, 21.

[82] D. Astruc, F. Lu, J. R. Aranzaes, *Angew. Chem. Int. Ed.* **2005**, *44*, 7852.

[83] a) S. Mössmer, J. P. Spatz, M. Möller, T. Aberle, J. Schmidt, W. Burchard, *Macromolecules* **2000**, *33*, 4791. b) N. N. Kariuki, L. Han, K. Ly, M. J. Patterson, M. M. Maye, G. Liu, C.-J. Zhong, *Langmuir* **2002**, *18*, 8255. c) M. Filali, M. A. R. Meier, U. Schubert, J.-F. Gohy, *Langmuir* **2005**, *21*, 7995.

[84] a) S. Nuss, H. Böttcher, H. Wurm, M. L. Hallensleben, *Angew. Chem. Int. Ed.* **2001**, *40*, 4016. b) K. Ohno, K. Koh, Y. Tsujii, T. Fukuda, *Macromolecules* **2002**, *35*, 8989. c) H. Zhao, X. Kang, L. Liu, *Macromolecules* **2005**, *38*, 10619. d) M. K. Corbierre, N. S. Cameron, M. Sutton, S. G. J. Mochrie, L. B. Lurio, A. Ruhm, R. B. Lennox, *J. Am. Chem. Soc.* **2001**, *123*, 10411.

[85] A. Kudelski, *Langmuir* **2003**, *19*, 3805

[86] H. Sakurai, H. Tsunoyama, T. Tsukuda, *Trans. Mater. Res. Soc. Jpn.* **2006**, *31*, 521.

[87] M. Okumura, Y. Kitagawa, T. Kawakami, *Int. J. Quantum. Chem.* **2010**, *110*, 2903.

[88] M. Okumura, Y. Kitagawa, T. Kawakami, M. Haruta, *Chem. Phys. Lett.* **2008**, *459*, 133.

[89] a) J. A. Rodriguez, D. W. Goodman, *Science* **1992**, *257*, 897. b) M. Jaime, R. Movshovich, G. R. Stewart, W. P. Beyermann, M. G. Berisso, M. F. Hundley, P. C. Canfield, J. L. Sarrao, *Nature* **2000**, *405*, 160.

[90] a) K. Gschneidner, A. Russell, A. Pecharsky, J. Morris, Z. H. Zhang, T. Lograsso, D. Hsu, C. H. C. Lo, Y. Y. Ye, A. Slager, D. Kesse, *Nature Mater.* **2003**, *2*, 587. b) T. Krenke, E. Duman, M. Acet, E. F. Wassermann, X. Moya, L. Manosa, A. Planes, *Nature Mater.* **2005**, *4*, 450.

[91] a) S. E. Habas, H. Lee, V. Radmilovic, G. A. Somorjai, P. Yang, *Nature Mater.* **2007**, *6*, 692. b) D. Xu, Z. P. Liu, H. Z. Yang, Q. S. Liu, J. Zhang, J. Y. Fang, S. Z. Zou, K. Sun, *Angew. Chem. Int. Ed.* **2009**, *48*, 4217. c) B. D. Adams, G. Wu, S. Nigro, A. Chen, *J. Am. Chem. Soc.* **2009**, *131*, 6930.

[92] D. Wang, Y. Li, *Adv. Mater.* **2011**, *23*, 1044.

[93] C. W. Yi, K. Luo, T. Wei, D. W. Goodman, *J. Phys. Chem. B* **2005**, *109*, 18535.

[94] a) F. Gao, Y. L. Wang, D. W. Goodman, *J. Am. Chem. Soc.* **2009**, *131*, 5734. b) J. K. Edwards, B. E. Solsona, P. Landon, A. F. Carley, A. Herzing, C. J. Kiely, G. J. Hutchings, *J. Catal.* **2005**, *236*, 69. c) T. Gracia, S. Agouram, A. Dejoz, J. F. Sanchez-Royo, L. Torrente-Murciano, B. Solsona, *Catal. Today* **2014**, doi: 10.1016/j.cattod.2014.03.039. d) M. O. Nutt, K. N. Heck, P. Alvarez, M. S. Wong, *Appl. Catal. B* **2006**, *69*, 115. e) N. E. Kolli, L. Delannoy, C. Louis, *J. Catal.* **2013**, *297*, 79. f) X. Liu, R. S. Ding, L. He, Y. M. Liu, Y. Cao, H. Y. He, K. N. Fan, *Chem. Sus. Chem*. **2013**, *6*, 604. g) J. Long, H. Liu, S. Wu, S. Liao, Y. Li, *ACS Catal.* **2013**, *3*, 647. h) N. Toshima, *Macromol. Sci. Chem.* **1990**, *27*, 1225. i) M. Chen, D. Kumar, C.-W. Yi, D. W. Goodman, *Science* **2005**, *310*, 291.

[95] a) H. Zhang, T. Watanabe, M. Okumura, M. Haruta, N. Toshima, *Nat. Mater.* **2012**, *11*, 49. b) Y. Hong, X. Jing, J. Huang, D. Sun, -W. Y. Odoom, F. Yang, M. Du, Q. Li, *Sustainable Chem. Eng.* **2014**, *2*, 1752. c) M. B. Griffin, A. A. Rodriguez, M. M. Montemore, J. R. Monnier, C. T. Williams, J. W. Meldin, *J. Catal.* **2013**, *307*, 111.

[96] a) N. K. Chaki, H. Tsunoyama, Y. Nigishi, H. Sakurai, T. Tsukuda, *J. Phys. Chem. C* **2007**, *111*, 4885. b) S. S. Yudha, R. N. Dhital, H. Sakurai, *Tetrahedron Lett.* **2011**, *52*, 2633. c) O. Sophiphun, J. Wittayakun, R. N. Dhital, S. Haesuwannakij, A. Murugadoss, H. Sakurai, *Aust. J. Chem.* **2012**, *65*, 1238. d) A. Murugadoss, K. Okumura, H. Sakurai, *J. Phys. Chem. C* **2012**, *116*, 26776. e) D. Wang, A. Villa, F. Porta, L. Prati, D. Su, *J. Phys. Chem. C* **2008**, *112*, 8617. f) C. Rossy, J. Majimel, E. Fouquet, C. Delacôte, M. Boujtita, C. Labrugère, M. Tréguer-Delapierre, F.-X. Felpin, *Chem. Eur. J.* **2013**, *19*, 14024. g) H. B. Liu, U. Pal, A. Medina, C. Maldonado, J. A. Ascencio, *Phys. Re*v. *B* **2005**, *71*, 075403. h) J. Cai, Y. Y. Ye, *Phys. Re*v. *B* **1996**, *54*, 8398. i) M.-L. Wu, D.-H. Chen, T.-C Huang, *Langmuir* **2001**, *17*, 3877.

[97] a) R. N. Dhital, C. Kamonsatikul, E. Somsook, K. Bobuatong, M. Ehara, S. Karanjit, H. Sakurai, *J. Am. Chem. Soc.* **2012**, *134*, 20250. b) R. N. Dhital, C. Kamonsatikul, E. Somsook, H. Sakurai, *Catal. Sci. Technol.* **2013**, *3*, 3030. c) R. N. Dhital, H. Sakurai, *Chem. Lett.* **2012**, *41*, 630.

Chapter 2

Investigation of Cluster Model for Reactions Catalyzed by Au:PVP through Mechanistic Study of Methanol Oxidation Reaction

2.1 Introduction

Among the different reactions, selective oxidation of alcohols to carbonylic compounds is one of the most important transformations in organic chemistry. It is the ultimate goal for metal nanocluster catalysts to be able to perform this reaction under ambient conditions at atmospheric pressure and room temperature. Au NCs stabilized on weakly coordinating porymer, solid support or other types have been found to be an effective catalyst for this reaction. In the case of solid-supported Au NCs, there are several reports about the synergetic effect between Au and metal oxide support, CeO_2 for example, which boost the catalytic activity in alcohol oxidation reaction. It was proposed that the lattice oxygen vacancies found abundantly in nanoparticulated ceria enhances the activity of the support by favouring interaction and dissociative chemisorption of molecular oxygen[1,2] that take part in reaction directly. So the mechanism of reaction is totally dependent on the type of catalyst used.

It was demonstrated that the activation of O_2 by Au/PVP is the primary step for aerobic oxidation of alcohols.[3-5] The small gold clusters with sizes of 1–5 nm shows best catalytic activity. Previous experimental and theoretical studies have revealed that cluster anions (Au_n^-) with small even-numbered ($n = 40 \leq 14$) and magic ($n = 18, 20$) sizes can generate superoxo-like species via electron transfer from the highest occupied molecular orbital (HOMO) of the gold cluster, which is negatively charged by electron donation from PVP, to the lowest unoccupied molecular orbital (LUMO) of the O_2 molecule.[6-11] This species subsequently activates the oxidation reaction of alcohol to the corresponding aldehydes and ketones, as well as carboxylic acids.[12,13] Another reaction mechanism has recently been proposed by Chechik and co-workers.[14] By using EPR spectroscopy and spin-trapping experiments, they showed that polymer encapsulated gold nanoparticles promote oxidation reaction. The hydrogen in the spin adduct (Au–H) originates from cleavage of the C–H bond in the alcohol molecule to the gold surface. The role of oxygen in this mechanism is to restore the catalytic activity rather than to oxidize the alcohol. Some theoretical investigations explain about the alcohol oxidation rection mechanism on the basis of dissociative adsorption of molecular oxygen on Au surface forming surface oxide like species.[2b] Nevertheless, the electronic mechanism or reaction pathway of aerobic oxidation remains a subject of considerable debate (Figure 1) and is yet to be fully understood. So detailed investigation of reaction mechanism is necessary and for that purpose selection of suitable model of the Au cluster that represent Au:PVP system is very important.

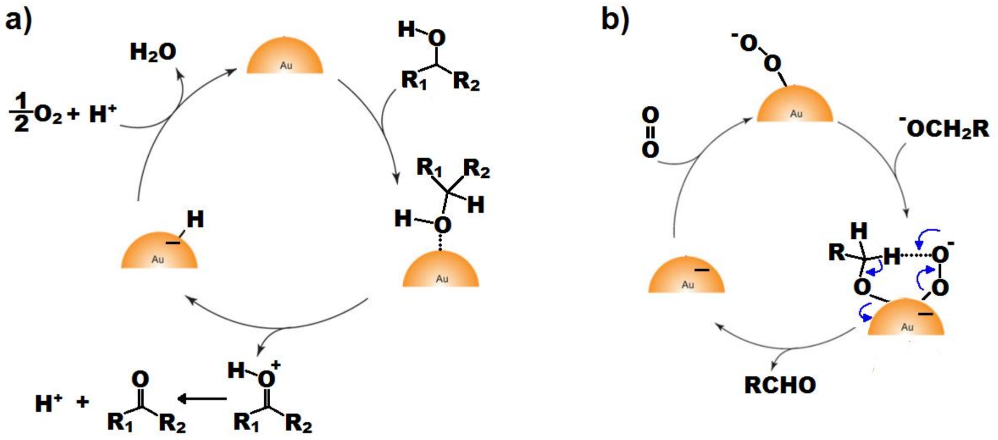

Figure 1: Proposed catalytic cycles for aerobic oxidation of alcohol indicating different role of O_2.

In this chapter, mechanism of the gold catalyzed aerobic oxidation of methanol to formic acid was systematically investigated on Au_8^- and Au_{20}^- cluster which can be regarded as a model for Au/PVP using density functional theory (DFT) to analyze the origin of high catalytic activity, especially the geometry of small gold clusters and to investigate nature of the active sites generated on the surface as a function of oxygen adsorption and to know their role in the reactions.

2.2 Calculation details

For the theoretical model of Au NC:PVP system, the anionic Au_{20} NC was used including the effects of the surrounding PVP molecules[15] on the energetics. In all our calculations, we employed a DFT with an M06 functional, which was recently recommended as a useful functional for simulating processes catalyzed by gold clusters.[16] We adopted the scalar relativistic effective core potential (ECP) with double-zeta basis sets [3s3p2d] (LANL2DZ) for all the gold atoms. This ECP treats the inner shell of gold (Xe core) as an effective potential, and treats the 19 valence electrons in the outer shell (5s5p5d6s) explicitly. The 6-31++G (d,p) basis sets were applied for the hydrogen, carbon, and oxygen atoms. Six-component d-functions were employed in all the calculations. All the ground-state optimized structures were local minima. Vibrational analysis performed on the optimized structures contained no imaginary frequencies. We performed a fully relaxed structural optimization, where the doublet spin state was maintained in this state throughout all of the calculations. Unrestricted Kohn–Sham equations were employed for open-shell systems. All of the optimized transition state structures possessed only a single imaginary frequency. All the calculations were carried out using the Gaussian 09 software package.[17]

2.3 Result and discussion

2.3.1 Geometry of Au cluster

The author selected Au_8^- and Au_{20}^- anionic gold clusters as the suitable model for the mechanistic study as these clusters show a strong decrease in its electron affinity (EA) compared to other gold clusters with up to 58 atoms (figure 1a).[18] The low EA of Au_8 and Au_{20} makes it energetically favorable for electron transfer to oxygen to occur during the aerobic oxidation process.[19] The mono anion of the gold clusters were chosen in accordance with previous studies of O_2 adsorption on Au_n^-.[19–24] Negative gold ions with an odd number of electrons bind O_2 efficiently, whereas neutral and cationic Au clusters with an odd number of electrons are inert toward O_2 (figure 1b).

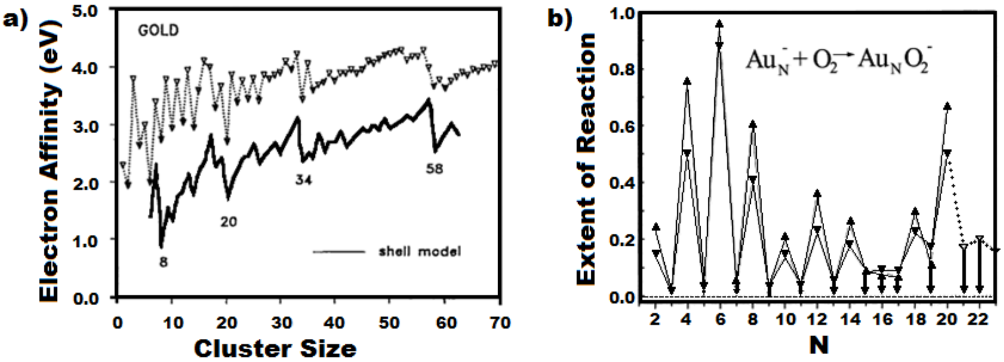

Figure 1: a) Electron affinities of $Au_{1\text{-}79}$ (reprinted from reference 18). b) Cluster-size dependence of the extent of reaction (reprinted from reference 19).

The geometric structures and mulliken charge were examined by taking into account the full structural relaxation of the gold clusters. The D2d structure for Au_{20}^- and D4h structure for Au_8^- are the most stable. This is in agreement with previous theortical and experimental findings that anionic gold clusters, Au_n^-, have planar structures for $n \leq 11$, and for $n = 12$ transition occurs from 2D to 3D structures.[25] The optimized structure shows bond lengths ranging from 2.768 Å to 2.797 Å in Au_8^- and 2.771 to 2.959 Å in Au_{20}^- which agrees well with previous experimental (2.79 Å) and theoretical studies (2.69 Å). The distribution of Mulliken charges indicates that high electron densities appear at the apex sites where the gold atoms are less coordinated (Figure 2), and the highly coordinated gold atoms have a lower electron density. Spin density is localized at the apex sites.

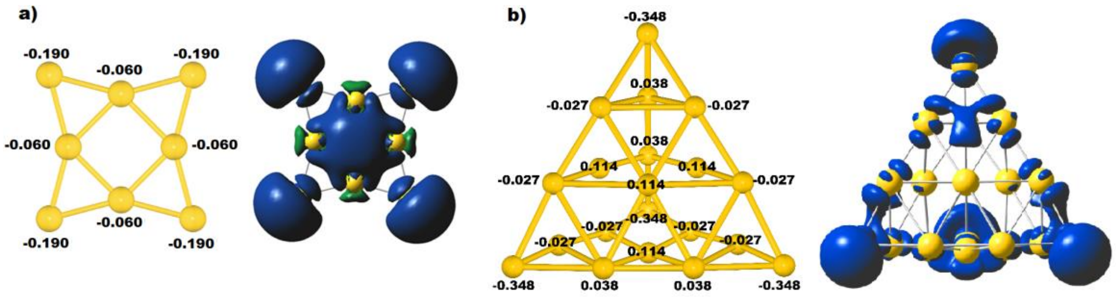

Figure 2: The optimized structure of a) Au_8^- and b) Au_{20}^- with Mulliken atomic charges and the calculated spin density isosurface.

2.3.2 Adsorption of molecular oxygen

Next, the adsorption site of O_2^- on the Au_8^- and Au_{20}^- clusters were examined. Geometry optimizations of $Au_{20}O_2^-$ were performed with the nine initial positions of O_2 (Figure 3a). The Au_{20}^- cluster have two possibilities for adsorption of O_2 on the long or short edge in the D2d structure. The fully relaxed structural optimizations was performed without any symmetry constraints for adsorption of a single O_2 on Au_{20}^- because it was experimentally found that an anionic gold cluster that adsorbs one O_2 molecule does not adsorb a second one.[19] The DFT calculations show that the adsorption energies of O_2 on Au_{20}^- are in the order of 6–17 kcal/mol (Table 1a). indicating both physisorption and chemisorption. The end-on adsorption (T1), with only one oxygen atom directly bonded to gold, has been found to be a stable adsorption complex on an apex of Au_{20}^-. This imply that O_2 adsorption site depends not only on particle size, but also on particle morphology.[14,25] The end-on adsorption has been frequently found in steps and defects involving low EA and low coordinated gold atoms.[26,27] The most stable structure belongs to adsorption at the BR1 site, which is located on the edge of Au_{20}^- and each oxygen atom in O_2 directly interacts with a gold atom; in contrast, adsorption over the FCC and HCP hollow sites is energetically unfavorable. The calculated adsorption energies at the BR1 and T1 sites are -18.1 and

-13.7 kcal/mol, respectively, while those of FCC and HCP are -2.3 and -0.9 kcal/mol, respectively. For Au_8^- cluster, T1 is the most stable adsorption complex with a calculated adsorption energy of –12.4 kcal/mol. On the other hand, the remaining optimized structures were found to be energetically unfavorable, showing that activity toward O_2 adsorption was not observed (Figure 3b, Table 1b).

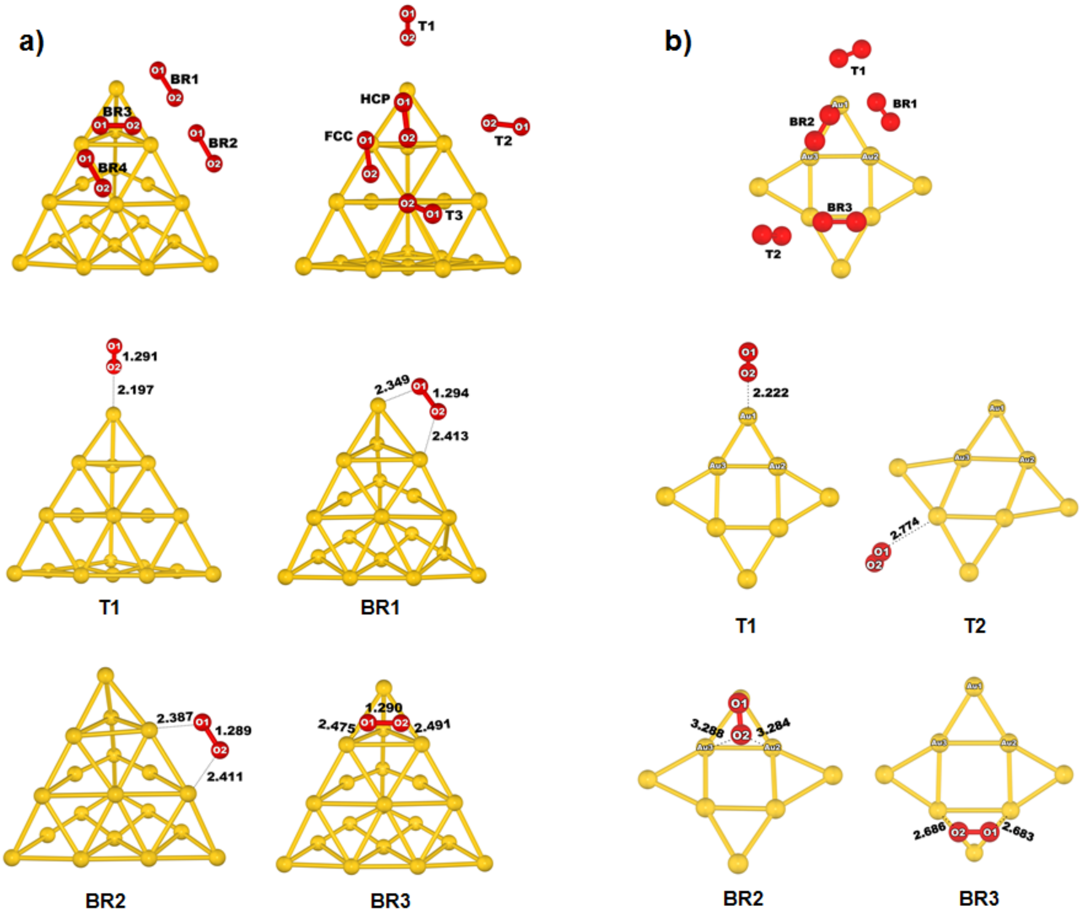

Figure 3: Initial positions of O_2 in the geometry optimization of a) $Au_{20}O_2^-$ and (b) $Au_8O_2^-$ the optimized structures with considerable adsorption energies. Distances are shown in Angstroms (Å).

Table 1: Optimized geometrical parameters, calculated adsorption energies (E_{O2}+BSSE), mulliken charge (q_{O1}, q_{O2}) and vibrational frequencies (freq.) of O–O bond for various adsorbed sites of oxygen molecules on a) Au_{20}^{-} b) Au_8^{-}

a)

Structure	O–O (Å)	$E_{O2+BSSE}$ (kcal/mol)	Freq (cm^{-1})	q_{O1}	q_{O2}
O_2	1.195	–	1705	0	0
O_2^{-}	1.322	–	1264	-0.500	-0.500
BR1	1.294	-17.0	1181	-0.275	-0.077
BR2	1.289	-4.6	1272	-0.121	0.119
BR3	1.290	-6.0	1273	-0.119	-0.120
BR4	Converge to BR1				
T1	1.291	-12.7	1235	-0.177	-0.228
T2	Converge to BR2				
T3	1.221	-1.4	1398	-0.091	-0.081
FCC	1.230	-1.3	1371	-0.071	-0.084
HCP	1.220	-0.4	1355	-0.051	-0.047

b)

Structure	Au–O (Å)	O–O (Å)	E_{O2} (kcal/mol)	freq. (cm^{-1})	q_{O1}	q_{O2}
O_2	–	1.207	–	1707	0	0
O_2^{-}	–	1.347	–	1264	-0.500	-0.500
T1	2.222	1.277	-12.4	1260	-0.145	-0.219
T2	2.774	1.226	-3.3	1467	-0.083	0.016
BR1	Converges to T1					
BR2	3.284	1.215	-4.3	1583	-0.040	0.075
BR3	2.683	1.254	6.2	1334	-0.092	-0.092

Based on the obtained results together with those reported previously,[26,28] we consider that O_2 prefers to adsorb on the edge and the apex of Au_8^{-} and Au_{20}^{-}, where high electron densities normally appear. This finding also confirms that a rough gold surface is more active for the adsorption of O_2 than a flat surface. Electron transfer accompanies the binding of O_2 to Au_{20}^{-}, as can be seen in the decrease of Mulliken charges on O_2, $\delta q = -0.275$ and -0.077 respect to free O_2 in the BR1. Consequently, the O–O bond of the adsorbed O_2 becomes longer and the vibrational frequency of the O–O bond is decreased. The O–O bond is elongated at all of the adsorption sites in between those of the experimental values of O_2 (1.207 Å) and O_2^- (1.347 Å) molecules.[29,30] The vibrational frequencies of the O–O bond are also decreased. Moreover, the Au–Au distances at the adsorption sites are slightly increased, reflecting the interaction between Au_{20}^- and O_2. The similar results for Au_8^- are shown in table 1b. At this point, one can expect that the electronic properties of the adsorbed O_2 molecule are affected by electron transfer from Au_{20}^-, resulting in the formation of superoxo-like species.

2.3.3 Cooperative adsorption with methanol

The coadsorption complexes are formed by adsorption of methoxy species, which are normally generated in high pH solution for aerobic oxidation catalyzed by polymer-stabilized gold clusters and O_2 on an Au_8^- and Au_{20}^- clusters.[5,12] The reason for using the methoxy species is that experimentally, the primary and secondary aliphatic alcohols were readily converted into the corresponding carboxylic acids and ketones, respectively, only in the high pH conditions.[31] None of the reactions proceeded in the absence of a base, in contrast to palladium or platinum-based catalysts indicating a different reaction mechanism and the oxidative addition of methanol on Au/PVP is also not favoured.

For Au_{20}^-, four of the most stable O_2 adsorption structures, BR1, BR2, BR3 and T1, were considered to study cooperative adsorption for the subsequent oxidation reaction Three structures A1–A3 are possible in the overall reaction (Figure 4 and Table 2), with the coadsorption energies ranging from -26 to -29 kcal/mol. At the local minima of the coadsorption, oxygen molecule keeps its molecular form and dissociative adsorption into atomic oxygen was not found. The coadsorption structures between methoxy species and O_2 located at the same apex site, A1–A3, in show a pronounced cooperative effect in the activation of molecular oxygen. These coadsorptions cause a modification of the electronic properties of O_2. The O–O bond lengths of the adsorbed O_2 are elongated from 1.289–1.294 Å to 1.351 Å and the corresponding vibrational frequencies of the O–O bonds are slightly decreased compared with those obtained for $Au_{20}O_2^-$. The Mulliken charges on O_2 are also increased. In contrast, the coadsorption complexes in which methoxy species and O_2 were located at different apex sites or the high coordinated gold atom do not show such an effect. This suggests that in the former case, the interaction between methoxy species and Au_{20}^- does not induce O_2 bond dissociation; rather, it exhibits electronic charge transfer from Au_{20}^- to O_2, resulting in the molecular adsorption of O_2 on Au_{20}^- with the superoxo state that could facilitate the oxidation of methoxy species.

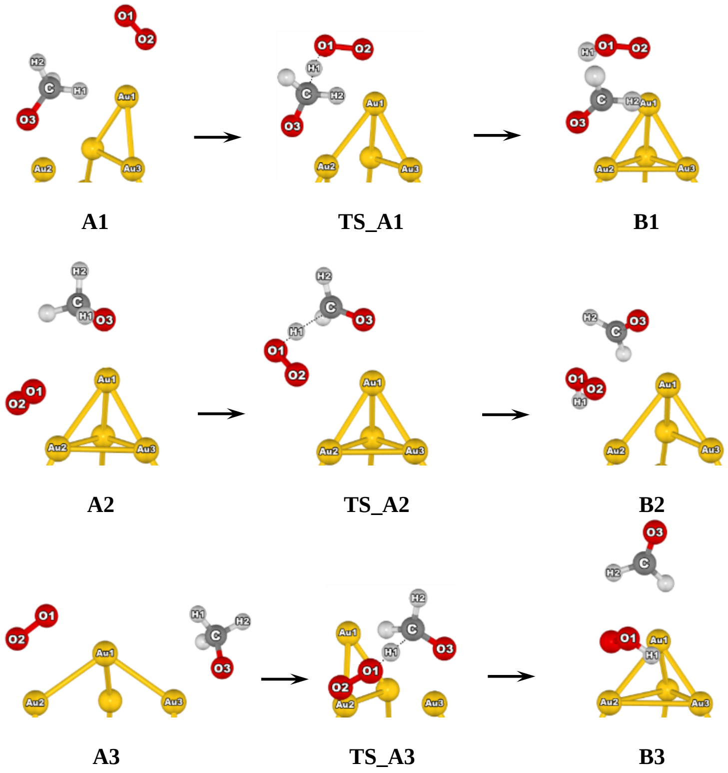

Figure 4: Possible reaction pathways from methoxy species to formaldehyde on $Au_{20}O_2^-$ (kcal/mol).

Table 2: Calculated energies (kcal/mol) of adsorption complexes (E_{ads}), transition states (E_{TS}), products (E_{prod}) and activation barriers (ΔE_{act}) involved in the reaction mechanism in Figure 4.

	A1	A2	A3
E_{ads}	-26.4	-28.8	-26.6
E_{TS}	-3.9	-0.9	8.2
E_{prod}	-49.1	-41.3	-47.5
ΔE_{act}	22.4	27.9	34.5

In the case of Au_8^-, although the A2 complex is the most stable coadsorption complex, we did not select it as the initial complex for further study of the reaction between O_2 and a methoxy species, because these two species are located far from each other. However, the second most stable complex (A1) shows the most pronounced cooperative effect in the activation of molecular oxygen, as discussed below. We found that coadsorption leads to a modification of the electronic properties of O_2. Methoxy species readily adsorb on Au_8^-, resulting in a weakening of the O–O bond of O_2. The O–O bond length of adsorbed O_2 elongates from 1.277 Å to 1.305 Å, and the vibrational frequency decreases to 1253 cm^{-1} compared with the values on $Au_8O_2^-$.

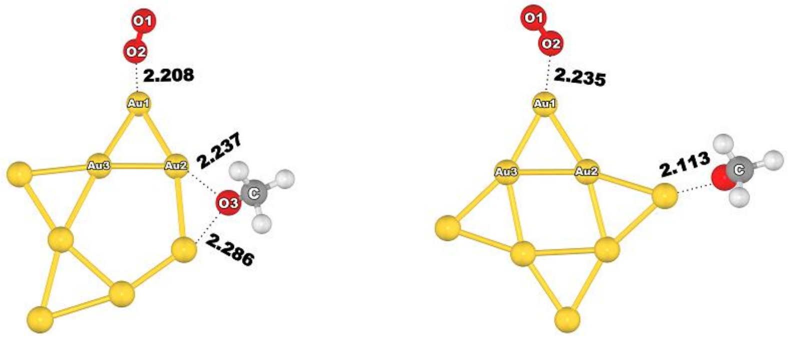

A1 (15.8)

A2 (22.9)

Figure 5: the optimized structures of the coadsorption complexes of $Au_8O_2^-$ and methoxy with adsorption energies (kcal/mol) in parenthesis. Distances are in angstroms (Å).

2.3.4 Mechanism of the whole reaction

The possible reaction pathways was examined on both Au_8^- and Au_{20}^- gold cluster. The proposed mechanism (Scheme 1, Figure 6) consists of formaldehyde formation as the first elementary step. The mechanism is initiated by the hydrogen abstraction of a methoxy species by a superoxo-like anion on the gold cluster, resulting in the formation of formaldehyde. At the TS_A1 structure, the C–H1 bond is elongated from 1.111 Å to 1.317 Å, whereas the O1–H1 distance contracts to 1.260 Å. The decrease in the C–O3 bond length to 1.359 Å indicates conversion into a carbonyl group. The structure of the gold cluster is also significantly affected by the reaction, and the orientations and local environment around the adsorption sites in all of the transition states are different. At the TS_A1 and TS_A3 structures, adsorbates are located on the edge and flat surface, respectively. The structural deformation at the apex site of the gold cluster leads to an increment in the negative charge on the oxygen and carbon atoms simultaneous with a decrease in the positive charge on the hydrogen atom of TS_A1 that is greater than for TS_A3. This implies that the charge distribution in TS_A1 is more pronounced than in TS_A3. This result can explain why the latter transition state is less stable than the former state. This step generates formaldehyde as the oxidation product.

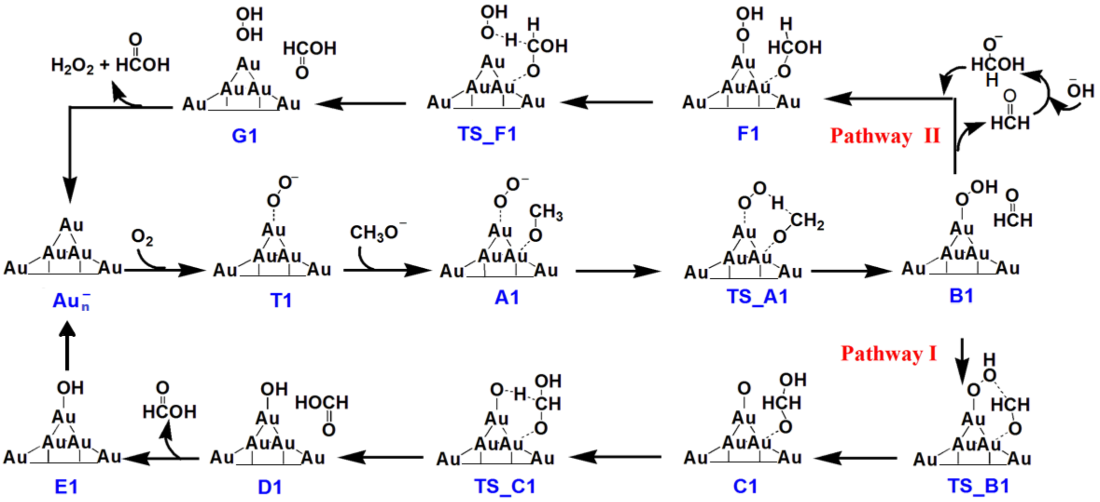

Scheme 1: Proposed reaction pathway for aerobic oxidation of methoxy species to formic acid.

Subsequently, the formaldehyde is activated by the hydroxyl group of a hydroperoxyl-like complex, or from base, leading to hydrogen abstraction producing formic acid through pathway I or II. In pathway I, the reaction is initiated by C–H bond dissociation of methoxy species with hydrogen transfer to a superoxo-like anion resulting in formaldehyde adsorbed on a hydroperoxyl-like complex ($Au_{20}OOH$). Then, the reaction further proceeds via nucleophilic attack by the hydroxyl group of the hydroperoxyllike complex on formaldehyde, leading to a hemiacetal intermediate and atomic oxygen attached to the gold cluster. Subsequently, the formic acid is generated by hydrogen transfer from the hemiacetal intermediate to atomic oxygen and desorbs from the gold cluster in the final step. For another possible reaction pathway that may compete with pathway I, it was assumed that formaldehyde generated in the first elementary step desorbs from the gold cluster, and nucleophilic addition of the hydroxyl anion to formaldehyde occurs in basic solution. Consequently, this leads to the formation of a hemiacetal intermediate that then adsorbs on the gold cluster. Finally, formic acid and hydrogen peroxide are produced by hydrogen abstraction from that intermediate and subsequent desorption from the Au cluster in the final step.

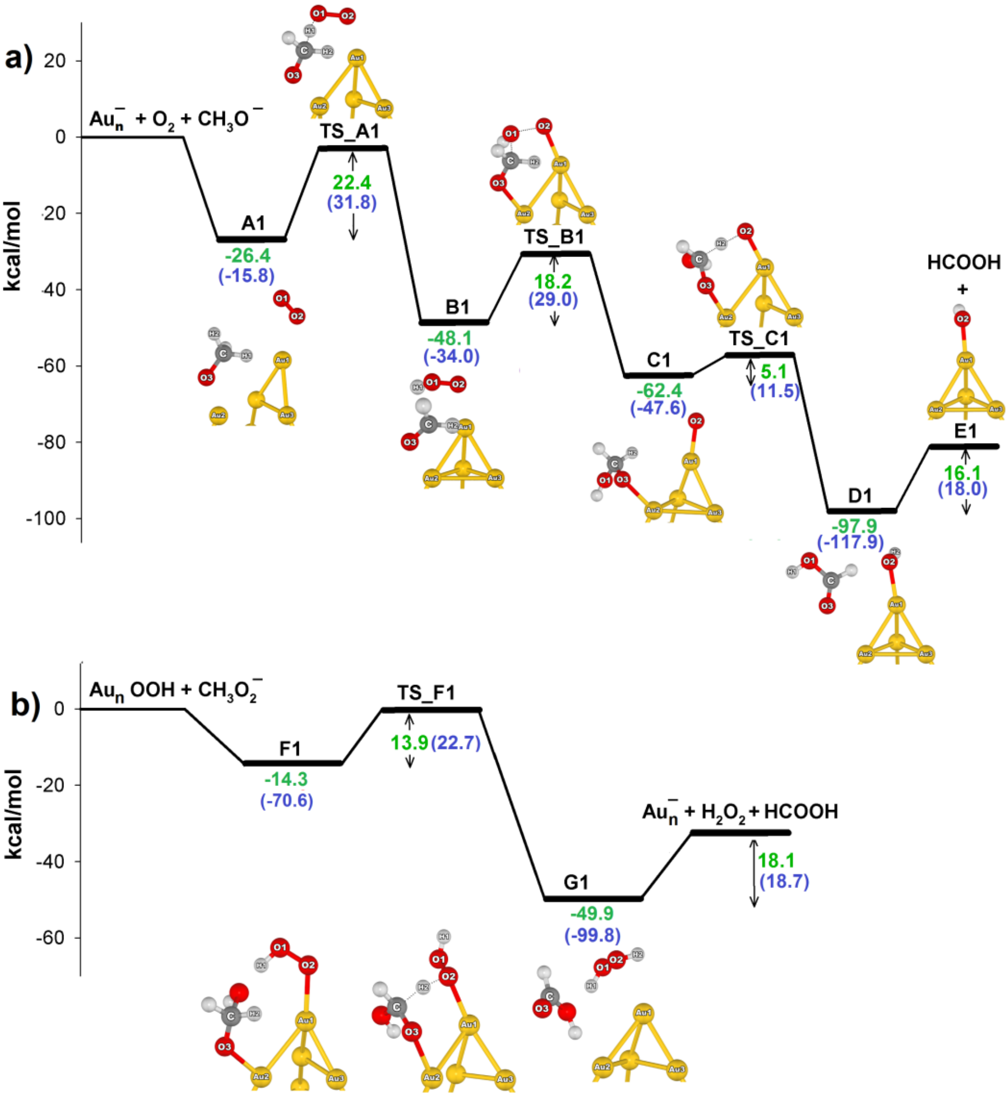

Figure 6: Energy profile diagram for methanol oxidation on Au_{20}^- and Au_8^-cluster (Energies for Au_8^- in parenthesis).

We could not find a reaction pathway that involves direct hydrogen transfer to the surface of the gold cluster. In the presence of an Au–H intermediate, the O_2 always desorbed from the gold cluster during the optimization. One possible explanation is that an electron occupying the singly occupied molecular orbital (SOMO) of Au cluster prefers to form a sigma bond to Au–H rather than interact with the less stable LUMO of O_2. The comparision between the energy diagram of Au_8^- and Au_{20}^- are shown in figure 5. Comparing the activation energies between proposed reaction pathways, we found that the reaction preferentially occurs via TS_A1, requiring an activation barrier of 22.4 kcal/mol. In this step, it appears that the geometric relaxation during the optimization and the charge contribution presented on the apex of Au_{20} are responsible for the observed reactivity.

2.4 Conclusion

In this chapter, it was found that, Au_{20}^- is a better model for the study reactions catalysed by PVP-supported collidal gold NCs through mechanistic investigation of methanol oxidation reaction because of the low energy barriers for reaction as compared with Au_8^-. Adsorption of O_2 in superoxide form activates Au NCs for adsorption of methoxy species and abstract hydrogen, leading to formaldehyde.

2.5 References

[1] F. Esch, S. Fabris, L. Zhou, L. Montini, C. Africh, P. Fomasiero, G. Comelli, R. Rosie, *Science* **2005**, *309*, 752.

[2] a) A. Abad, A. Corma, H. Gracia, *Chem. Eur. J.* **2008**, *14*, 212. b) M. Boronat, A. Corma, *J. Catal.* **2011**, *284*, 138.

[3] H. Tsunoyama, Y. Liu, T. Akita, N. Ichikuni, H. Sakurai, S. Xie and T. Tsukuda, *Catal. Surv. Asia*, **2011**, 1.

[4] I. Kamiya, H. Tsunoyama, T. Tsukuda and H. Sakurai, *Chem. Lett.* **2007**, ***36***, 646.

[5] H. Tsunoyama, N. Ichikuni and T. Tsukuda, *Langmuir* **2008**, *24*, 11327.

[6] B. Yoon, H. Häkkinen and U. Landman, *J. Phys. Chem. A.* **2003**, *107*, 4066.

[7] M. Okumura, Y. Kitagawa, T. Kawakami, M. Haruta, *Chem. Phys. Lett.* **2008**, *459*, 133.

[8] T. Ishida, M. Nagaoka, T. Akita and M. Haruta, *Chem. Euro. J* **2008**, *14*, 8456.

[9] L. M. Molina and B. Hammer, *J. Chem. Phys.* **2005**, *123*, 161104.

[10] B. Thorsten M, *Int. J. Mass. Spectro.* **2005**, *243*, 1.

[11] Y. Kim, *Chem. Phys. Lett.* **2003**, *377*, 170.

[12] H. Tsunoyama, H. Sakurai, Y. Negishi, T. Tsukuda, *J. Am. Chem. Soc.* **2005**, *127*, 9374.

[13] H. Tsunoyama, H. Sakurai, T. Tsukuda, *Chem. Phys. Lett.* **2006**, *429*, 528.

[14] a) M. Conte, H. Miyamura, S. Kobayashi and V. Chechik, *J. Am. Chem. Soc.* **2009**, *131*, 7189. b) M. Conte, H. Miyamura, S. Kobayashi and V. Chechik, *Chem. Commun.* **2010**, *46*, 145.

[15] a) M. Okumura, Y. Kitagawa, T. Kawakami, *Int. J. Quantum. Chem.* **2010**, *110*, 2903. b) M. Okumura, Y. Kitagawa, T. Kawakami, M. Haruta, *Chem. Phys. Lett.* **2008**, *459*, 133. c) B. Boekfa, E. Pahl, N. Gaston, H. Sakurai, J. Limtrakul, M. Ehara, *J. Phys. Chem. C*. **2014**, *118*, 22188.

[16] M. Mantina, R. Valero, D. G. Truhlar, *J. Chem. Phys.* **2009**, *131*, 064706.

[17] M. J. Frisch, G. W. Trucks, H. B. Schlegel, G. E. Scuseria, M. A. Robb, J. R. Cheeseman, G. Scalmani, V. Barone, B. Mennucci, G. A. Petersson, H. Nakatsuji, M. Caricato, X. Li, H. P. Hratchian, A. F. Izmaylov, J. Bloino, G. Zheng, J. L. Sonnenberg, M. Hada, M. Ehara, K. Toyota, R. Fukuda, J. Hasegawa, M. Ishida, T. Nakajima, Y. Honda, O. Kitao, H. Nakai, T. Vreven, J. Montgomery, J. A., J. E. Peralta, F. Ogliaro, M. Bearpark, J. J. Heyd, E. Brothers, K. N. Kudin, V. N. Staroverov, R. Kobayashi, J. Normand, K. Raghavachari, A. Rendell, J. C. Burant, S. S. Iyengar, J. Tomasi, M. Cossi, N. Rega, N. J. Millam, M. Klene, J. E. Knox, J.

B. Cross, V. Bakken, C. Adamo, J. Jaramillo, R. Gomperts, R. E. Stratmann, O. Yazyev, A. J. Austin, R. Cammi, C. Pomelli, J. W. Ochterski, R. L. Martin, K. Morokuma, V. G. Zakrzewski, G. A. Voth, P. Salvador, J. J. Dannenberg, S. Dapprich, A. D. Daniels, Ö. Farkas, J. B. Foresman, J. V. Ortiz, J. Cioslowski, D. J. Fox, *Gaussian 09, Revision B.01*, Gaussian, Inc., Wallingford CT, **2012**.

[18] K. J. Taylor, C. L. Pettiette-Hall, O. Cheshnovsky, R. E. Smalley, *J. Chem. Phys.* **1992**, *96*, 3319.

[19] B. E. Salisbury, W. T. Wallace, R. L. Whetten, *Chem. Phys.* **2000**, *262*, 131.

[20] C. Luo, W. Fa, J. Dong, *J. Chem. Phys.* **2006**, *125*, 084707(1-5).

[21] D. M. Cox, R. Brickman, K. Creegan, A. Kaldor, *Z. Phys. D.* **1991**, *19*, 353.

[22] W. Huang, H.-J. Zhai, L.-S. Wang, *J. Am. Chem. Soc.* **2010**, *132*, 4344.

[23] Y. Kim, *Chem. Phys. Lett.* **2003**, *377*, 170.

[24] G. Mills, M. S. Gordon, H. Metiu, *Chem. Phys. Lett.* **2002**, *359*, 493.

[25] a) L. M. Molina, B. Hammer, *Appl. Catal. A: General* **2005**, *291*, 21. b) H. Häkkinen, B. Yoon, U. Landman, X. Li, H.-J. Zhai, L.-S. Wang, *J. Phys. Chem. A* **2003**, *107*, 6168. c) F. J. Furche, *Chem. Phys.* **2002**, *117*, 6982.

[26] G. Mills, M. S. Gordon and H. Metiu, *J. Chem. Phys.* **2003**, *118*, 4198.

[27] F. Tielens, J. Andrés, M. Van Brussel, C. Buess-Hermann and P. Geerlings, *J. Phys. Chem B.* **2005**, *109*, 7624.

[28] X. Wu, L. Senapati, S. K. Nayak, A. Selloni and M. Hajaligol, *J. Chem. Phys.* **2002**, *117*, 4010.

[29] K. P. Huber and G. Herzberg, *Molecular Spectra and Molecular Structure, Van Nostrand Reinhold*, *New York*, 1979.

[30]. M. J. Travers, D. C. Cowles and G. B. Ellison, *Chem. Phys. Lett.* **1989**, *164*, 449.

[31] H. Tsunoyama, T. Tsukuda and H. Sakurai, *Chem. Lett.* **2007**, *36*, 212.

Chapter 3

Application of Cluster Model to the Mechanistic Study of Reactions Catalyzed by Au:PVP

3.1 Introduction

Biaryls, an important class of organic compounds, has become targets for many research groups due to its increasing application in pharmaceuticles, natural products, and agrochemicals[1] and as ligands in catalytic reactions. The oxidative homocoupling of arylboronic acids in the presence of a transition-metal catalyst is among the best ways of synthesizing symmetrical biaryls.[2] This coupling reaction between two nucleophiles requires the presence of molecular oxygen or a chemical oxidant. Palladium is the metal predominantly used in catalysts for this reaction,[3] however, Au,[2,4,5] is one of the most selective catalyst.

Au-catalyzed reactions have also been emerging as powerful synthetic tools for synthesizing many types of C-C or C-hetero bonds due to its scope and application in various fields. Au:PVP-catalyzed aerobic homocoupling of phenylboronic acid is one of them.[4a] It provided a convenient method for C-C bond formation under mild condition. Since O_2 is necessary for this reaction, as well as the aerobic oxidation reactions, it is proposed that an electron-deficient site at the cluster surface is generated by adsorption of O_2, which behaves as a formal Lewis acid providing a site for transmetalation of aryl moieties eventhough detailed mechanism has not been studied, yet.

A general mechanism for the oxidative homocoupling involves a double transmetalation of two nucleophiles to give a biaryl–metal intermediate that undergoes reductive elimination to form the biaryl as a coupling product. The oxidant helps to oxidize the metal species, regenerating the catalyst for a further catalytic cycle. Despite a number of reports on the progress of oxidative homocoupling reactions of various organometallic reagents, precise mechanistic details of the catalytic reaction are still lacking. However, several mechanistic investigations have been performed on the Pd-catalyzed homocoupling reaction which involves activation of phenylboronic acid by the palladium peroxo complex (**4**) through a classic Lewis acid–base interaction. Coordination of one oxygen atom of the peroxo complex to the boron atom activates the arylboronic acid to form a transmetalated product. A second transmetalation gives a biaryl Pd^{2+} species, and the final step involves reductive elimination of the biaryl with concomitant regeneration of Pd^0 for the next catalytic cycle (scheme 1).

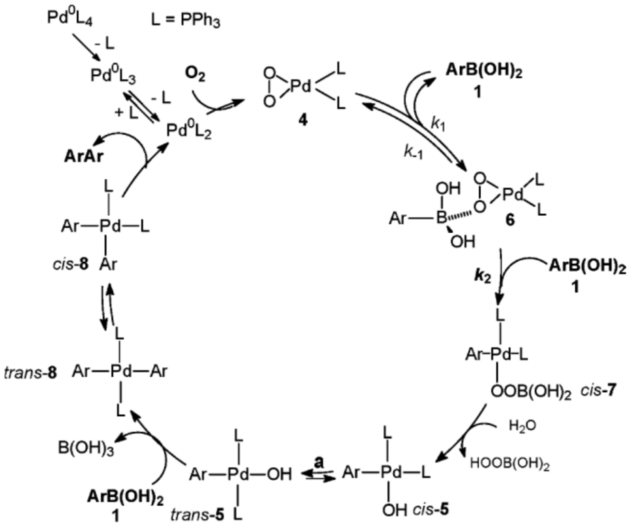

Scheme 1. Proposed mechanism of Pd-catalyzed homocoupling reaction (reprinted from reference 3h).

Recently, homocoupling reactions using various Au-based catalysts, in which cationic Au species are the catalytically active sites, have been reported,[5a,b,e,h] however, our previous report on the Au:[poly(*N*-vinylpyrrolidin-2-one)] (Au:PVP) nanocluster (NC)-catalyzed aerobic homocoupling reaction was based on a zero-valent Au as catalytic unit that carries a slight negative charge as a result of electron donation from the surrounding polymer, PVP in this case.[4] Some catalytic systems are based on zero-valent gold, for example, Au NCs supported on Mg–Al mixed oxide (MAO),[6] for which the mechanism of homocoupling of phenylboronic acid involves the role of O_2 as an oxidant in the presence of water to regenerate the Au NCs by oxidation of the negatively charged Au NCs that are formed during the reaction. The surface hydroxy groups of MAO interact with phenylboronic acid, resulting in weakening of the C–B bond, thereby facilitating the transmetalation process. Another report suggests that the homocoupling reaction catalyzed by carbon NC-stabilized Au relies on oxidation of the surfaces of the Au NCs by dissolved molecular oxygen,[5f] which generates a positively charged surface Au species linked to oxygenated ligands such as O_2^{2-}, O_2^{-}, or OH^{-}. In contrast, Boronat and Corma[7] considered the activation and dissociation of a O_2 molecule to form several oxygen species adsorbed on the oxidized Au surface. This system generates various types of low-coordinated Au sites, such as neutral Au^0, cationic Au^I, and $Au^{\delta+}$. In catalytic systems containing cationic gold species, such as Au/CeO_2, direct influence of oxygen in the C–C bond-forming step rather than adsorption and activation of phenylboronic acid has been described (Figure 1). However, there has been no detailed mechanistic study on aerobic homocoupling reactions catalyzed by Au NCs, such as Au:PVP, in which anionic Au is the catalytic species.

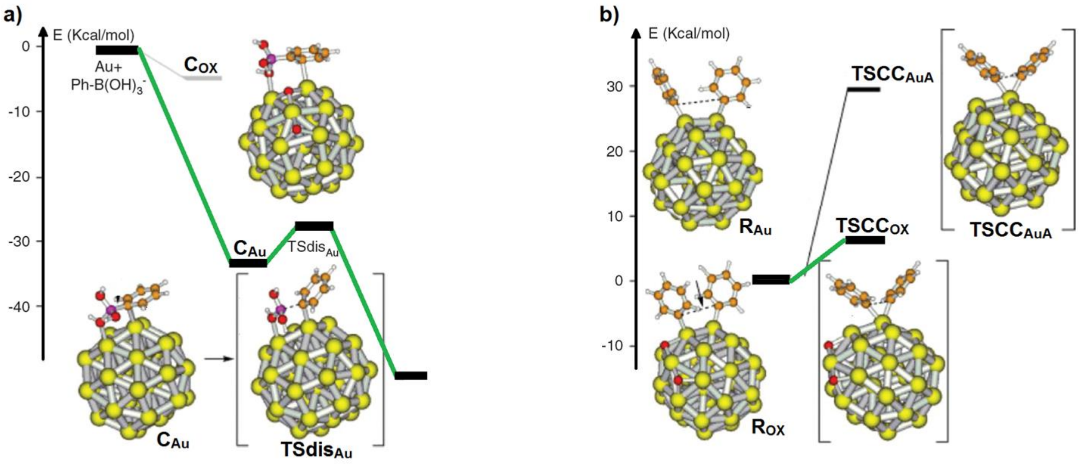

Figure 1: Calculated energy profile for a) dissociation of $PhB(OH)_3^{-}$ and b) coupling of two phenyl fragments on a naked Au_{38} nanoparticle (black line) and on a partially oxidized Au_{38} (green line). (reprinted from reference 7)

Many theoretical studies have demonstrated the importance of activation of O_2 in various oxidation reactions by transition metals in the form of superoxide or peroxide species. For Au in particular, molecular O_2 is adsorbed and activated in the form of the superoxide, and dissociated species is difficult to form, as reported by Nakatsuji et al.[8] and by Roldán et al.[9] During previous mechanistic investigations on the aerobic oxidation of methanol to formic acid,[10,11] we found that Au_{20}^{-} can be regarded as a good model for the Au:PVP system and that the low electron affinity of this cluster is energetically favorable for electron transfer from Au to the $2\pi^*$ orbital of O_2, resulting in nondissociative chemisorption on Au of O_2 in the form of the superoxide. This electronic charge transfer plays a crucial role in selective oxidations of various substances. The self-coupling reaction of phenylboronic acid also requires O_2, even though this is not an oxidation reaction.

So, in this chapter, the mechanism of the aerobic homocoupling of phenylboronic acid on the Au:PVP system was investigated by using the Au_{20}^{-} NC model and density functional theory (DFT) calculations to represent the experimental conditions that we described in the first report on the Au nanoparticle-catalyzed C–C bond-forming reaction.[4] In particular, the key role of molecular oxygen and the necessity for basic aqueous conditions for this reaction was analyzed in detail.

3.2 Calculation details

For the theoretical model of Au NC:PVP system, the anionic Au_{20} NC was used including the effects of the surrounding PVP molecules[12] on the energetics. All the calculations were carried out by using the *Gaussian 09* suite of programs (revision B.01).[13] DFT calculations with the M06 functional, which has been reported as reliable for reactions on Au NC through several benchmark calculations[14] has been applied with scalar relativistic effective core potential (ECP) and double-zeta basis sets [3s3p2d] (LANL2DZ) for the gold atom. The 6-31G (d,p) basis sets were used for the hydrogen, carbon, and oxygen atoms. Six-component d-functions were employed in all the calculations. A fully relaxed structural optimization was performed, where the doublet spin state was maintained throughout the reaction pathway. The unrestricted Kohn–Sham scheme was employed for open-shell electronic structure calculations. All the ground-state optimized structures were local minima containing no imaginary frequencies, and all of the optimized transition-state structures possessed only a single imaginary frequency, as confirmed by vibrational analysis.

3.3 Result and discussion

3.3.1 Effect of O_2 and water in the adsorption and dissociation of phenylboronate

For the formation of biphenyl via Au-catalyzed homocoupling reaction, molecular oxygen was expected to play a vital role.[4-9] It was proposed that electron-deficient site are generated at the cluster surface, by adsorption of O_2, which behaves as a Lewis acid and provides a site for transmetalation of aryl moieties during this reaction (Figure 2). Phenol was formed as a side product which is expected to be formed by oxidation of phenylboronic acid.

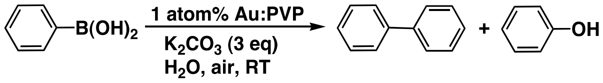

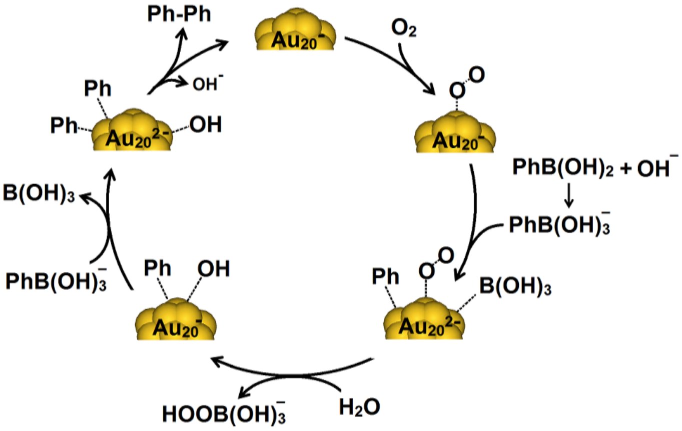

Figure 2: Proposed Catalytic reaction cycle for the formation of biphenyl.

It would be expected that the mechanism associated with the Au NC catalyst stabilized by PVP, which involves anionic Au species, should differ from that of catalytic systems involving cationic Au species. Experiments have shown that the present reaction proceeds in a basic aqueous medium in the presence of dissolved oxygen. The molecular oxygen would be expected to play a key role in the Au NCs-catalyzed homocoupling reaction. The overall aerobic homocoupling of phenylboronic acid to yield biphenyl can be represented as follows:

$$2PhB(OH)_2 + 2H_2O + Au + O_2 \quad \rightarrow \quad Ph–Ph + 2B(OH)_3 + Au + H_2O_2 \qquad (1)$$

Phenols are often formed as byproducts in the homocoupling of arylboronic acids in water in the presence of dioxygen. We therefore propose that phenol is produced by oxidation of the phenylboronic acid by H_2O_2 generated during the process of formation of the biaryl.[3i] This H_2O_2 is probably generated in solution by hydrolysis of $HOOB(OH)_2$ as follows:

$$HOOB(OH)_2 + H_2O \quad \rightarrow \quad B(OH)_3 + H_2O_2 \qquad (2)$$

$$H_2O_2 + ArB(OH)_2 \quad \rightarrow \quad B(OH)_3 + ArOH. \qquad (3)$$

The most stable geometry is the structure in which the oxygen atom is bound directly to the apex site of the Au_{20}^{-} NC. Adsorption of O_2 on the Au NC surface causes elongation of Au–Au bond and alteration of the charge distribution on each Au atom. The electronic structure of the adsorbed O_2 molecule is influenced by electron transfer from Au_{20}^{-}, resulting in the formation of a superoxo-like species that, in turn, modifies the electronic structure of the Au cluster surface, providing favorable sites for the adsorption of arylboronic acids in the homocoupling reactions (Figure 3).

For the formation of biphenyl, adsorption and dissociation of $PhB(OH)_3^{-}$ was investigated including the effects of adsorbed oxygen. This $PhB(OH)_3^{-}$ anion might be generated at high pH values under basic conditions. The role of oxygen has been well explained by Wang et al. in their experiments,[6] in which no biphenyl was obtained in the absence of oxygen, a similar finding to our previous experimental results.[2,4]

In this regard, as a first step, the adsorption of $PhB(OH)_3^{-}$ was studied on bare Au_{20}^{-} as well as oxidized Au_{20}^{-} with molecular oxygen adsorbed in the form of superoxide ($Au_{20}O_2^{-}$). The presence of an inorganic base is necessary for this reaction. The effect of the base was realized on the generation of tetracoordinated borate from phenylboronic acid. This causes elongation of the C–B bond from 1.558 Å in phenylboronic acid to 1.640 Å in its anion, facilitating the dissociation process. $PhB(OH)_3^{-}$ adsorbs on Au_{20}^{-} with an adsorption energy of 15.2 kcal/mol. Here, the phenyl ring interacts with the flat face of the Au NC surface. Upon adsorption, the length of the C–B bond of $PhB(OH)_3^{-}$ decreases to 1.631 Å, due to the interaction with the Au NC. On oxidized Au_{20}^{-} ($Au_{20}O_2^{-}$), the adsorption energy increases by 24 kcal/mol (Figure 3) and the C–B bond length is 1.635 Å. This larger adsorption energy can be explained by an enhanced Lewis acid–base-type interaction between partially oxidized Au ($Au_{20}O_2^{-}$) and $PhB(OH)_3^{-}$. As can be seen in Figure 4, the

Mulliken charge is such that adsorption of molecular oxygen provides Lewis acidic sites on Au NC (red font), thereby favoring the adsorption of anionic tetracoordinated borate species. The O1-O2 bond length increases from 1.272 Å (in $Au_{20}O_2^-$) to 1.301 Å (in A_1) and 1.302 Å (in TS_1) upon hydrogen bonding between O2 and H1.

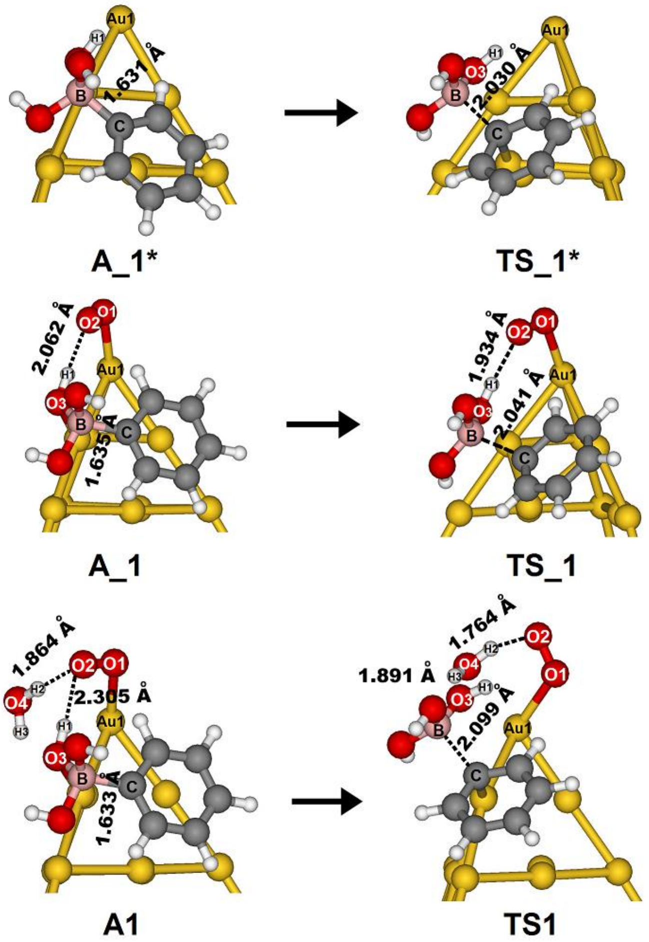

Figure 3: Optimized structures of adsorption complexes and transition states.

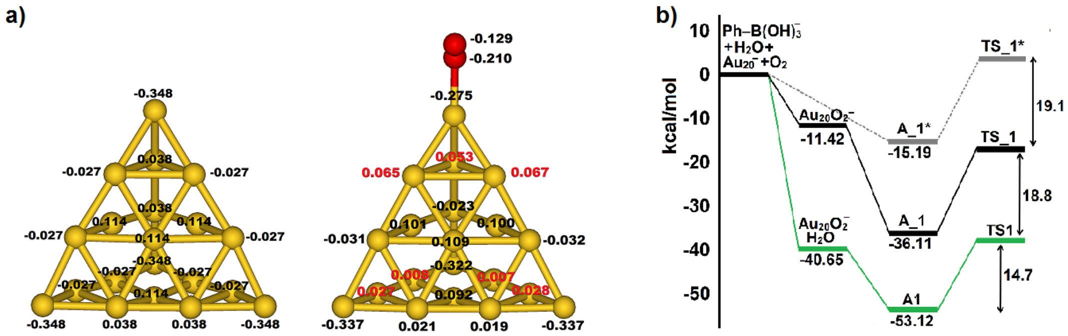

Figure 4: a) Mulliken charge on Au_{20}^{-} and $Au_{20}O_2^{-}$, b) Energy diagram of C-B bond activation step (adsorption of $PhB(OH)_3^{-}$ on bare Au_{20}^{-} (grey), on Au_{20}^{-} and O_2 (black), on Au_{20}^{-}, O_2 and H_2O (green). All 'A' are adsorption complexes and all 'TS' are transition.

In the adsorption complex **A_1**, $PhB(OH)_3^{-}$ forms a hydrogen bond with the O_2 atoms of $Au_{20}O_2^{-}$, which also facilitates dissociation of the C–B bond (Figure 3). The distance between the O2 atom of the dioxygen and the H1 atom of $PhB(OH)_3^{-}$ is 2.062 Å. In addition, the O1–O2 bond is elongated to 1.301 Å in **A_1** from 1.272 Å in $Au_{20}O_2^{-}$. This hydrogen bond also remains intact at transition state **TS_1** for the C–B bond dissociation. We studied the base-mediated activation of phenylboronic acid; however, ligand (O_2^{-})-induced transmetalation might also be possible. However, the activation barrier in the case of $Au_{20}O_2^{-}$ is nearly the same as that in the case of bare Au_{20}^{-}.

H_2O and O_2 are vital components in the homocoupling of phenylboronic acid. In many previous studies,[2,4,5] for example, on the homocoupling reaction catalyzed by gold–carbon nanoparticle composites, water was used as a cosolvent. The Au:PVP-catalyzed homocoupling reaction was performed in water as a the sole solvent.[4] Therefore, the inclusion of the solvent effect of water is relevant in the present system. We believe that several water molecules are associated with the NC catalyst surface along with PVP and that they participate in the reaction. Here, on the basis of the hydrogen-bonding distance, we considered one water molecule that interacts directly with the reactants or participates in the reaction.

When one water molecule is included explicitly on the surface of the partially oxidized Au cluster ($Au_{20}O_2^-$), the adsorption of $PhB(OH)_3^-$ is exothermic by 53.12 kcal/mol (Figure 4). The water molecule forms a hydrogen-bonded network with both O_2 and $PhB(OH)_3^-$**,** with significant stabilization of the transition state; the activation barrier for the C–B bond dissociation decreases from 18.4 to 14.7 kcal/mol at TS1.

The presence of a hydrogen-bonding network is manifested in the bond lengths, the distances between the O2 atom of oxygen and the H2 atom of H_2O (1.864 Å) or the H1 atom of $PhB(OH)_3^-$ (2.305 Å). The O1–O2 bond length becomes 1.305 Å, which is longer than that in **A_1**. Dissociation of the C–B bond on Au NC requires an energy barrier of 19.1 kcal/mol from **A_1*** and 18.8 kcal/mol from **A_1**. Interestingly, the energy for dissociation of the C–B bond over partially oxidized Au in the presence of a water molecule is only 14.4 kcal/mol. This result demonstrates that the water molecule is important for C–B bond dissociation, lowering the energy barrier by about 4 kcal/mol. We therefore compared the structures of the transition states for bare Au, Au–O_2, and Au–O_2–H_2O (Figure 4b). In the transition state **TS_1***, the C–B bond is elongated from 1.631 Å to 2.030 Å. On $Au_{20}O_2^-$, the stronger hydrogen-bonding interaction between dioxygen and the substrate molecule as a result of the shorter H1–O2 distance (1.394 Å) causes additional elongation of the C–B bond (2.041 Å) at **TS_1**. More importantly, **TS1** contains two short contacts: O2–H2 (1.764 Å) and O3–H3 (1.891 Å). These cause significant stabilization of the transition state from **A1**. As a result, the C–B bond is significantly elongated to 2.099 Å (Figure 3).

Dissociation of the C–B bond results in adsorption of a phenyl group on Au NC and interaction of $B(OH)_3$ with O_2 through hydrogen bonding in intermediate **B1***.

Because of the oxophilic nature of boron, we considered another intermediate **B1** (Figure 5) that might be generated by nucleophilic attack of oxygen adsorbed on Au NC. Calculated energies for these two intermediates without considering the solvent molecule show that **B1** is less stable than **B1***. In contrast, inclusion of one water molecule stabilizes intermediate **B1*** and both intermediates have similar relative energies. We therefore considered intermediate **B1*** for the next step to generate intermediate **C1** by a hydrolysis process. However, we could not locate the transition state for O–H bond dissociation of H_2O.

As described earlier, the adsorption and activation of $PhB(OH)_3^-$ is favored on the surface of the partially oxidized Au cluster ($Au_{20}O_2^-$). This phenomenon might be induced by the presence of an inorganic base in the reaction or by the O_2^- adsorbed on Au surface. However, both processes generate a phenyl fragment and a peroxyborate [$–OOB(OH)_3^-$] species attached to the Au NC surface, as seen in intermediate **B1**. In the presence of water, [$–OOB(OH)_3^-$] can undergo hydrolysis to form a hydroperoxyborate [$HOOB(OH)_3^-$] species attached to the Au NC (intermediate **C1**). This [$HOOB(OH)_3^-$] species readily desorbs from the Au cluster to leave an –OH species adsorbed on the Au_{20} cluster ($Au_{20}OH^-$) (Figure 5).

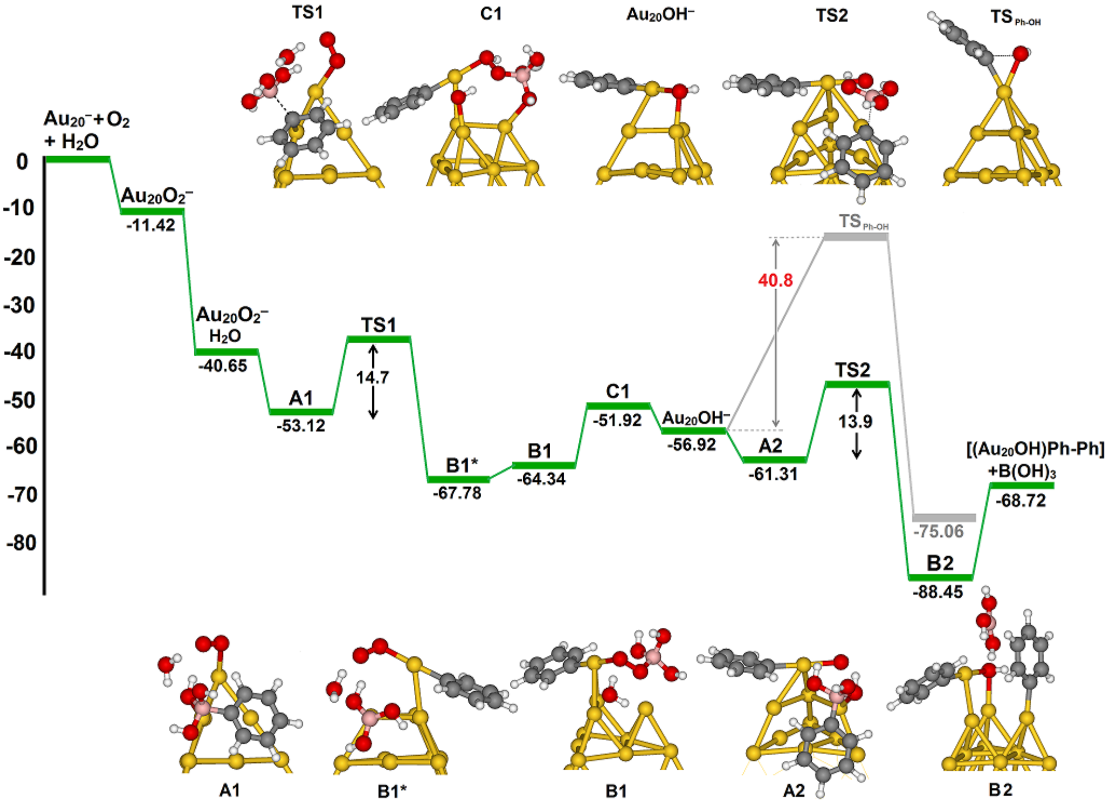

Figure 5: Energy diagram up to formation of [**(**Au$_{20}$OH**)**Ph–Ph].

Coupling of two phenyl fragment is necessary for the formation of biphenyl. Therefore, the adsorption and dissociation of a second PhB(OH)$_3$$^{-}$ molecule was considered (Figure 5). The adsorption of PhB(OH)$_3$$^{-}$ on Au$_{20}$OH^{-} gives the adsorption complex **A2** with an adsorption energy of 4.4 kcal/mol. As in the case of **A1**, the phenyl ring interacts with the flat surface of the Au NC and one of the hydrogen atoms of PhB(OH)$_3$$^{-}$ interacts with oxygen atom of OH with a distance of 2.220 Å at the apex site of the Au NC. C–B bond dissociation occurs via the transition state **TS2** to form intermediate **B2** with an activation barrier of 13.9 kcal/mol, which is nearly the same as that in the first step (**TS1**). In **TS2**, the interaction becomes stronger as the distance of hydrogen bonding decreases to 1.895 Å as a result of the significant increase in the C–B bond length (to 2.068 Å from 1.630 Å). The intermediate **B2** contains two phenyl fragments with $B(OH)_3$ and OH^- attached to the Au NC. The desorption process of $B(OH)_3$ is endothermic by 19.7 kcal/mol. Subsequently, the two phenyl and –OH species remain adsorbed on the Au NC surface, as required for the formation of the biphenyl product by a reductive elimination process.

3.3.2 Migration of phenyl group on Au NC and reductive elimination process

For the effective coupling, two phenyl fragments should approach to each other at the closest distance. Reductive elimination of two phenyl group leading to biphenyl occur at the edge or facet site with low-energy-barrier through spillover of phenyl group on Au NC. Three possible structures were considered for the reductive elimination process from top (Au_{20}Ph-Ph_T), edge (Au_{20}Ph-Ph_E) and flat face (Au_{20}Ph-Ph_F) (Figure 6). Calculated activation energy at top site is in the range of 7.1 to 9.3 kcal/mol and at face site is in the range of 12.6-13.2 kcal/mol depending on the interaction with the water and/or OH^- species. So, both sites are possible for the reductive elimination. The OH^- and H_2O species apparently assist the reductive elimination or coupling reaction.

Wiberg bond indices (WBI) for the Au1–C1 and Au2–C2 bonds of some selected structures of $(Au_{20}Ph\text{-}Ph)^-$ that include H_2O, OH^-, or both are shown in table 2. The values were significantly reduced when we considered the effects of both species in (Au_{20}Ph-Ph_T_OH_H_2O). This implies that the presence of both OH^- and H_2O adsorbed on the cluster surface in basic aqueous reaction medium facilitates the reductive elimination process by weakening the Au–C bond, thereby enhancing biphenyl formation. Simultaneously, the C1–C2 distance is significantly reduced and the C1–Au1–C2 bond angle is decreased.

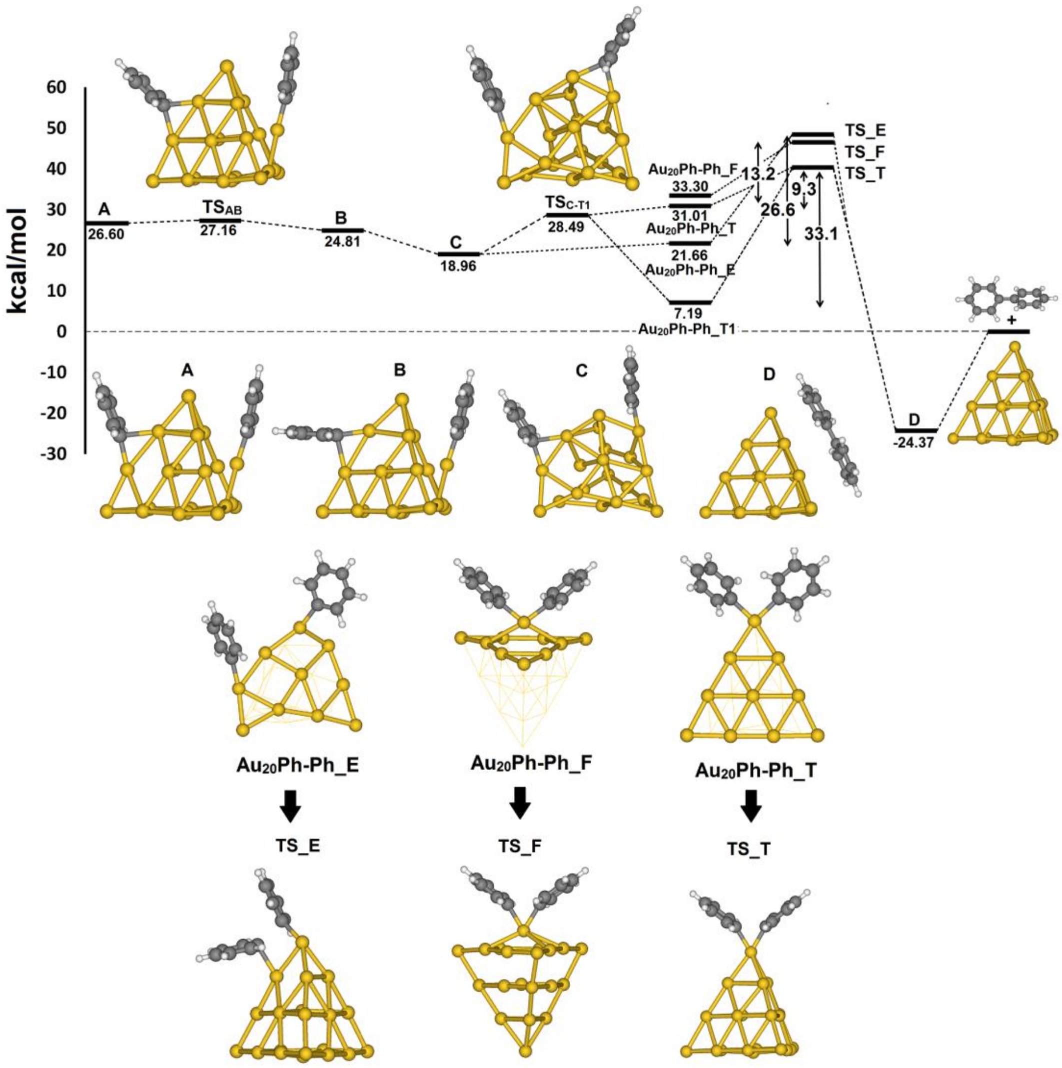

Figure 6: Energy diagram for spillover of phenyl group and reductive elimination process with optimized structures of Au_{20}^{-} with phenyl groups.

Table 1. Role of O_2 and H_2O in the reductive elimination

Structure	Activation energy (kcal/mol)		
	Au_{20}^{-}	Au_{20}^{-} and $-OH^{-}$	Au20^{-}, $-OH^{-}$, and H_2O
Au_{20}Ph-Ph_T	9.3	8.5	7.1
Au_{20}Ph-Ph_E	26.6	–	24.6
Au_{20}Ph-Ph_F	13.2	12.8	12.6

Table 2. Wiberg bond indices in Au_{20}Ph-Ph showing the roles of the base and H_2O.

	$(Au_{20}Ph\text{-}Ph\_T)^{-}$	$(Au_{20}Ph\text{-}Ph\_T\_OH)^{-2}$	$(Au_{20}Ph\text{-}Ph\_T\_H_2O)^{-2}$	$(Au_{20}Ph\text{-}Ph\_T\_OH\_H_2O)^{-2}$
Au1–C1	0.5682	0.5648	0.5690	**0.5606**
Au1–C2	0.5674	0.5690	0.5662	**0.5624**
$R_{C1–C2}$ (Å)	3.099	3.036	3.178	**2.946**
$\theta_{C1\text{-}Au1\text{-}C2}$ (˚)	93.90	92.13	96.25	**89.14**

3.3.3 Mechaism of phenol formation

When the reaction is conducted in a protic polar solvent such as water, considerable amounts of phenol are formed as a byproduct together with biphenyl. Conversion of the C–B bond into a C–O bond via a phenylperoxyborate intermediate might be promoted in protic solvents, resulting in phenol formation. In the Au:PVP-catalyzed homocoupling, even though the reaction is conducted in an aqueous solvent, the selectivity toward biphenyl is higher than that toward phenol. This implies that the conversion of the C–B bond into a C–O bond has a higher activation barrier than that to a C–C bond.

To understand the selectivity of the reaction, the mechanism of phenol formation on Au_{20}^{-} was studied. The same mechanism was calculated as a noncatalytic process, and compared with the catalytic one. As shown in Scheme 3, nucleophilic attack by OOH^{-} on $PhB(OH)_2$ generates the hydroperoxyborate complex **X1**. Oxidation of the C–B bond to a C–O bond takes place through the transition state **TS_X1**. This step has an activation barrier of 25.8 kcal/mol in the gas phase. However, on the surface of Au NC, this step requires an energy of 18.2 kcal/mol, which is much lower than that for the noncatalyzed process (Figure 7). This would suggest that phenol formation should be accelerated on the catalyst surface. However, this energy barrier is higher than the highest barrier (14.7 kcal/mol) required for C–C bond formation. This explains the high selectivity toward biphenyl over phenol. Direct reductive elimination of phenyl group and –OH from the more negatively charged Au NC surface can be ruled out because of very high energy barrier (40.8 kcal/mol) calculated for the process (figure 5).

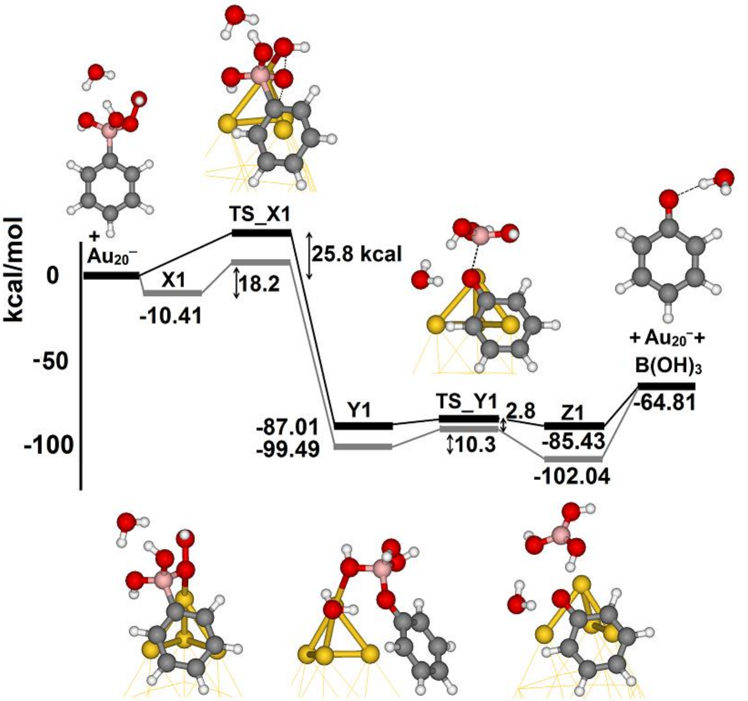

Figure 7: Energy diagram for Au-catalyzed (gray line) and noncatalytic (black line) processes for the formation of phenol.

3.4 Conclusion

In this chapter, the author successfully investigated the mechanism of aerobic homocoupling of phenylboronic acid on Au NC surface. The surface of the Au NC is oxidized by the dissolved molecular oxygen in the form of superoxide O_2^- in the first step of the catalytic cycle which is important for transmetallation step. In parallel, mechanism of phenol formation was also studied. It is illustrate that base and water play non-negligible role in activating Au NCs through electron donation and hydrogen bonding.

3.5 References

[1] a) D. A. Horton, G. T. Bourne, M. L. Smythe, *Chem. Rev.* **2003**, *103*, 893. b) J. H. Schön, H. Meng, Z. Bao, *Nature* **2001**, *413*, 713.

[2] R. N. Dhital, A. Murugadoss, H. Sakurai, *Chem. Asian J.* **2012**, *7*, 55.

[3] a) K. Mitsudo, T. Shiraga, D. Kagen, D. Shi, J. Y. Becker, H. Tanaka, *Tetrahedron* **2009**, *65*, 8384. b) L. Yin, J. Liebscher, *Chem. Rev.* **2007**, *107*, 133. c) Z. Jin, S.-X. Guo, X.-P. Gu, L.-L. Qiu, H.-B. Song, J.-X. Fang, *Adv. Synth. Catal.* **2009**, *351*, 1575. d) S. R. Cicco, G. M. Farinola, C. Martinelli, F. Naso, M. Tiecco, *Eur. J. Org. Chem.* **2010**, 2275. e) A. Prastaro, P. Ceci, E. Chiancone, A. Boffi, G. Fabrizi, S. Cacchi, *Tetrahedron Lett.* **2010**, *51*, 2550. f) C. Amatore, C. Cammoun, A. Jutand, *Eur. J. Org. Chem.* **2008**, 4567. g) M. J. Burns, I. J. S. Fairlamb, A. R. Kapdi, P. Sehnal, R. J. K. Taylor, *Org. Lett.* **2007**, *9*, 5397. h) C. Adamo, C. Amatore, I. Ciofini, A. Jutand, H. Lakmini, *J. Am. Chem. Soc.* **2006**, *128*, 6829. i) H. Yoshida, Y. Yamaryo, J. Ohshita, A. Kunai, *Tetrahedron Lett.* **2003**, *44*, 1541. j) D. J. Koza, E. Carita, *Synthesis* **2002**, 2183. k) M. Moreno-Mañas, M. Pérez, R. Pleixats, *J. Org. Chem.* **1996**, *61*, 2346. l) A. Lei, X. Zhang, *Tetrahedron Lett.* **2002**, *43*, 2525.

[4] a) H. Tsunoyama, H. Sakurai, N. Ichikuni, Y. Negishi and T. Tsukuda, *Langmuir* **2004**, *20*, 11293. b) H. Sakurai, H. Tsunoyama, T. Tsukuda, *J. Organomet. Chem.* **2007**, *692*, 368. c) R. N. Dhital, A, Murugadoss, H. Sakurai, *Chem. Asian J.* **2012**, *7*, 55. d) O. Sophiphun, J. Wittayakun, R. N. Dhital, S. Haesuwannakij, A. Murugadoss, H. Sakurai, *Aust. J. Chem.* **2012**, *65*, 1238.

[5] a) S. Carrettin, J. Guzman, A. Corma, *Angew. Chem. Int. Ed.* **2005**, *44*, 2242. b) K. M. Parida, S. Singha, P. C. Sahoo, S. Sahu, *J. Mol. Catal. A: Chem.* **2011**, *342*, 11. c) L. Wang, W. Zhang, D. S. Su, X. Meng, F.-S. Xiao, *Chem. Commun.* **2012**, *48*, 5476. d) K. Rahme, M. T. Nolan, T. Doody, G. P. McGlacken, M. A. Morris, C.

O’Driscoll, J. D. Holmes, *RSC Adv*. **2013**, *3*, 21016. e) C. G. Arellano, A. Corma, M. Iglesias, F. Sánchez, *Chem. Commun.* **2005**, 1990. f) M. P. Sk, C. K. Jana, A. Chattopadhyay, *Chem. Commun.* **2013**, *49*, 8235. g) A. Primo, F. Quignard, *Chem. Commun.* **2010**, *46*, 5593. h) A. Kar, N. Mangu, H. M. Kaiser, M. Bellerab, M. K. Tse, *Chem. Commun.* **2008**, 386.

[6] L. Wang, H. Wang, W. Zhang, J. Zhang, J. P. Lewis, X. Meng, F.-S. Xiao, *J. Catal.* **2013**, *298*, 186.

[7] M. Boronat, A. Corma, *J. Catal.* **2011**, *284*, 138.

[8] H. Nakatsuji, Z.-M. Hu, H. Nakai, K. Ikeda, *Surf. Sci*. **1997**, *387*, 328.

[9] A. Roldán, S. González, J. M. Ricart, F. Illas, *ChemPhysChem*. **2009**, *10*, 348.

[10] K. Bobuatong, S. Karanjit, R. Fukuda, M. Ehara, H. Sakurai, *Phys. Chem. Chem. Phys.* **2012**, *14*, 3103.

[11] S. Karanjit, K. Bobuatong, R. Fukuda, M. Ehara, H. Sakurai, *Int. J. Quantum Chem.* **2013**, *113*, 428.

[12] a) M. Okumura, Y. Kitagawa, T. Kawakami, *Int. J. Quantum. Chem.* **2010**, *110*, 2903. b) M. Okumura, Y. Kitagawa, T. Kawakami, M. Haruta, *Chem. Phys. Lett.* **2008**, *459*, 133. c) B. Boekfa, E. Pahl, N. Gaston, H. Sakurai, J. Limtrakul, M. Ehara, *J. Phys. Chem. C*. **2014**, *118*, 22188.

[13] M. J. Frisch, G. W. Trucks, H. B. Schlegel, G. E. Scuseria, M. A. Robb, J. R. Cheeseman, G. Scalmani, V. Barone, B. Mennucci, G. A. Petersson, H. Nakatsuji, M. Caricato, X. Li, H. P. Hratchian, A. F. Izmaylov, J. Bloino, G. Zheng, J. L. Sonnenberg, M. Hada, M. Ehara, K. Toyota, R. Fukuda, J. Hasegawa, M. Ishida, T. Nakajima, Y. Honda, O. Kitao, H. Nakai, T. Vreven, J. Montgomery, J. A., J. E. Peralta, F. Ogliaro, M. Bearpark, J. J. Heyd, E. Brothers, K. N. Kudin, V. N. Staroverov, R. Kobayashi, J. Normand, K. Raghavachari, A. Rendell, J. C. Burant,

S. S. Iyengar, J. Tomasi, M. Cossi, N. Rega, N. J. Millam, M. Klene, J. E. Knox, J. B. Cross, V. Bakken, C. Adamo, J. Jaramillo, R. Gomperts, R. E. Stratmann, O. Yazyev, A. J. Austin, R. Cammi, C. Pomelli, J. W. Ochterski, R. L. Martin, K. Morokuma, V. G. Zakrzewski, G. A. Voth, P. Salvador, J. J. Dannenberg, S. Dapprich, A. D. Daniels, Ö. Farkas, J. B. Foresman, J. V. Ortiz, J. Cioslowski, D. J. Fox, *Gaussian 09, Revision B.01*, Gaussian, Inc., Wallingford CT, **2012**.

[14] M. Mantina, R. Valero, D. G. Truhlar, *J. Chem. Phys.* **2009**, *131*, 064706.

Chapter 4

Theoreoretical and Experimental Studies on Gold-based Bimetallic Nanocluster Catalysts

4.1 Introduction

The concept of impurity doping of one metal on the other to generate bimetallic system have become very useful because of the enhanced catalytic activities, selectivities, and stabilities of bimetallic NCs in comparison to their single-metal counterparts.[1] Especially, Au/Pd bimetallic alloy has superior catalytic activities in various types of reaction under mild conditions.[2-8] The activity and selectivity of Pd catalyst can be enhanced by alloying with Au due to the synergistic effects of bimetallic surfaces,7d–e such as ensemble and the ligand effect.1b Furthermore, bimetallization can result in stabilization of nanoparticles in cases where one metal acts as stabilizer for the other, preventing aggregation1b,7e-f which is a major limitation of Pd NPs chemistry in coupling reactions because once oxidative addition happens, Pd^{2+} will form and it will no longer stay on the surface in the absence of a strong ligand or stabilizer (Scheme 1).

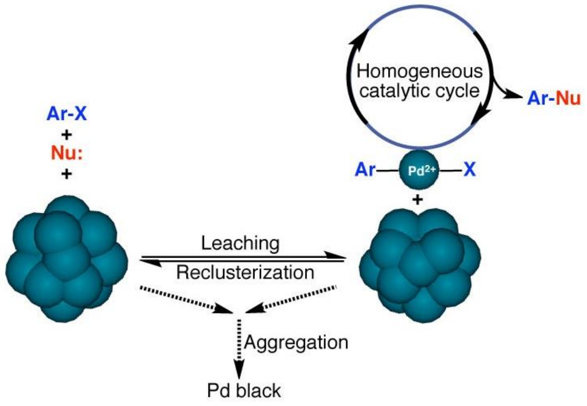

Scheme 1: a) Proposed oxidative addition mechanism on Pd catalyst resulting in leaching and aggregation.

PVP-stabilized bimetallic Au/Pd alloy NCs show efficient catalytic activity for C-Cl bond activation towards Ullmann coupling reaction using DMF as solvent and reducing agent (Scheme 2a path a). Through DFT calculation of the reaction mechanism, the author realized that both Au and Pd cooperatively participate in oxidative addition step of C-Cl bond and spillover of Cl over gold is a crucial step in the reaction, that drives the reaction through heterogeneous path due to spillover process of chlorine atom on the bimetallic surfaces preventing the homogeneous path (Scheme 2b) which is unlikely in the case of monometallic Pd surgaces.[8a] This reaction cannot be catalyzed by Pd NCs because of difficulty in Pd^{2+}/Pd^{4+} cycle during second oxidative addition process. To understand the effect of Pd doping on Au, hydrodechlorination reaction is a good model reaction. For Pd, eventhough it is difficult to activate C-Cl bond, once it is activated, Pd may be released as Pd^{2+} ion in solution due to oxidative addition process (Scheme 2b). Instead, if the author uses a hydride source (Scheme 2a path b), it will possibly undergo reduction, giving arene as the product even through usual homogenous mechanism and release the Pd^0 which can be captured by Au as a stabilizing ligand. In this work, the author attempts to trap it by Au during hydrodechlorination reaction and tune the reaction mechanism from homogenous to heterogenous.

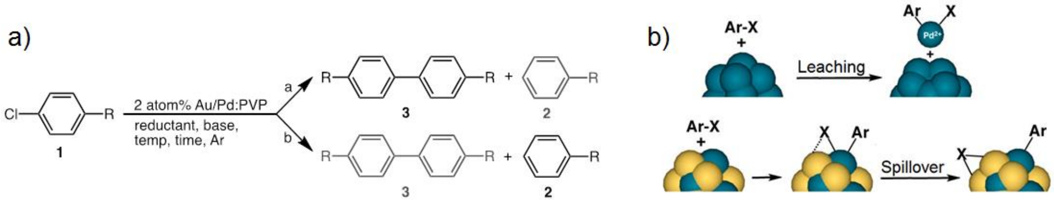

Scheme 2: a) Proposed oxidative addition mechanism on Pd and Au/Pd catalyst, b) C-Cl bond activation by Au/Pd:PVP bimetallic catalyst.

4.2 Experimental Section

Preparation of monometallic Au, Pd and bimetallic Au/Pd NCs

Monometallic Au:PVP, Pd:PVP and bimetallic Au/Pd:PVP nanoclusters were prepared by the method reported in our previous reports.1-3 278 mg (2.50 mmol, monomer unit of polymer) of PVP (K-30) was placed in a hard glass test tube (φ = 42 mm) and dissolved in 44 mL of Milli-Q water. Require amount of $HAuCl_4$ (from 25 mM stock solution) and $PdCl_2$ (from 12.5 mM stock solution) was added to the solution and final concentration of metal solution were made 0.5 mM (1:100 metals to polymer ratios). The resulting solution was stirred for 30 min at 27 °C. The solution was maintained 15 °C except for the case of Au NCs (at 0 °C) before reduction in organic synthesizer (EYELA, PPS-2510) and an aqueous solution (5 mL) of $NaBH_4$ (20 mg, 0.52 mmol) was added rapidly under vigorous stirring (1700 rpm). The color of the mixture was changed, indicating the formation of nanoparticle. Thus obtained Au, Pd and Au/Pd:PVP clusters were deionized subsequently by passing the colloidal solution through a membrane filter with a cut-off molecular weight of 10 kDa using a centrifugal ultrafiltration device (Vivascience, Vivaspin 20). The collected dispersion was then dried using a lyophilizer for catalytic reactions and characterizations.

***General Procedure for dechlorination of 4-Chloro-1-methoxybenzene (1a) in the presence of Au, Pd or bimetallic Au/Pd as a catalyst*.**

A 15-mm-diameter test tube was charged with 4-chloro-1-methoxybenzene (**1a**; 0.1 mmol) and KOH (0.15 mmol, 150 mol%) under argon. A hydrosol of 2 atom% Au:PVP, Pd:PVP, a mixture of Pd:PVP and Au:PVP, or Au/Pd:PVP in *i*-PrOH (3 mL) was added, and the mixture was stirred at 1300 rpm at the desired temperature in an organic synthesizer (EYELA, PPS-2510). The reaction was then quenched with 1 M HCl and the mixture was extracted with EtOAc (3 × 10 mL). The extracts were combined, dried (Na_2SO_4), and diluted to an exact volume in a volumetric flask. The yields were determined by GC, with hexadecane as a standard reference.

Dechlorination reaction of other chloroarenes were performed in similar conditions as optimized for 4-chloro-1-methoxybenzene using 2-4 atom% Au/Pd:PVP catalyst, 3-5 ml *i*-PrOH, 150-400 mol% base and 25-65 °C under argon. Yields of the desired products were reported as isolated yield or GC yield.

Kinetics of 4-Chloro-1-methoxybenzene:

0.3 mmol of **1** and 150 mol% of NaOH (0.45 mmol, 18.0 mg) were placed in a test tube (φ=30 mm). A hydrosol of Au:PVP, Pd:PVP or Au/Pd:PVP (2 atom%) in *i*-PrOH (9 ml) was added and argon was supplied from balloon without degassing the solution. The reaction was stirred vigorously (1300 rpm) at 25 °C. 0.1 mL of reaction mixture was sampled in each time intervals, then immediately quenched by 1 M HCl and extracted with ethyl acetate (0.5 mL x 3 times). GC yields of product were determined by using hexadecane as internal standard. The decay of substrate was monitored by the time dependent curve of yield of products or decay of substrates.

Characterization of catalyst before and after reaction

Two parallel sets of reaction were carried out in organic synthesizer (EYELA, PPS-2510). In one test tube (T1) (φ = 15 mm), 4-Chloro-1-methoxybenzene (0.1 mmol) and base KOH (150 mol%) were charged. A hydrosol of Au:PVP (1 atom%) and Pd:PVP (1 atom%) in i-PrOH (3 ml) was added and argon was supplied from balloon without degassing the solution. Same process was followed for the second test tube (T2) except the substrate 4-Chloro-1-methoxybenzene. Both the reaction were stirred vigorously (1300 rpm) at 45 °C for 12 h. Then the reaction mixtures were filtered and washed by water to remove organic and inorganic compounds. Both of the catalyst after treatment was subjected to transmission electron microscopy (TEM, JEOL JEM-3100FE and JEM-2100F) and scanning transmission electron microscopy–energy dispersive X-ray spectroscopy (STEM-EDX) analysis. The sample from test tube T1 is considered as after reaction and T2 as before reaction. The scanning transmission electron microscope (HITACHI, HD-2700) attached an energy-dispersive X-ray detector (EDAX, Apolio XLT) was operated at 200 kV.

4.3 Result and discussion

4.3.1 Hydrodechlorination of Aryl Chlorides: Catalyst test

Dechlorination reaction of 4-chloroanisole **1** was investigated in 2-propanol as solvent and hydrogen donor. First, we attempted to identify optimal conditions for the dechlorination reaction on the basis of the optimized conditions for Ullmann coupling reaction (Table 1a, entry 1). The reaction was carried out in the presence of Au/Pd:PVP as a catalyst and potassium hydroxide as the base in dimethyl sulfoxide (DMSO), no reaction occurred because of the nonreducing nature of the solvent (entry 2). However, the yield of dechlorination product methoxybenzene (**2**) increased in alcohol solvents. Reactions in 1:1 mixtures of methanol, ethanol, or propan-2-ol with water gave 2 in yields of 22%, 63%, and 70%, respectively (entries 3–5) and without water in ethanol (78%) and propanol (>95%) (entries 6–7). The best conditions involved the use of anhydrous propan-2-ol as the sole solvent; under these conditions, the reaction was completed within one hour at 45 °C and five hours at 25 °C giving >95% yield of **2** (entry 7-8). The optimized or slightly modified reaction conditions were applied to the dechlorination of various substrates including polychlorinated compounds and the results are summarized in Table 2. Under the conditions, polychlorinated compound such as dichlorobiphenyl and dichloroanthracene can be completely dechlorinated.

The efficiency of various Au and Pd catalysts for the dechlorination reaction was compared by performing the reaction of 1-chloro-4-methoxybenzene (**1**) for 1 h (Table 1). The highest catalytic activity was shown by Au/Pd bimetallic alloy nanoparticles, which gave **2** quantitatively (Table 1, entry 7). The dechlorination reaction of **1** did not proceed when Au:PVP was used as a catalyst (entry 9), whereas Pd:PVP did give **2**. only 24% (entry 10), while the physical mixture of the two monometallic catalysts Au:PVP and Pd:PVP (Au + Pd) gave 51% yield, which was higher than that obtained with Pd:PVP alone (entry 11). To test the effect of Au on the catalytic activity of Pd, we performed the reaction under identical conditions using physical mixtures of the two monometallic catalysts in varying Au and Pd ratios (Figure 1) . Even a small amount of Pd in Au, or vice versa, enhanced the catalytic activity to a value higher than that displayed by Au or Pd alone.

Table 1: Optimization of reaction condition and catalyst test

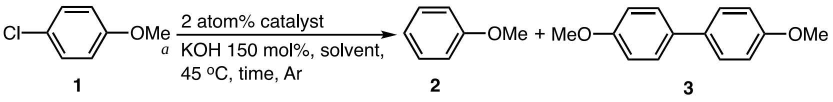

entry	solvent	t (h)	catalyst	yield (%)[b]	
				2	3
1	DMF-H_2O (1:2)	24	Au/Pd:PVP	6	92
2	DMSO-H_2O (1:1)	24	Au/Pd:PVP	0	0
3	MeOH-H_2O (1:1)	24	Au/Pd:PVP	22	20
4	EtOH-H_2O (1:1)	24	Au/Pd:PVP	63	14
5	*i*PrOH-H_2O (1:1)	24	Au/Pd:PVP	70	17
6	EtOH	24	Au/Pd:PVP	78	11
7	*i*PrOH	1	Au/Pd:PVP	>95	trace
8[c]	*i*PrOH	5	Au/Pd:PVP	>95	trace
9	*i*PrOH	1	Au:PVP	0	0
10	*i*PrOH	1	Pd:PVP	24	0
11	*i*PrOH	1	Au:PVP[d] + Pd:PVP[d]	51	trace

[a] Reaction conditions: 1 (0.1 mmol), catalyst (2 atom%), KOH (150 mol%), solvent (3 mL), 45 °C, under argon. [b] Yield by GC analysis. [c] At 25 °C. [d] 1 atom%.

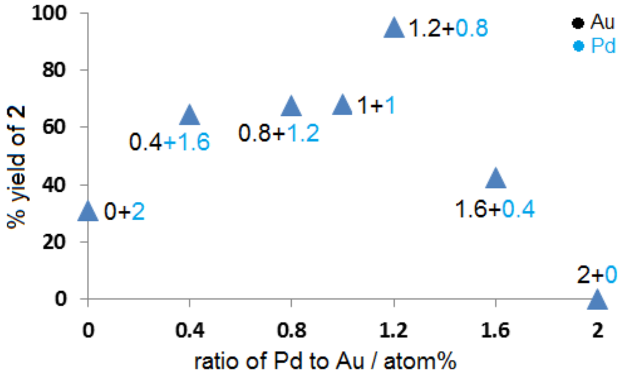

Figure 1: Relationship between catalytic activity and various Au/Pd ratios in physical mixture of Au:PVP and Pd:PVP.

Table 2: Catalytic dechlorination reaction of chloroarenes using Au/Pd:PVP catalyst

entry	substrate	product	T (°C)	t (h)	yield[a] (%)
1[b]	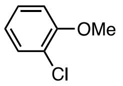	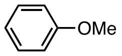	25	5	80
2[b]	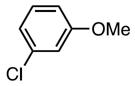	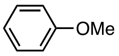	25	5	70
3[c]	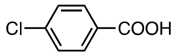	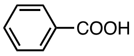	45	9	94
4	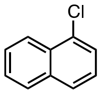	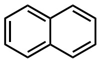	45	3	93
5	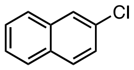	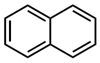	45	3	90
6[d]	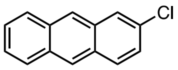	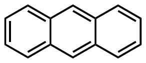	45	15	95
7[f]	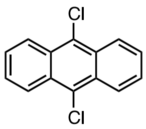	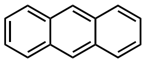	65	10	96
8[d]	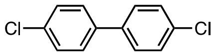	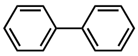	45	8	97
9[e]	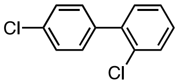	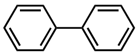	45	20	98

[a] Isolated yield. General reaction conditions: 2 atom% catalyst, 150 mol% KOH, solvent *i*-PrOH (3 mL). [b] GC yield. [c] 400 mol% KOH. [d] solvent *i*-PrOH (5 mL). [e] 400 mol% KOH. [f] 4 atom% catalyst, 600 mol% KOH, solvent *i*-PrOH (5 mL).

4.3.2 Kinetic studies of Hydrodechlorination of Aryl Chlorides

Measurements of the kinetics of consumption of **1** (Figure 2) showed differences in the catalytic activities of Au/Pd alloy, Pd, and (Au + Pd) nanoparticles. The reaction with bimetallic Au/Pd:PVP was a very fast second-order reaction with a rate constant for consumption of **1** of k = 5.6 × 10–1 Lmol^{-1}h^{-1}. The reaction with monometallic Pd:PVP, on the other hand, was very slow and showed first-order kinetics. The 1:1 physical mixture of Au:PVP and Pd:PVP show a reactivity that was intermediate between those of the two monometallic catalysts. At the beginning of the reaction, the catalytic activity of Pd:PVP (2 atom%) was higher, and the reaction rate was almost double than that observed with Au:PVP (1 atom%) + Pd:PVP (1 atom%) mixture. However, after two hours, the activity of the Au + Pd mixture gradually increased in comparison to that of Pd alone. The kinetic of consumption of 1 in the presence of the Au + Pd mixture at 25 °C showed a linear fit to the first-order plot of –ln[A] versus time, with an observed rate of consumption of **1** (k_{1a}) = 3.7 × 10^{-2} h^{-1} for the initial 2 hours of reaction. However, the slope then increased significantly, corresponding to an increase in the rate to 4.6 × 10^{-2} h^{-1} and a change in the order of the reaction (Figure 2b).

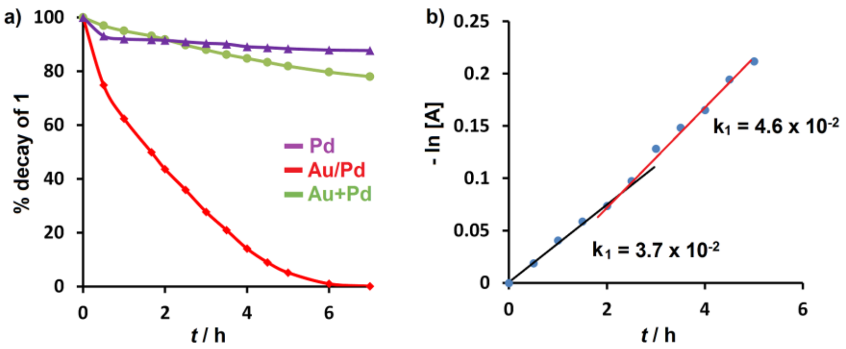

Figure 2: (a) Time-dependent consumption of **1** at 25 °C in hydrodechlorination reaction; (b) plot of –ln[A] vs time for (Au+Pd). ([A] = concentration of **1** with time).

On the basis of the above results, we hypothesized that leaching might occur from the surface during catalysis by monometallic Pd due to oxidative addition of the C–Cl bond. This species must be exclusively responsible for the initial catalytic activity through a homogeneous mechanism because Au:PVP on its own shows no activity in the reaction. In the presence of gold, *in situ* reduction of Pd(II) under the reaction condition might lead to the Au/Pd bimetallic catalyst with high dispersion of Pd on Au (Table 1, entry 11).

4.3.3. Characterization of catalyst before and after reaction

In order to test the hypothesis, the reaction **1** were carried out using base KOH and physical mixture of two catalyst Au:PVP (1 atom%) and Pd:PVP (1 atom%) in *i*-PrOH at 45 °C for 12 h and the catalyst recovered from the reaction mixture was subjected to

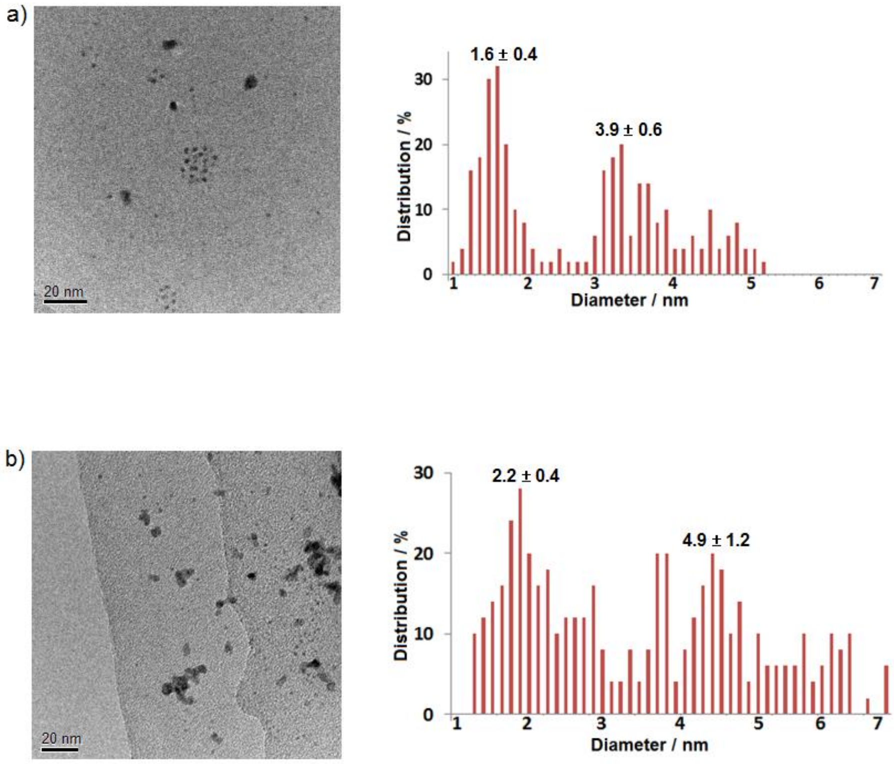

Figure 3: TEM images and size distribution of (Au+Pd):PVP a) before and b) after reaction.

transmission electron microscopy (TEM) analysis. TEM images shows that before reaction, only Au:PVP (1.6 ± 0.4 nm) and Pd:PVP (3.9 ± 0.6 nm) NCs exists separately [Figure 3], however, after the reaction, morphology of nanoclusters changes with a growth in the size of the NCs. STEM-EDX data showed the existence of bimetallic NCs containing various amounts of Au and Pd (Table 3). Most of the particles are polymorphological with non-uniform lattice pattern. But, some particles show uniform lattice pattern with single crystallinity possessing two metals (Figure 4). This supports that the enhanced catalytic activity of Pd is due to the dilution of surface Pd atoms by gold in forming these very few numbers of Au rich Au/Pd bimetallic NCs *in situ*.

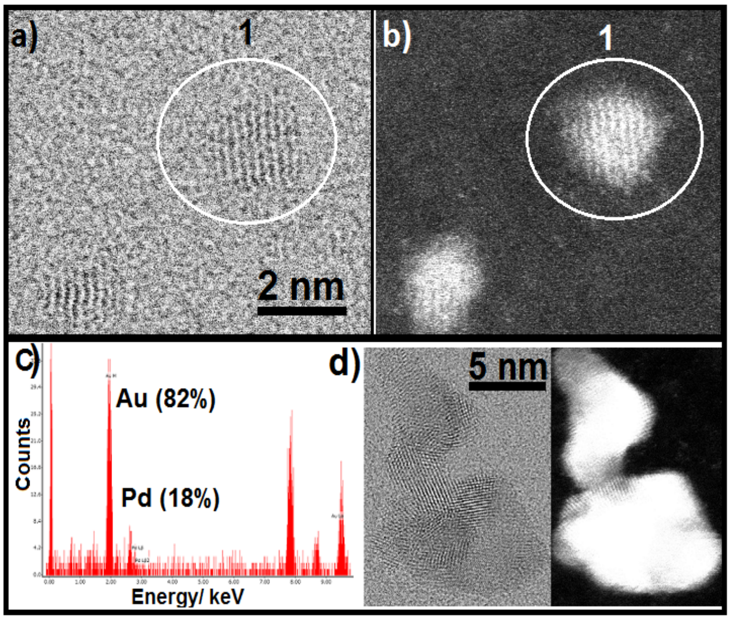

Figure 4: a) Bright-field and b) high-angle annular dark-field (HAADF) STEM images of particle 1 after reaction. c) STEM-EDX spectrum of particle 1. d) Bright-field (left) and HAADF STEM images of a polymorphic particle formed after reaction.

Table 3: Composition of Au/Pd bimetallic nanoparticle formed during the reaction (STEM-EDX). The particle numbers correspond to the numbers marked on the nanoparticles in the HAADF-STEM image

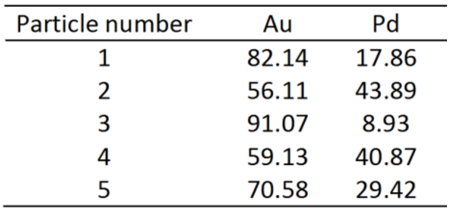

Particle number	Au	Pd
1	82.14	17.86
2	56.11	43.89
3	91.07	8.93
4	59.13	40.87
5	70.58	29.42

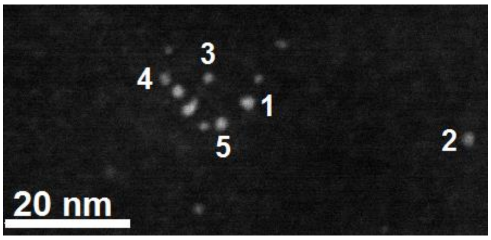

4.3.4 Mehanism of reaction

Therefore two catalytic cycles were proposed for the observed reactivities of monometallic and bimetallic nanoparticles, respectively, (Figure 5). The catalytic reaction involving the bimetallic nanoparticles follows a heterogeneous mechanism and occurs on the surface of the catalyst (cycle A) because of the spillover of Cl over gold. The process is very fast, with no aggregation or deactivation of the catalyst at any stage of the reaction. In the case of monometallic Pd:PVP in the absence of Au, the catalyst shows a homogeneous reaction mechanism (cycle B) through leached Pd. This is a slow process and, as the reaction proceeds, the Pd^0 species becomes gradually deactivated through aggregation, with the formation of Pd black. In the presence of Au, however, the leached palladium species that are present in solution are captured by Au to form bimetallic Au/Pd:PVP And both catalytic cycles operating simultaneously in the case of physical mixtures of Au:PVP and Pd:PVP.

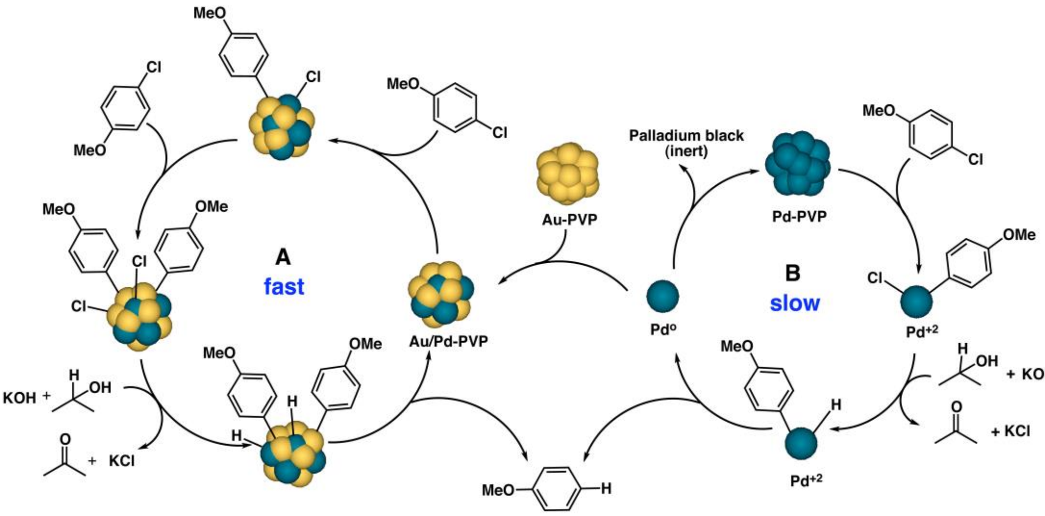

Figure 5: Proposed reaction mechanism for Pd and Au/Pd nanocluster.

4.4 Conclusion

In this chapter, the author found that the mutual influence of two metals Au and Pd can lead to higher catalytic behavior which is different than that of the monometallic NCs, through “synergistic effects”. The author found that, Au helps to capture and stabilize Pd, and the produce a bimetallic system *in situ* that catalyzes the reaction by a different mechanism, enhancing the catalytic activity. This can be a potential method for stabilization of leached Pd using Au as a stabilizer.

4.5 References

[1] a) C. W. Yi, K. Luo, T. Wei, D. W. Goodman, *J. Phys. Chem. B* 2005, **109**, 18535. b) F. Gao, D. W. Goodman, *Chem. Soc. Rev.*, 2012, **41**, 8009.

[2] a) J. Xu, T. White, P. Li, C. H. He, J. G. Yu, W. K. Yuan, Y. –F. Han, *J. Am. Chem. Soc.* 2010, **132**, 10398. b) T. Gracia, S. Agouram, A. Dejoz, J. F. Sanchez-Royo, L. Torrente-Murciano, B. Solsona, *Catal. Today* 2014, doi: 10.1016/ j.cattod.2014.03.039. c) M. O. Nutt, K. N. Heck, P. Alvarez, M. S. Wong, *Appl.*

Catal. B 2006, **69**, 115. d) A. Sárkány, O. Geszti, G. Sáfrán, *Appl. Catal. A*, 2008, **350**, 157. e) N. E. Kolli, L. Delannoy, C. J. Louis, *Catal.* 2013, **297**, 79. f) T. Longfei, W. Xiaoli, C. Dong, L. Huiyu, M. Xianwei, T. Fangqiong, *J. Mater. Chem. A* 2013, **1**, 10382. g) J. Long, H. Liu, S. Wu, S. Liao, Y. Li, *ACS Catal.* 2013, **3**, 647.

[3] a) X. Wei, X. F. Yang, A. Q. Wang, L. Li, X. Y. Liu; T. Zhang, *J. Phys. Chem.* 2012, **116**, 6222. b) S. Carrettin, P. McMorn, P. Johnston, K. Griffin, C. J. Kielyc, G. J. Hutchings, *Phys. Chem. Chem. Phys.,* 2003, **5**, 1329.

[4] N. Toshima, *Macromol. Sci. Chem.,* 1990, **27**, 1225.

[5] M. Chen, D. Kumar, C.-W. Yi, D. W. Goodman, *Science,* 2005, **310**, 291.

[6] H. Zhang, T. Watanabe, M. Okumura, M. Haruta, N. Toshima, *Nat. Mater.* 2012, **11**, 49.

[7] a) N. K. Chaki, H. Tsunoyama, Y. Nigishi, H. Sakurai, T. Tsukuda, *J. Phys. Chem. C*, 2007, **111**, 4885. b) S. S. Yudha, R. N. Dhital, H. Sakurai, *Tetrahedron Lett*, 2011, **52**, 2633. c) O. Sophiphun, J. Wittayakun, R. N. Dhital, S. Haesuwannakij, A. Murugadoss, H. Sakurai, *Aust. J. Chem.* 2012, **65**, 1238. d) A. Murugadoss, K. Okumura, H. Sakurai, *J. Phys. Chem. C*, 2012, **116**, 26776. e) D. Wang, A. Villa, F. Porta, L. Prati, D. Su, *J. Phys. Chem. C*, 2008, **112**, 8617. f) C. Rossy, J. Majimel, E. Fouquet, C. Delacôte, M. Boujtita, C. Labrugère, M. Tréguer-Delapierre, F. X. Felpin, *Chem. Eur. J.*, 2013, **19**, 14024. g) H. B. Liu, U. Pal, A. Medina, C. Maldonado, J. A. Ascencio, *Phys. Rev. B*, 2005, **71**, 075403. h) J. Cai, Y. Y. Ye, *Phys. Rev. B,* 1996, **54**, 8398. i) M. L. Wu, D. H. Chen, T. C. Huang, *Langmuir*, 2001, **17**, 3877.

[8] a) R. N. Dhital, C. Kamonsatikul, E. Somsook, K. Bobuatong, M. Ehara, S. Karanjit, H. Sakurai, *J. Am. Chem. Soc.* 2012, **134**, 20250. b) R. N. Dhital, H.

Sakurai, *Chem. Lett.* 2012, **41**, 630.

Conclusion

In this thesis, the mechanism of reactions catalyzed by gold and gold-based bimetallic nanocluster catalysts were investigated theoretically and experimentally.

In chapter 2, through mechanistic study of methanol oxidation reaction, The author found that the shape of cluster model can affect coordination number of the gold atom, and charge distribution on Au which in turn can affect the reaction pathways of the aerobic oxidation of methanol. In addition, it was realized that Au_{20}^- can be considered as a good model to reperesent Au:PVP system which can be applied for further investigation of other reactions catalyzed by Au:PVP NCs.

In chapter 3, the mechanism of aerobic homocoupling reaction of phenylboronic acid was studied comprehensively on Au_{20}^-. The results clearly explained that O_2 adsorption activates Au NCs by generating lewis acid sites and the cooperative effect of O_2 and H_2O play an important role in the adsorption and dissociation steps of C-B bond for transmetallation and reductive elimination. The spillover process of phenyl group on Au NCs facilitated reductive elimination from top and facet sites with low energy barrier. Furthermore, mechanism of phenol formation was also studied..

In chapter 4, bimetallic effect of the Pd doped on Au was studied for C-Cl bond activation in Ullmann coupling and Hydrodechlorination reaction. Monometallic and bimetallic catalysts were found to behave differently in the hydrodechlorination reaction following different mechanism. This doping strategy is helpful for design of new catalyst employing bimetallic effects.

Publications:

1. Aerobic oxidation of methanol to formic acid on Au_{20}^{-}: a theoretical study on the reaction mechanism,

   Karan Bobuatong, **Sangita Karanjit**, Ryoichi Fukuda, Masahiro Ehara, Hidehiro Sakurai, *Phys. Chem. Chem. Phys.* **2012**, 14, 3103.
2. Mechanism of the aerobic oxidation of methanol to formic acid on Au_{8}^{-}: A DFT study,

   Sangita Karanjit, Karan Bobuatong, Ryoichi Fukuda, Masahiro Ehara, Hidehiro Sakurai, *Int. J. Quantum Chem.* **2013**, 113, 428.
3. Mechanism of the aerobic homocoupling of Phenylboronic acid on Au_{20}^{-}: A DFT study,

   Sangita Karanjit, Masahiro Ehara, Hidehiro Sakurai, *Chem. Asian J.* **2015**, DOI: 10.1002/asia.201500535.
4. Significant Stabilization of Palladium by Gold in the Bimetallic Nanocatalyst Leading to an Enhanced Activity in the Hydrodechlorination of Aryl Chlorides,

   Sangita Karanjit, Atchaleeya Jinasan, Ekasith Somsook, Raghu Nath Dhital, Kenichi Motomiya, Yoshinori Sato, Kazuyuki Tohji, Hidehiro Sakurai, *Chem. Commun.* **2015**, 51, 12724.

List of Related Publication

1. Low-temperature carbon–chlorine bond activation by bimetallic gold/palladium alloy nanoclusters : an application to Ullmann Coupling

   Raghu Nath Dhital, Chao Kamonsatikul, Ekasith Somsook, Karan Bobuatong, Masahiro Ehara, **Sangita Karanjit**, Hidehiro Sakurai, *J. Am. Chem. Soc.* **2012**, 134, 20250.

2. Enantioselective synthesis of a chiral nitrogen–doped buckybowl

   Qitao Tan, Shuhei Higashibayashi, **Sangita Karanjit**, Hidehiro Sakurai, *Nat. Commun.* DOI: 10.1038/ncomms1896.

3. Synthesis of Substituted Sumanenes by Aromatic Electrophilic Substitution Reactions

   Binod Babu Shrestha, **Sangita Karanjit**, Gautam Panda, Shuhei Higashibayashi, Hidehiro Sakurai, *Chem. Lett.* **2013**, 42, 386.

4. Correlation between Bowl-Inversion Energy and Bowl Depth in Substituted Sumanenes

   Binod Babu Shrestha, **Sangita Karanjit**, Shuhei Higashibayashi, Hidehiro Sakurai, *Pure Appl. Chem.* **2014**, 86, 747.

5. Investigation on the Dynamic Behavior of Bisumanenyl

   Binod Babu Shrestha, **Sangita Karanjit**, Shuhei Higashibayashi, Toru Amaya, Toshikazu Hirao, Hidehiro Sakurai, *Asian J. Org. Chem.* **2015**, 4, 62.

Acknowledgement

The work in this thesis has been made possible by the contribution of many people. This doctoral thesis would not have been possible without the help and support of these kind people around me.

First and foremost I would like to express my deepest gratitude to my supervisor Professor Dr. Hidehiro Sakurai for providing me a golden oppurtinity to persue this work, as well as his scientific advice, invaluable time, continuous encouragement, guidance and all supports through this entire work. I would also like to thank Professor Dr. Masahiro Ehara in the Institute for molecular Science for his great help in computational analysis of my work through his valuable comments and suggestions and for providing acess to supercomputers.

I wish to express my especial gratitude to Assistant Professor Dr. Suhei Higashibayashi, Assistant Professor Dr. Ryoichi Fukuda and Dr. Karan Bobuatong, whose tuition, guidance and good company were a huge help during his time at Institute for Molecular Science. I am also grateful to Professor Dr. Yumi Yakiyama, Professor Dr. Ken Kokubo and Assistant Professor Dr. Naohiko Ikuma for fruitful discussion and valuable suggestions during meeting and seminars and their generous help.

My research project has been all the more enjoyable due to the good company of many colleagues at the Tohoku University, and Mahidol University. I would particularly like to thank Professor Dr. Yoshinori Sato and his group members for TEM and STEM-EDX measurements and data analysis. I would like to thank Professor Dr. Yasuhiro Uozumi and his group members for allowing me to use the spectroscopy instruments and Ms. Setsiri Haesuwanakiij for helping me during operating the TEM instruments.

I am profoundly grateful to Professor Dr. Mitsutaka Okumura and Professor Dr.

Ken-ichi Machida for their valuable comments and suggestions on preparation of this thesis during the reviewing process.

I would like to thank all the members of Sakurai group for creating a friendly, pleasant and innovative working environment in the lab. I enjoyed many discussions and working in the lab with them and achieved many fruitful suggestions in the group meetings and seminars.

Finally, I would like to say a huge thank you to my parents, whose hard work, guidance and encouragement have afforded me every opportunity to pursue whichever path I chose. For better or worse, this has led to the production of this thesis, and I will be forever in their debt. My especial thanks to my husband Mr. Binod Babu Shrestha, who is always with me as a collegue, a friend and a life partner in every moment of my life to give his helping hands whenever I need.

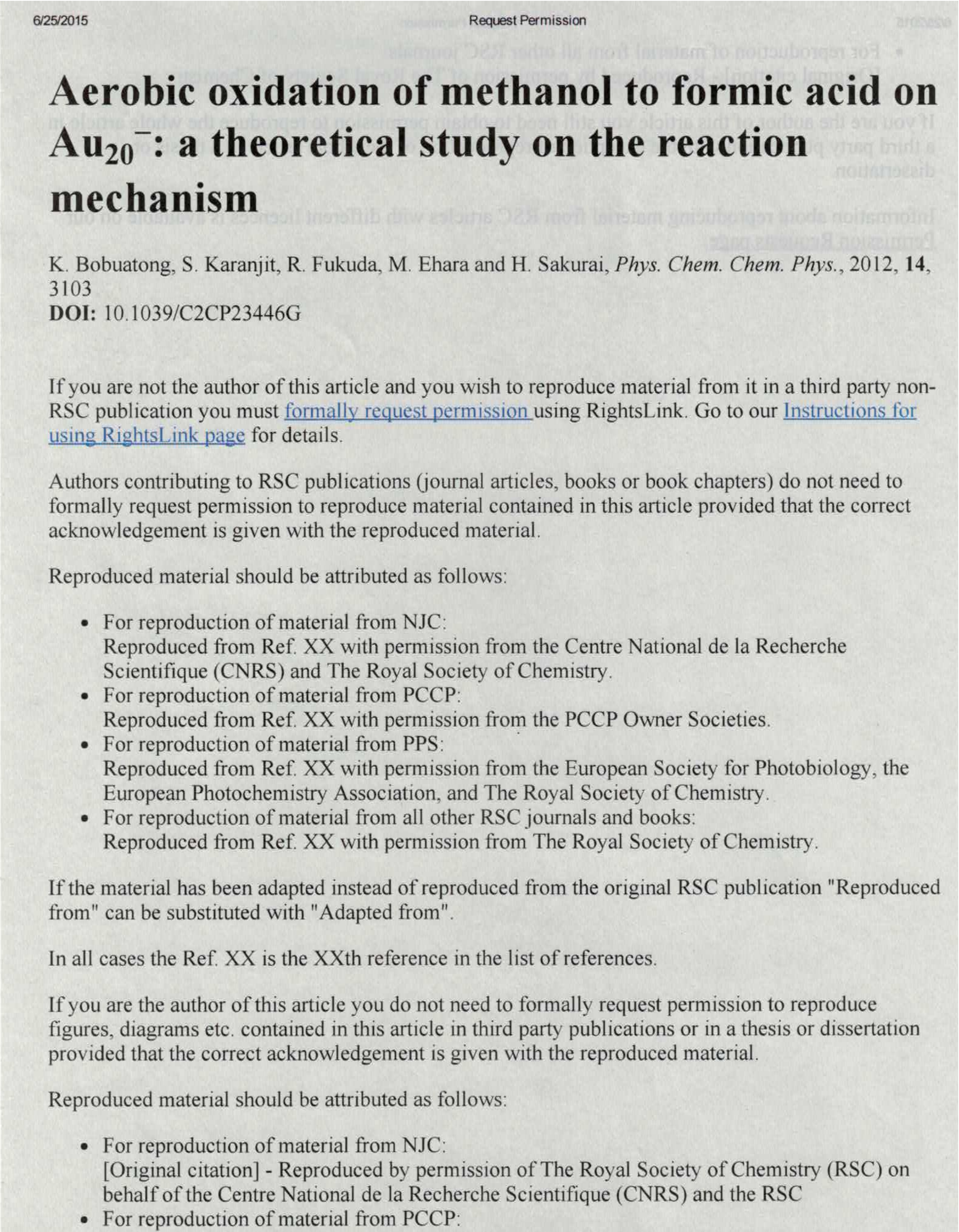

Aerobic oxidation of methanol to formic acid on Au_{20}^{-}: a theoretical study on the reaction mechanism

K. Bobuatong, S. Karanjit, R. Fukuda, M. Ehara and H. Sakurai, *Phys. Chem. Chem. Phys.*, 2012, **14**, 3103
DOI: 10.1039/C2CP23446G

If you are not the author of this article and you wish to reproduce material from it in a third party non-RSC publication you must formally request permission using RightsLink. Go to our Instructions for using RightsLink page for details.

Authors contributing to RSC publications (journal articles, books or book chapters) do not need to formally request permission to reproduce material contained in this article provided that the correct acknowledgement is given with the reproduced material.

Reproduced material should be attributed as follows:

- For reproduction of material from NJC:
  Reproduced from Ref. XX with permission from the Centre National de la Recherche Scientifique (CNRS) and The Royal Society of Chemistry.
- For reproduction of material from PCCP:
  Reproduced from Ref. XX with permission from the PCCP Owner Societies.
- For reproduction of material from PPS:
  Reproduced from Ref. XX with permission from the European Society for Photobiology, the European Photochemistry Association, and The Royal Society of Chemistry.
- For reproduction of material from all other RSC journals and books:
  Reproduced from Ref. XX with permission from The Royal Society of Chemistry.

If the material has been adapted instead of reproduced from the original RSC publication "Reproduced from" can be substituted with "Adapted from".

In all cases the Ref. XX is the XXth reference in the list of references.

If you are the author of this article you do not need to formally request permission to reproduce figures, diagrams etc. contained in this article in third party publications or in a thesis or dissertation provided that the correct acknowledgement is given with the reproduced material.

Reproduced material should be attributed as follows:

- For reproduction of material from NJC:
  [Original citation] - Reproduced by permission of The Royal Society of Chemistry (RSC) on behalf of the Centre National de la Recherche Scientifique (CNRS) and the RSC
- For reproduction of material from PCCP:
  [Original citation] - Reproduced by permission of the PCCP Owner Societies
- For reproduction of material from PPS:
  [Original citation] - Reproduced by permission of The Royal Society of Chemistry (RSC) on behalf of the European Society for Photobiology, the European Photochemistry Association, and RSC

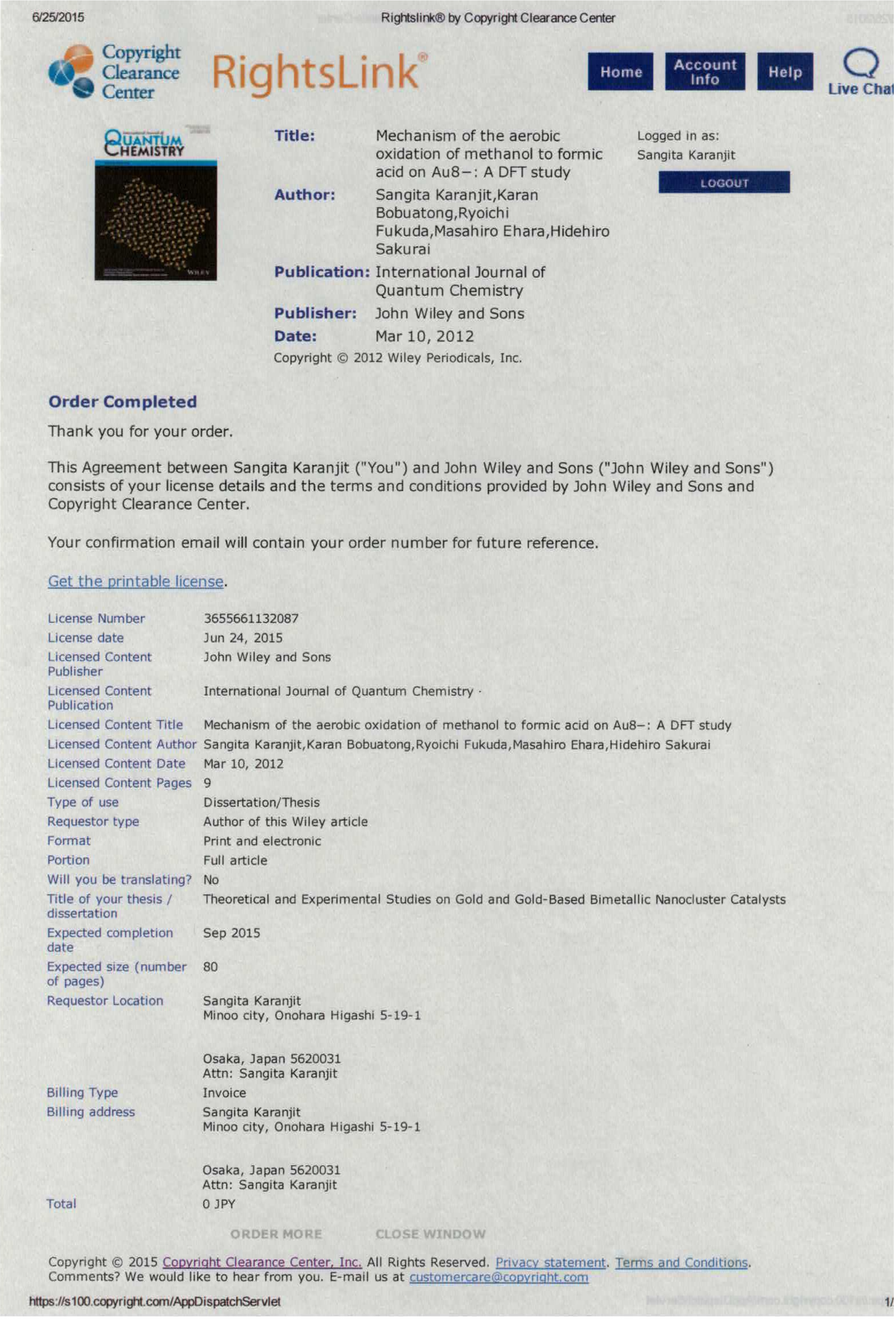

6/25/2015 Rightslink® by Copyright Clearance Center

Title:	Mechanism of the aerobic oxidation of methanol to formic acid on Au8−: A DFT study
Author:	Sangita Karanjit,Karan Bobuatong,Ryoichi Fukuda,Masahiro Ehara,Hidehiro Sakurai
Publication:	International Journal of Quantum Chemistry
Publisher:	John Wiley and Sons
Date:	Mar 10, 2012

Copyright © 2012 Wiley Periodicals, Inc.

Logged in as:
Sangita Karanjit

Order Completed

Thank you for your order.

This Agreement between Sangita Karanjit ("You") and John Wiley and Sons ("John Wiley and Sons") consists of your license details and the terms and conditions provided by John Wiley and Sons and Copyright Clearance Center.

Your confirmation email will contain your order number for future reference.

Get the printable license.

License Number	3655661132087
License date	Jun 24, 2015
Licensed Content Publisher	John Wiley and Sons
Licensed Content Publication	International Journal of Quantum Chemistry
Licensed Content Title	Mechanism of the aerobic oxidation of methanol to formic acid on Au8−: A DFT study
Licensed Content Author	Sangita Karanjit,Karan Bobuatong,Ryoichi Fukuda,Masahiro Ehara,Hidehiro Sakurai
Licensed Content Date	Mar 10, 2012
Licensed Content Pages	9
Type of use	Dissertation/Thesis
Requestor type	Author of this Wiley article
Format	Print and electronic
Portion	Full article
Will you be translating?	No
Title of your thesis / dissertation	Theoretical and Experimental Studies on Gold and Gold-Based Bimetallic Nanocluster Catalysts
Expected completion date	Sep 2015
Expected size (number of pages)	80
Requestor Location	Sangita Karanjit Minoo city, Onohara Higashi 5-19-1 Osaka, Japan 5620031 Attn: Sangita Karanjit
Billing Type	Invoice
Billing address	Sangita Karanjit Minoo city, Onohara Higashi 5-19-1 Osaka, Japan 5620031 Attn: Sangita Karanjit
Total	0 JPY

Copyright © 2015 Copyright Clearance Center, Inc. All Rights Reserved. Privacy statement. Terms and Conditions.
Comments? We would like to hear from you. E-mail us at customercare@copyright.com

https://s100.copyright.com/AppDispatchServlet 1/

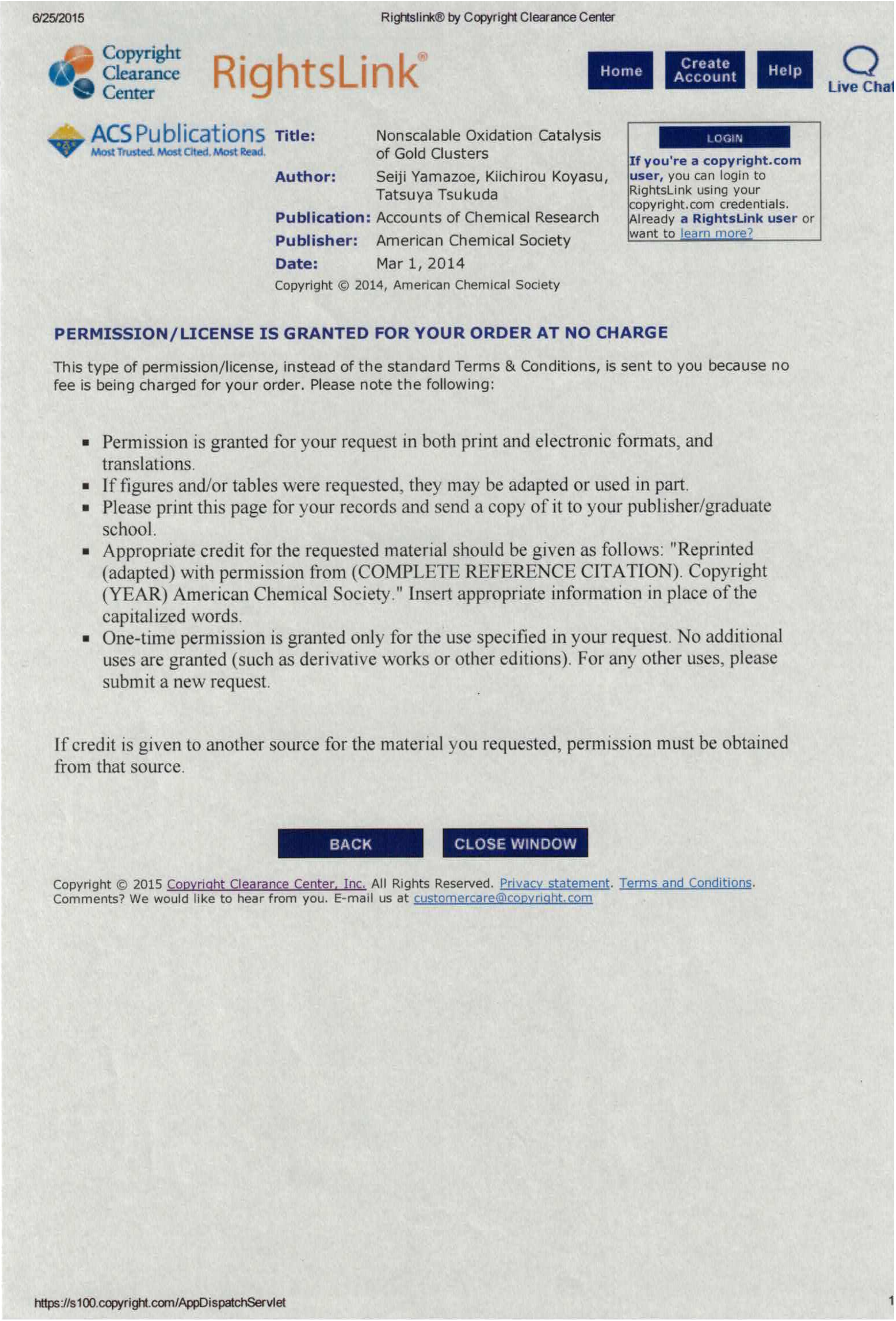

Title: Nonscalable Oxidation Catalysis of Gold Clusters
Author: Seiji Yamazoe, Kiichirou Koyasu, Tatsuya Tsukuda
Publication: Accounts of Chemical Research
Publisher: American Chemical Society
Date: Mar 1, 2014

Copyright © 2014, American Chemical Society

If you're a copyright.com user, you can login to RightsLink using your copyright.com credentials. Already **a RightsLink user** or want to learn more?

PERMISSION/LICENSE IS GRANTED FOR YOUR ORDER AT NO CHARGE

This type of permission/license, instead of the standard Terms & Conditions, is sent to you because no fee is being charged for your order. Please note the following:

- Permission is granted for your request in both print and electronic formats, and translations.
- If figures and/or tables were requested, they may be adapted or used in part.
- Please print this page for your records and send a copy of it to your publisher/graduate school.
- Appropriate credit for the requested material should be given as follows: "Reprinted (adapted) with permission from (COMPLETE REFERENCE CITATION). Copyright (YEAR) American Chemical Society." Insert appropriate information in place of the capitalized words.
- One-time permission is granted only for the use specified in your request. No additional uses are granted (such as derivative works or other editions). For any other uses, please submit a new request.

If credit is given to another source for the material you requested, permission must be obtained from that source.

Copyright © 2015 Copyright Clearance Center, Inc. All Rights Reserved. Privacy statement. Terms and Conditions.
Comments? We would like to hear from you. E-mail us at customercare@copyright.com

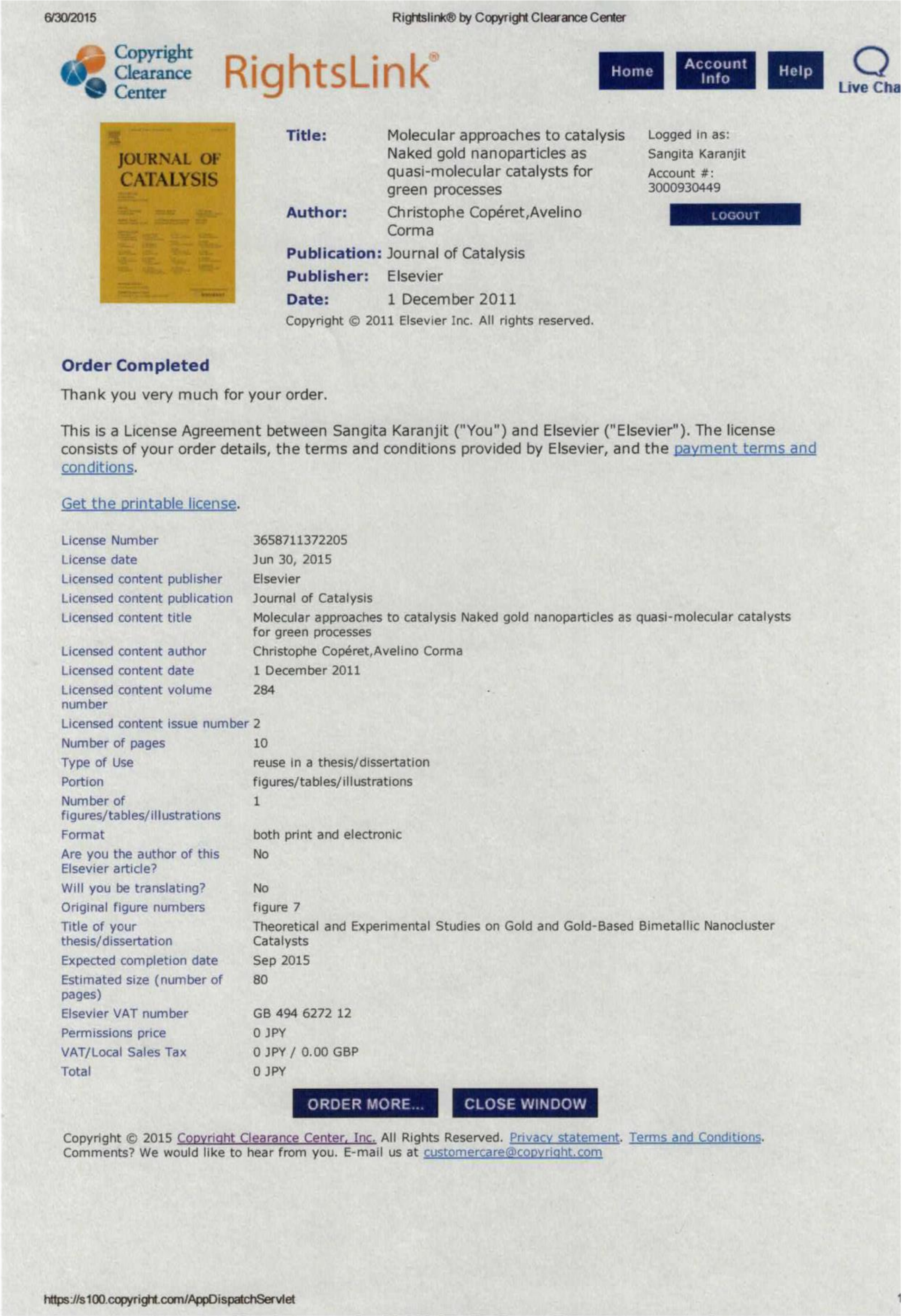

6/30/2015 Rightslink® by Copyright Clearance Center

Title: Molecular approaches to catalysis Naked gold nanoparticles as quasi-molecular catalysts for green processes

Author: Christophe Copéret,Avelino Corma

Publication: Journal of Catalysis

Publisher: Elsevier

Date: 1 December 2011

Copyright © 2011 Elsevier Inc. All rights reserved.

Logged in as:
Sangita Karanjit
Account #:
3000930449

Order Completed

Thank you very much for your order.

This is a License Agreement between Sangita Karanjit ("You") and Elsevier ("Elsevier"). The license consists of your order details, the terms and conditions provided by Elsevier, and the payment terms and conditions.

Get the printable license.

License Number	3658711372205
License date	Jun 30, 2015
Licensed content publisher	Elsevier
Licensed content publication	Journal of Catalysis
Licensed content title	Molecular approaches to catalysis Naked gold nanoparticles as quasi-molecular catalysts for green processes
Licensed content author	Christophe Copéret,Avelino Corma
Licensed content date	1 December 2011
Licensed content volume number	284
Licensed content issue number	2
Number of pages	10
Type of Use	reuse in a thesis/dissertation
Portion	figures/tables/illustrations
Number of figures/tables/illustrations	1
Format	both print and electronic
Are you the author of this Elsevier article?	No
Will you be translating?	No
Original figure numbers	figure 7
Title of your thesis/dissertation	Theoretical and Experimental Studies on Gold and Gold-Based Bimetallic Nanocluster Catalysts
Expected completion date	Sep 2015
Estimated size (number of pages)	80
Elsevier VAT number	GB 494 6272 12
Permissions price	0 JPY
VAT/Local Sales Tax	0 JPY / 0.00 GBP
Total	0 JPY

Copyright © 2015 Copyright Clearance Center, Inc. All Rights Reserved. Privacy statement. Terms and Conditions.
Comments? We would like to hear from you. E-mail us at customercare@copyright.com

https://s100.copyright.com/AppDispatchServlet

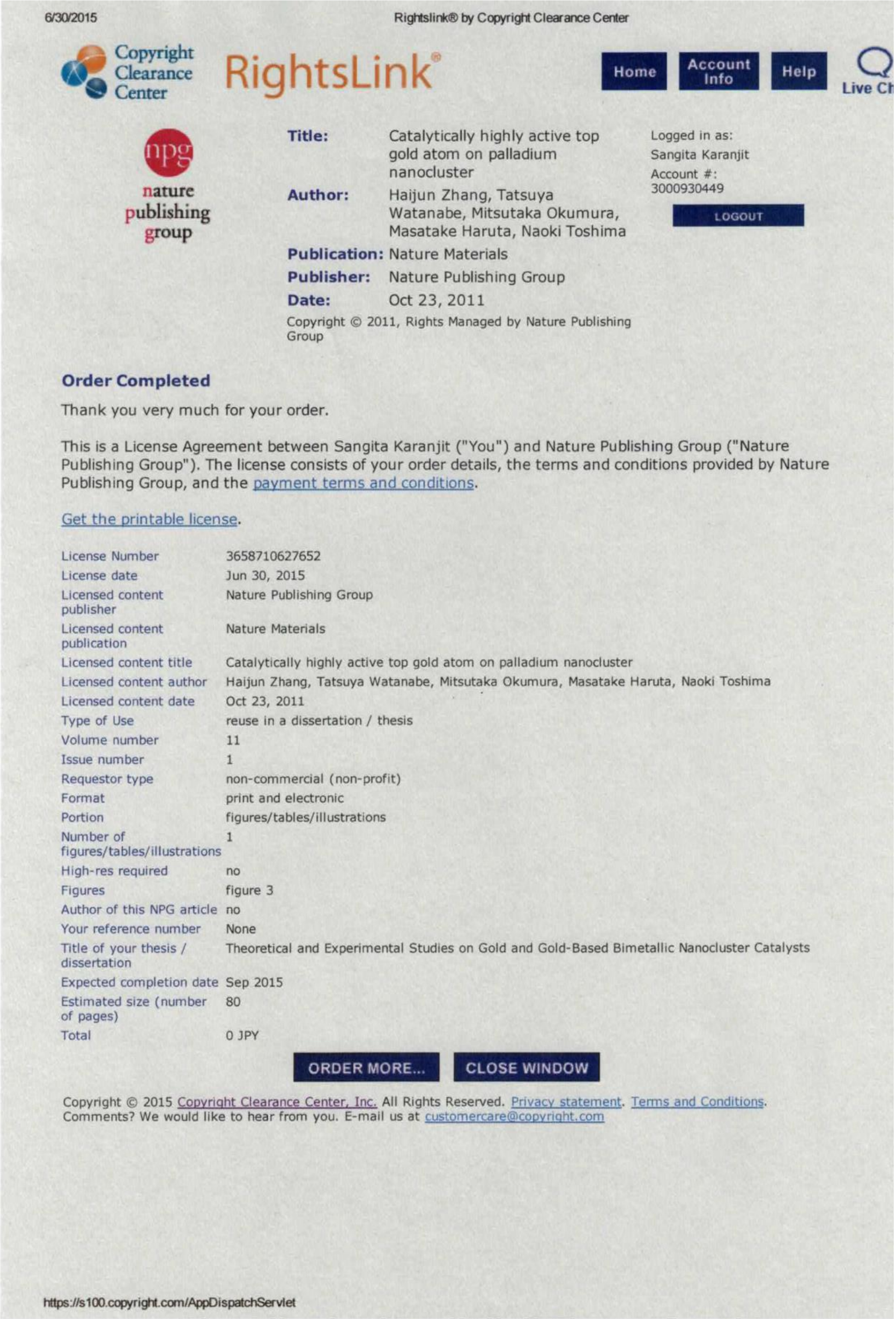

6/30/2015 Rightslink® by Copyright Clearance Center

Title: Catalytically highly active top gold atom on palladium nanocluster

Author: Haijun Zhang, Tatsuya Watanabe, Mitsutaka Okumura, Masatake Haruta, Naoki Toshima

Publication: Nature Materials

Publisher: Nature Publishing Group

Date: Oct 23, 2011

Copyright © 2011, Rights Managed by Nature Publishing Group

Logged in as:
Sangita Karanjit
Account #:
3000930449

Order Completed

Thank you very much for your order.

This is a License Agreement between Sangita Karanjit ("You") and Nature Publishing Group ("Nature Publishing Group"). The license consists of your order details, the terms and conditions provided by Nature Publishing Group, and the payment terms and conditions.

Get the printable license.

License Number	3658710627652
License date	Jun 30, 2015
Licensed content publisher	Nature Publishing Group
Licensed content publication	Nature Materials
Licensed content title	Catalytically highly active top gold atom on palladium nanocluster
Licensed content author	Haijun Zhang, Tatsuya Watanabe, Mitsutaka Okumura, Masatake Haruta, Naoki Toshima
Licensed content date	Oct 23, 2011
Type of Use	reuse in a dissertation / thesis
Volume number	11
Issue number	1
Requestor type	non-commercial (non-profit)
Format	print and electronic
Portion	figures/tables/illustrations
Number of figures/tables/illustrations	1
High-res required	no
Figures	figure 3
Author of this NPG article	no
Your reference number	None
Title of your thesis / dissertation	Theoretical and Experimental Studies on Gold and Gold-Based Bimetallic Nanocluster Catalysts
Expected completion date	Sep 2015
Estimated size (number of pages)	80
Total	0 JPY

Copyright © 2015 Copyright Clearance Center, Inc. All Rights Reserved. Privacy statement. Terms and Conditions.
Comments? We would like to hear from you. E-mail us at customercare@copyright.com

https://s100.copyright.com/AppDispatchServlet

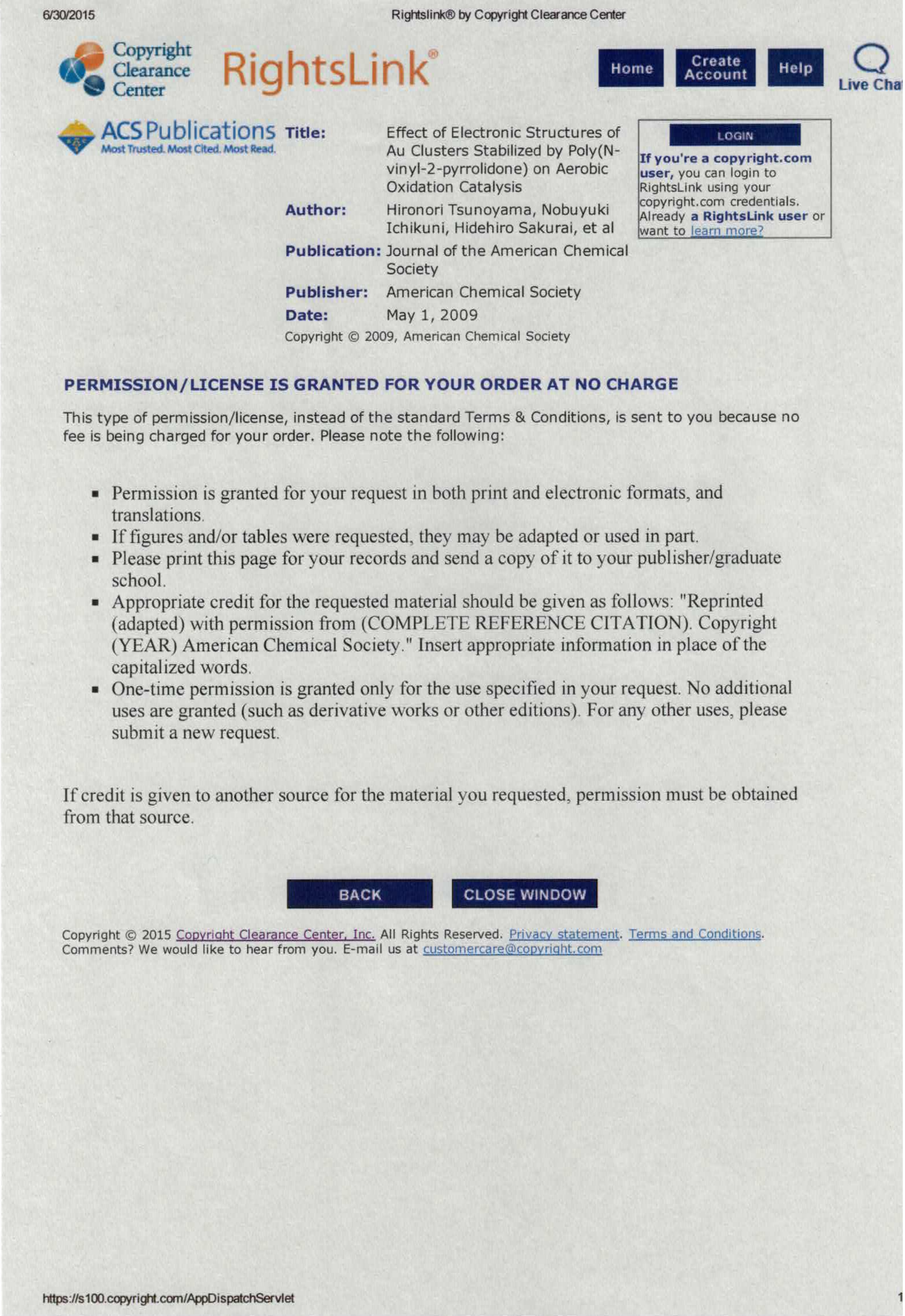
6/30/2015 Rightslink® by Copyright Clearance Center

Title:	Effect of Electronic Structures of Au Clusters Stabilized by Poly(N-vinyl-2-pyrrolidone) on Aerobic Oxidation Catalysis
Author:	Hironori Tsunoyama, Nobuyuki Ichikuni, Hidehiro Sakurai, et al
Publication:	Journal of the American Chemical Society
Publisher:	American Chemical Society
Date:	May 1, 2009

Copyright © 2009, American Chemical Society

If you're a copyright.com user, you can login to RightsLink using your copyright.com credentials. Already **a RightsLink user** or want to learn more?

PERMISSION/LICENSE IS GRANTED FOR YOUR ORDER AT NO CHARGE

This type of permission/license, instead of the standard Terms & Conditions, is sent to you because no fee is being charged for your order. Please note the following:

- Permission is granted for your request in both print and electronic formats, and translations.
- If figures and/or tables were requested, they may be adapted or used in part.
- Please print this page for your records and send a copy of it to your publisher/graduate school.
- Appropriate credit for the requested material should be given as follows: "Reprinted (adapted) with permission from (COMPLETE REFERENCE CITATION). Copyright (YEAR) American Chemical Society." Insert appropriate information in place of the capitalized words.
- One-time permission is granted only for the use specified in your request. No additional uses are granted (such as derivative works or other editions). For any other uses, please submit a new request.

If credit is given to another source for the material you requested, permission must be obtained from that source.

Copyright © 2015 Copyright Clearance Center, Inc. All Rights Reserved. Privacy statement. Terms and Conditions.
Comments? We would like to hear from you. E-mail us at customercare@copyright.com

https://s100.copyright.com/AppDispatchServlet 1

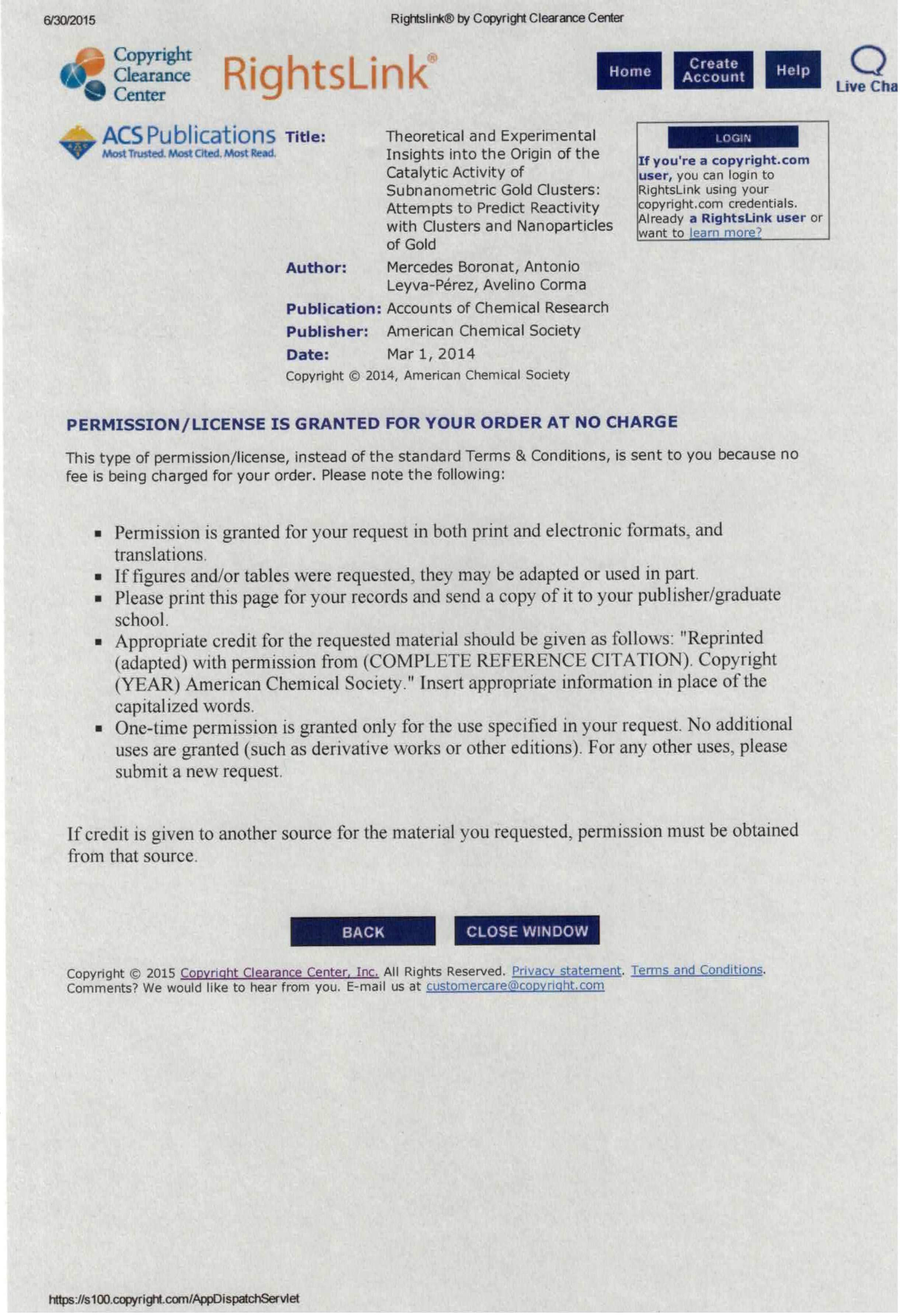

Copyright Clearance Center RightsLink®

ACS Publications
Most Trusted. Most Cited. Most Read.

Title: Theoretical and Experimental Insights into the Origin of the Catalytic Activity of Subnanometric Gold Clusters: Attempts to Predict Reactivity with Clusters and Nanoparticles of Gold

Author: Mercedes Boronat, Antonio Leyva-Pérez, Avelino Corma

Publication: Accounts of Chemical Research

Publisher: American Chemical Society

Date: Mar 1, 2014

Copyright © 2014, American Chemical Society

If you're a copyright.com user, you can login to RightsLink using your copyright.com credentials. Already **a RightsLink user** or want to learn more?

PERMISSION/LICENSE IS GRANTED FOR YOUR ORDER AT NO CHARGE

This type of permission/license, instead of the standard Terms & Conditions, is sent to you because no fee is being charged for your order. Please note the following:

- Permission is granted for your request in both print and electronic formats, and translations.
- If figures and/or tables were requested, they may be adapted or used in part.
- Please print this page for your records and send a copy of it to your publisher/graduate school.
- Appropriate credit for the requested material should be given as follows: "Reprinted (adapted) with permission from (COMPLETE REFERENCE CITATION). Copyright (YEAR) American Chemical Society." Insert appropriate information in place of the capitalized words.
- One-time permission is granted only for the use specified in your request. No additional uses are granted (such as derivative works or other editions). For any other uses, please submit a new request.

If credit is given to another source for the material you requested, permission must be obtained from that source.

Copyright © 2015 Copyright Clearance Center, Inc. All Rights Reserved. Privacy statement. Terms and Conditions.
Comments? We would like to hear from you. E-mail us at customercare@copyright.com

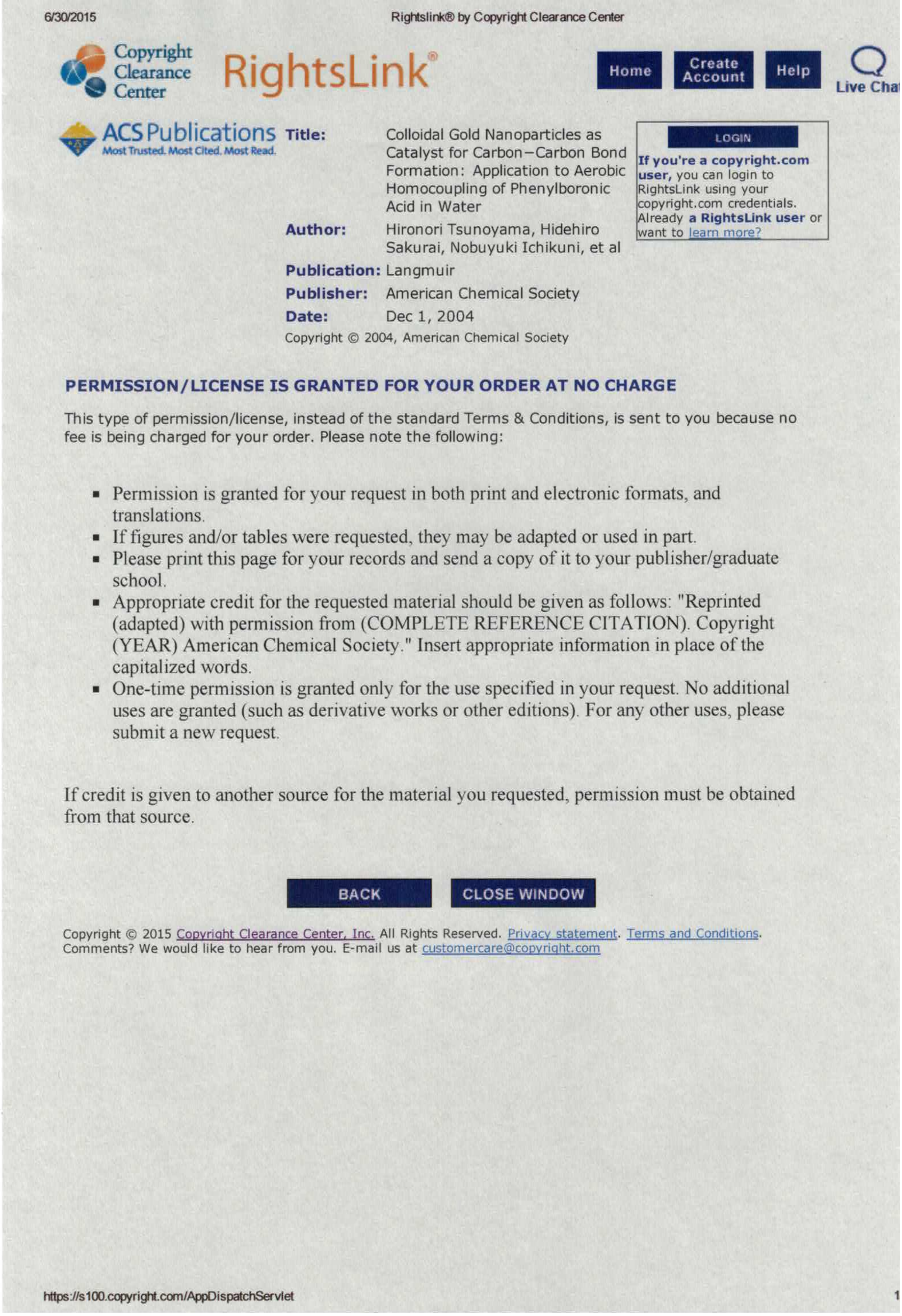

6/30/2015 Rightslink® by Copyright Clearance Center

Copyright Clearance Center RightsLink®

ACS Publications
Most Trusted. Most Cited. Most Read.

Title: Colloidal Gold Nanoparticles as Catalyst for Carbon−Carbon Bond Formation: Application to Aerobic Homocoupling of Phenylboronic Acid in Water

Author: Hironori Tsunoyama, Hidehiro Sakurai, Nobuyuki Ichikuni, et al

Publication: Langmuir

Publisher: American Chemical Society

Date: Dec 1, 2004

Copyright © 2004, American Chemical Society

If you're a copyright.com user, you can login to RightsLink using your copyright.com credentials. Already **a RightsLink user** or want to learn more?

PERMISSION/LICENSE IS GRANTED FOR YOUR ORDER AT NO CHARGE

This type of permission/license, instead of the standard Terms & Conditions, is sent to you because no fee is being charged for your order. Please note the following:

- Permission is granted for your request in both print and electronic formats, and translations.
- If figures and/or tables were requested, they may be adapted or used in part.
- Please print this page for your records and send a copy of it to your publisher/graduate school.
- Appropriate credit for the requested material should be given as follows: "Reprinted (adapted) with permission from (COMPLETE REFERENCE CITATION). Copyright (YEAR) American Chemical Society." Insert appropriate information in place of the capitalized words.
- One-time permission is granted only for the use specified in your request. No additional uses are granted (such as derivative works or other editions). For any other uses, please submit a new request.

If credit is given to another source for the material you requested, permission must be obtained from that source.

Copyright © 2015 Copyright Clearance Center, Inc. All Rights Reserved. Privacy statement. Terms and Conditions.
Comments? We would like to hear from you. E-mail us at customercare@copyright.com

https://s100.copyright.com/AppDispatchServlet 1

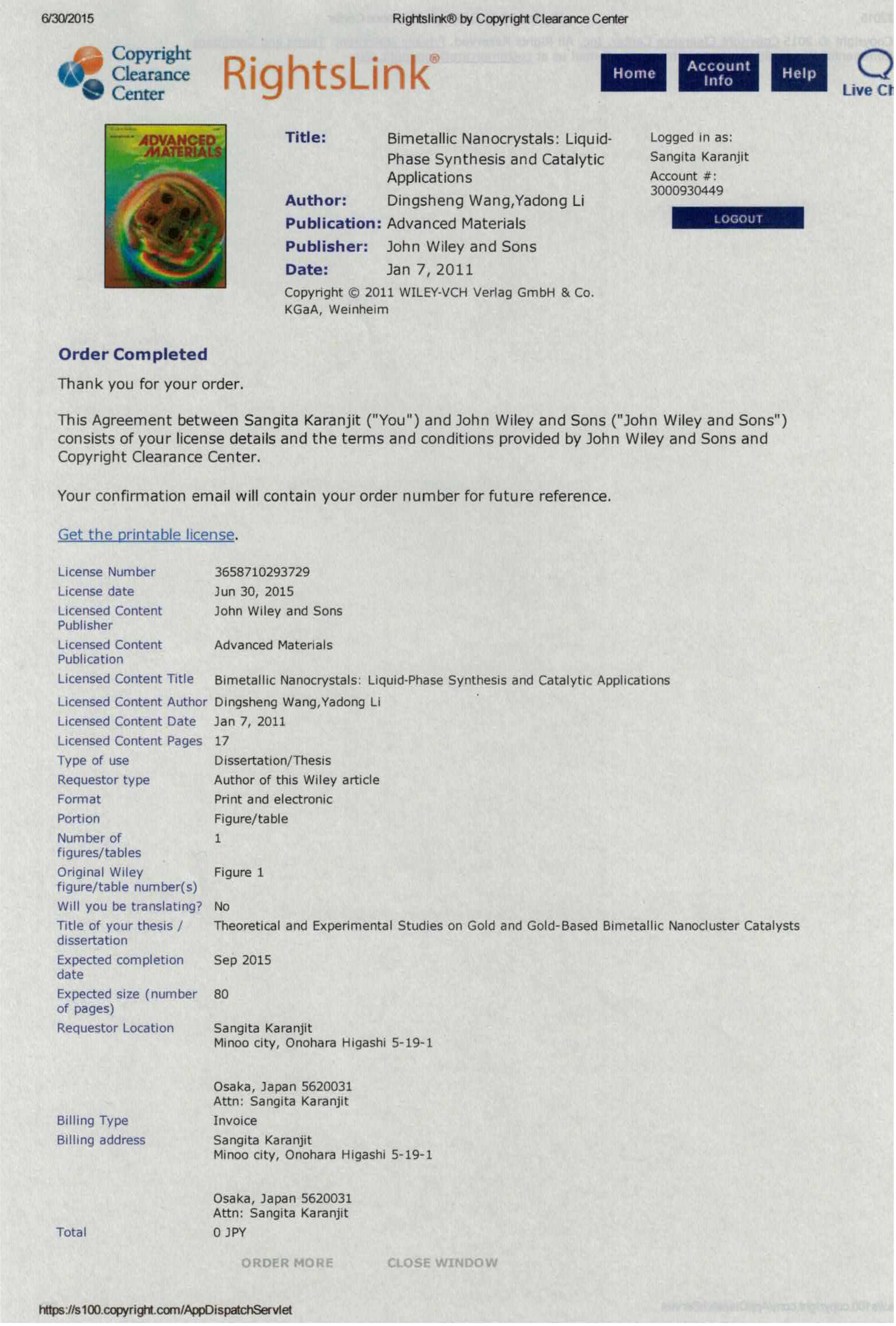

6/30/2015 Rightslink® by Copyright Clearance Center

Title: Bimetallic Nanocrystals: Liquid-Phase Synthesis and Catalytic Applications
Author: Dingsheng Wang,Yadong Li
Publication: Advanced Materials
Publisher: John Wiley and Sons
Date: Jan 7, 2011

Copyright © 2011 WILEY-VCH Verlag GmbH & Co. KGaA, Weinheim

Logged in as:
Sangita Karanjit
Account #:
3000930449

Order Completed

Thank you for your order.

This Agreement between Sangita Karanjit ("You") and John Wiley and Sons ("John Wiley and Sons") consists of your license details and the terms and conditions provided by John Wiley and Sons and Copyright Clearance Center.

Your confirmation email will contain your order number for future reference.

Get the printable license.

License Number	3658710293729
License date	Jun 30, 2015
Licensed Content Publisher	John Wiley and Sons
Licensed Content Publication	Advanced Materials
Licensed Content Title	Bimetallic Nanocrystals: Liquid-Phase Synthesis and Catalytic Applications
Licensed Content Author	Dingsheng Wang,Yadong Li
Licensed Content Date	Jan 7, 2011
Licensed Content Pages	17
Type of use	Dissertation/Thesis
Requestor type	Author of this Wiley article
Format	Print and electronic
Portion	Figure/table
Number of figures/tables	1
Original Wiley figure/table number(s)	Figure 1
Will you be translating?	No
Title of your thesis / dissertation	Theoretical and Experimental Studies on Gold and Gold-Based Bimetallic Nanocluster Catalysts
Expected completion date	Sep 2015
Expected size (number of pages)	80
Requestor Location	Sangita Karanjit Minoo city, Onohara Higashi 5-19-1 Osaka, Japan 5620031 Attn: Sangita Karanjit
Billing Type	Invoice
Billing address	Sangita Karanjit Minoo city, Onohara Higashi 5-19-1 Osaka, Japan 5620031 Attn: Sangita Karanjit
Total	0 JPY

https://s100.copyright.com/AppDispatchServlet

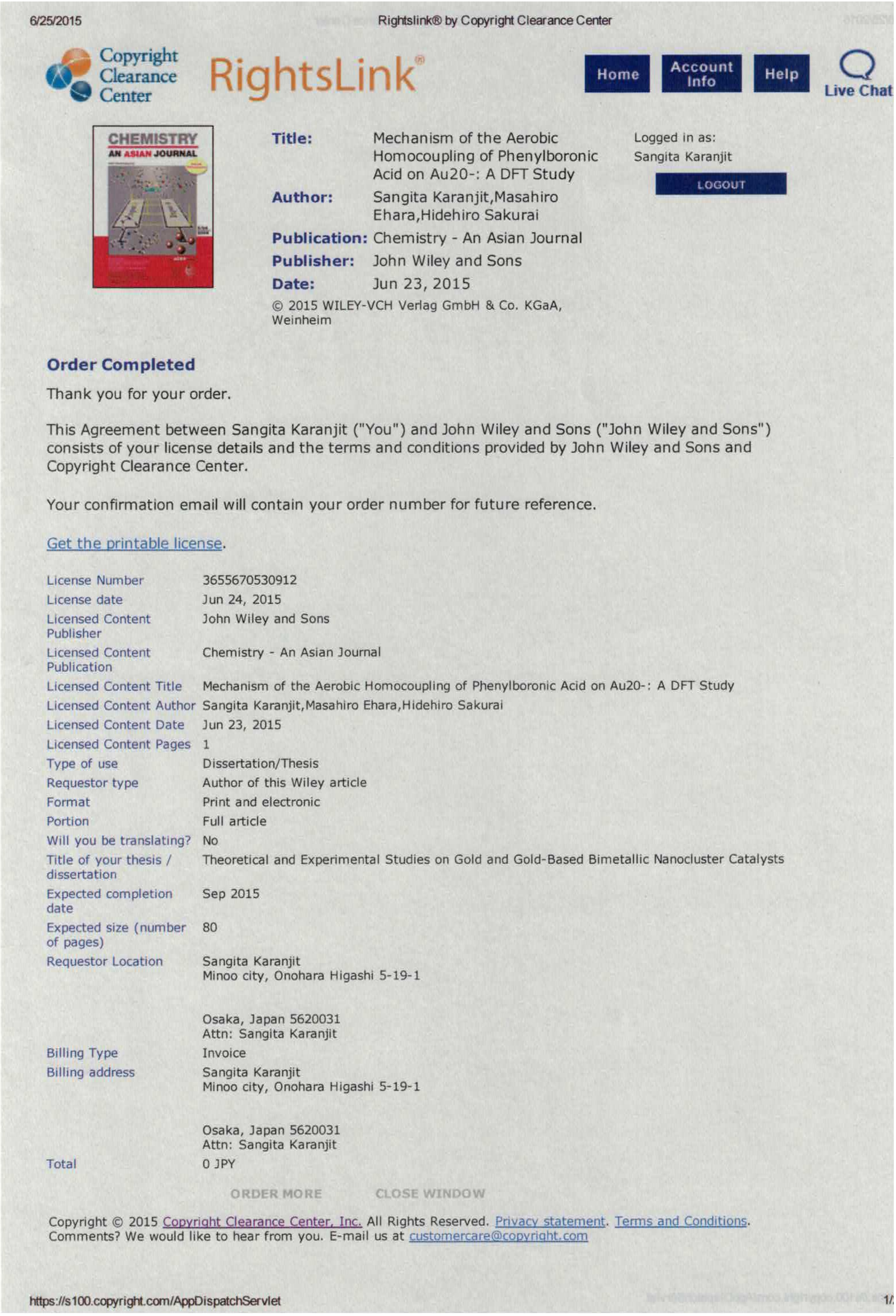

6/25/2015 Rightslink® by Copyright Clearance Center

Title: Mechanism of the Aerobic Homocoupling of Phenylboronic Acid on Au20-: A DFT Study
Author: Sangita Karanjit,Masahiro Ehara,Hidehiro Sakurai
Publication: Chemistry - An Asian Journal
Publisher: John Wiley and Sons
Date: Jun 23, 2015

© 2015 WILEY-VCH Verlag GmbH & Co. KGaA, Weinheim

Logged in as:
Sangita Karanjit

Order Completed

Thank you for your order.

This Agreement between Sangita Karanjit ("You") and John Wiley and Sons ("John Wiley and Sons") consists of your license details and the terms and conditions provided by John Wiley and Sons and Copyright Clearance Center.

Your confirmation email will contain your order number for future reference.

Get the printable license.

License Number	3655670530912
License date	Jun 24, 2015
Licensed Content Publisher	John Wiley and Sons
Licensed Content Publication	Chemistry - An Asian Journal
Licensed Content Title	Mechanism of the Aerobic Homocoupling of Phenylboronic Acid on Au20-: A DFT Study
Licensed Content Author	Sangita Karanjit,Masahiro Ehara,Hidehiro Sakurai
Licensed Content Date	Jun 23, 2015
Licensed Content Pages	1
Type of use	Dissertation/Thesis
Requestor type	Author of this Wiley article
Format	Print and electronic
Portion	Full article
Will you be translating?	No
Title of your thesis / dissertation	Theoretical and Experimental Studies on Gold and Gold-Based Bimetallic Nanocluster Catalysts
Expected completion date	Sep 2015
Expected size (number of pages)	80
Requestor Location	Sangita Karanjit Minoo city, Onohara Higashi 5-19-1 Osaka, Japan 5620031 Attn: Sangita Karanjit
Billing Type	Invoice
Billing address	Sangita Karanjit Minoo city, Onohara Higashi 5-19-1 Osaka, Japan 5620031 Attn: Sangita Karanjit
Total	0 JPY

Copyright © 2015 Copyright Clearance Center, Inc. All Rights Reserved. Privacy statement. Terms and Conditions.
Comments? We would like to hear from you. E-mail us at customercare@copyright.com

https://s100.copyright.com/AppDispatchServlet

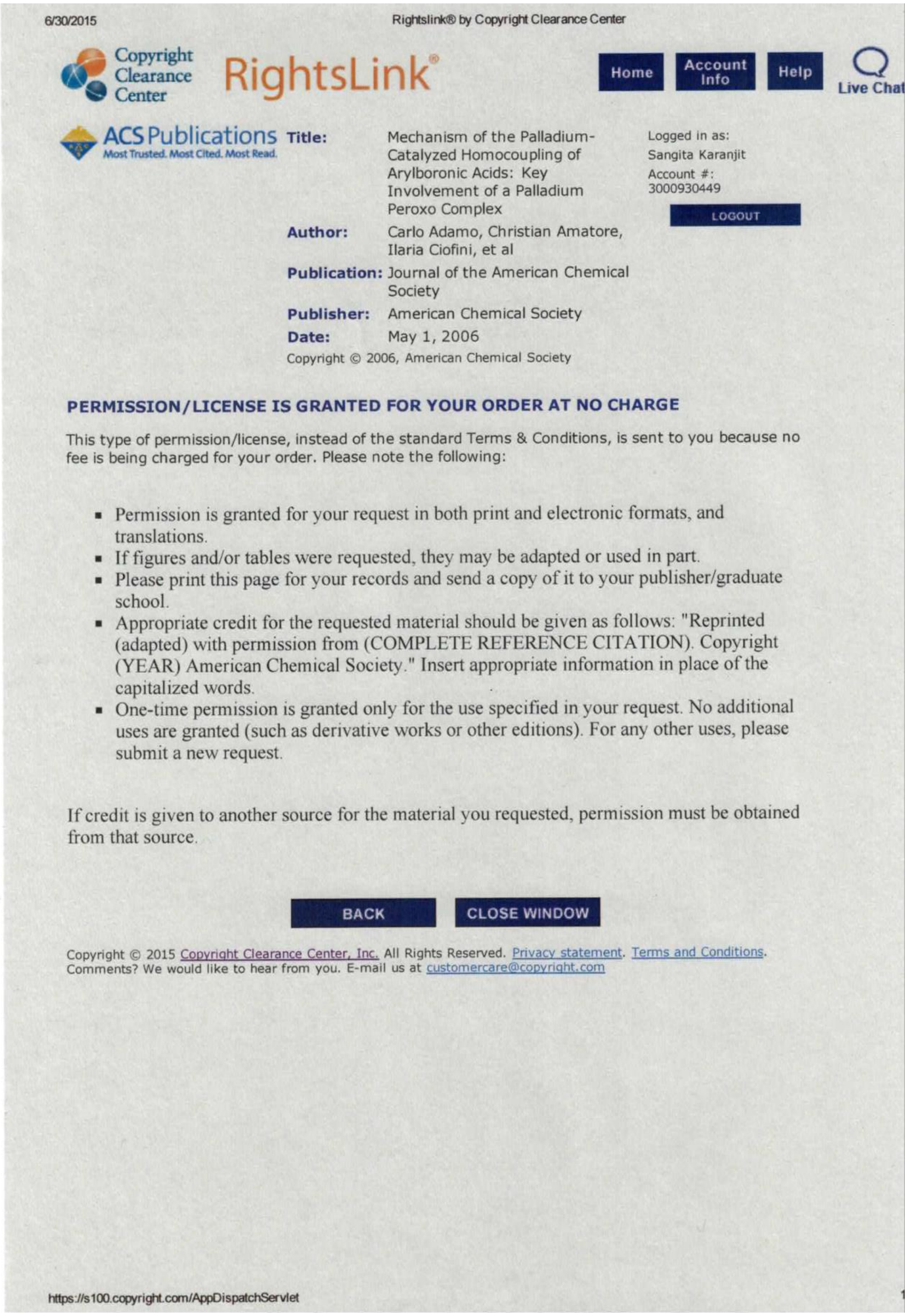

6/30/2015 Rightslink® by Copyright Clearance Center

Title: Mechanism of the Palladium-Catalyzed Homocoupling of Arylboronic Acids: Key Involvement of a Palladium Peroxo Complex

Author: Carlo Adamo, Christian Amatore, Ilaria Ciofini, et al

Publication: Journal of the American Chemical Society

Publisher: American Chemical Society

Date: May 1, 2006

Copyright © 2006, American Chemical Society

Logged in as:
Sangita Karanjit
Account #:
3000930449

PERMISSION/LICENSE IS GRANTED FOR YOUR ORDER AT NO CHARGE

This type of permission/license, instead of the standard Terms & Conditions, is sent to you because no fee is being charged for your order. Please note the following:

- Permission is granted for your request in both print and electronic formats, and translations.
- If figures and/or tables were requested, they may be adapted or used in part.
- Please print this page for your records and send a copy of it to your publisher/graduate school.
- Appropriate credit for the requested material should be given as follows: "Reprinted (adapted) with permission from (COMPLETE REFERENCE CITATION). Copyright (YEAR) American Chemical Society." Insert appropriate information in place of the capitalized words.
- One-time permission is granted only for the use specified in your request. No additional uses are granted (such as derivative works or other editions). For any other uses, please submit a new request.

If credit is given to another source for the material you requested, permission must be obtained from that source.

Copyright © 2015 Copyright Clearance Center, Inc. All Rights Reserved. Privacy statement. Terms and Conditions.
Comments? We would like to hear from you. E-mail us at customercare@copyright.com

https://s100.copyright.com/AppDispatchServlet 1

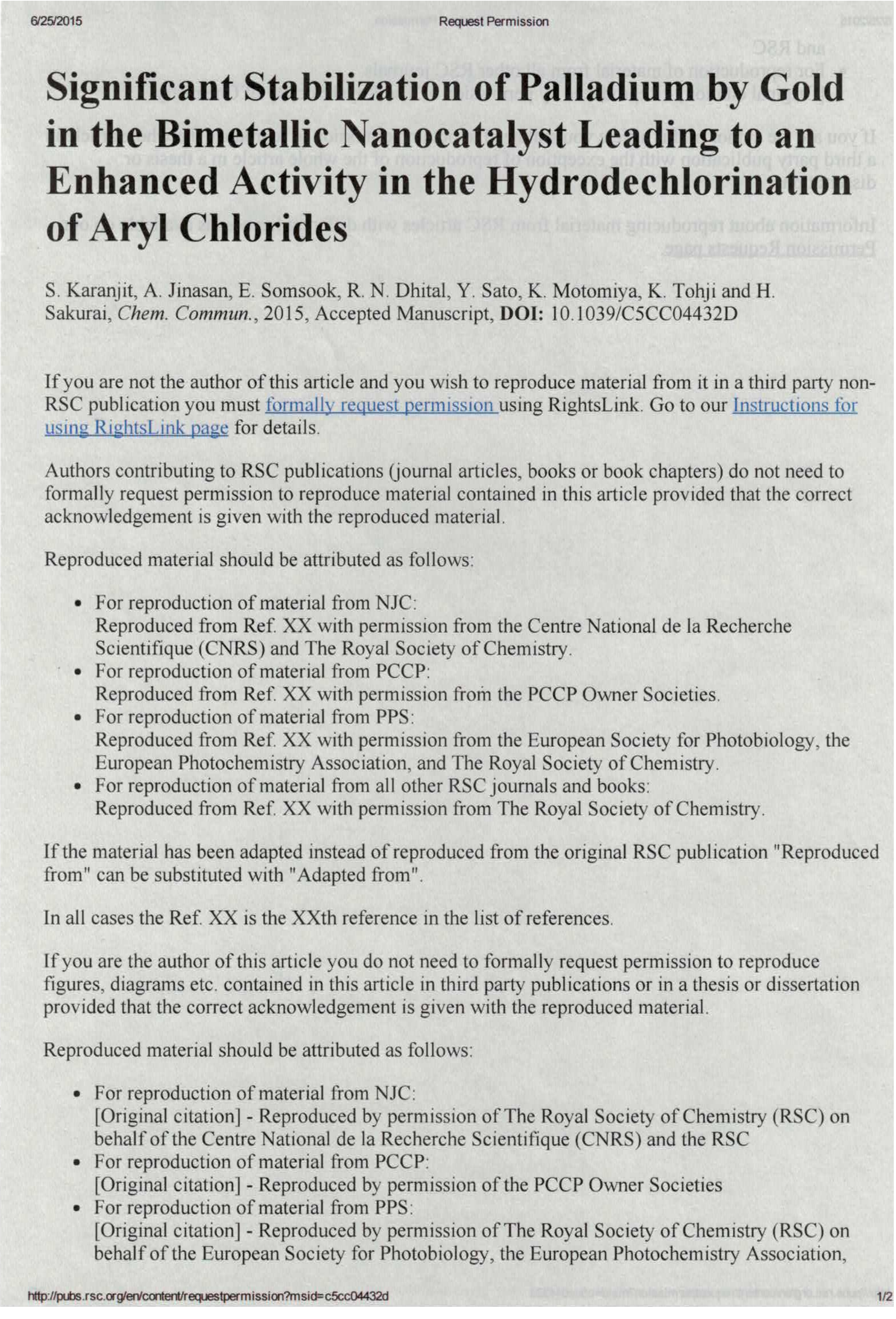

Significant Stabilization of Palladium by Gold in the Bimetallic Nanocatalyst Leading to an Enhanced Activity in the Hydrodechlorination of Aryl Chlorides

S. Karanjit, A. Jinasan, E. Somsook, R. N. Dhital, Y. Sato, K. Motomiya, K. Tohji and H. Sakurai, *Chem. Commun.*, 2015, Accepted Manuscript, **DOI:** 10.1039/C5CC04432D

If you are not the author of this article and you wish to reproduce material from it in a third party non-RSC publication you must formally request permission using RightsLink. Go to our Instructions for using RightsLink page for details.

Authors contributing to RSC publications (journal articles, books or book chapters) do not need to formally request permission to reproduce material contained in this article provided that the correct acknowledgement is given with the reproduced material.

Reproduced material should be attributed as follows:

- For reproduction of material from NJC:
  Reproduced from Ref. XX with permission from the Centre National de la Recherche Scientifique (CNRS) and The Royal Society of Chemistry.
- For reproduction of material from PCCP:
  Reproduced from Ref. XX with permission from the PCCP Owner Societies.
- For reproduction of material from PPS:
  Reproduced from Ref. XX with permission from the European Society for Photobiology, the European Photochemistry Association, and The Royal Society of Chemistry.
- For reproduction of material from all other RSC journals and books:
  Reproduced from Ref. XX with permission from The Royal Society of Chemistry.

If the material has been adapted instead of reproduced from the original RSC publication "Reproduced from" can be substituted with "Adapted from".

In all cases the Ref. XX is the XXth reference in the list of references.

If you are the author of this article you do not need to formally request permission to reproduce figures, diagrams etc. contained in this article in third party publications or in a thesis or dissertation provided that the correct acknowledgement is given with the reproduced material.

Reproduced material should be attributed as follows:

- For reproduction of material from NJC:
  [Original citation] - Reproduced by permission of The Royal Society of Chemistry (RSC) on behalf of the Centre National de la Recherche Scientifique (CNRS) and the RSC
- For reproduction of material from PCCP:
  [Original citation] - Reproduced by permission of the PCCP Owner Societies
- For reproduction of material from PPS:
  [Original citation] - Reproduced by permission of The Royal Society of Chemistry (RSC) on behalf of the European Society for Photobiology, the European Photochemistry Association,